

# **Proteomic investigation of the molecular targets of mycophenolic acid in human cells**

Dissertation

for the award of the degree

**“Doctor of Philosophy (Ph.D.)”**

Division of Mathematics and Natural Sciences

of the Georg-August University Goettingen

Submitted by

**Muhammad Qasim**

from Mardan, Pakistan

Goettingen, 2012

## D7

Reviewer 1: Prof. Dr. Uwe Groß  
Director, Department of Medical Microbiology,  
University Medical Center,  
Georg-August University, Goettingen, Germany.

Reviewer 2: Prof. Dr. Stefanie Pöggeler  
Director, Department of Genetics of Eukaryotic Microorganisms,  
Institute of Microbiology and Genetics,  
Georg-August University, Goettingen, Germany.

Date of oral examination: 20/01/2012

## **DECLARATION**

I hereby declare that the Ph.D. thesis entitled “Proteomic investigation of the molecular targets of mycophenolic acid in human cells” has been written independently, with no other sources than quoted, and no portion of the work referred to in the thesis has been submitted in support of an application for another degree.

Muhammad Qasim

# Table of contents

<b>List of abbreviations</b> .....	<b>1</b>
<b>List of Figure</b> .....	<b>4</b>
<b>List of Tables</b> .....	<b>5</b>
<b>1. General introduction</b> .....	<b>6</b>
<b>1.1 Mycophenolic acid</b> .....	<b>6</b>
1.1.1 Metabolism.....	7
1.1.2 Cellular and adverse effects of MPA .....	10
<b>1.2 Intestinal epithelial barrier</b> .....	<b>13</b>
1.2.1 Tight junctions.....	15
1.2.2 Factors modulating intestinal permeability .....	18
1.2.3 Regulation of TJ structure and function.....	20
1.2.4 Caco-2 cells as an in vitro model for intestinal epithelial integrity .....	21
<b>1.3 Rationale for proposed research</b> .....	<b>23</b>
<b>2. Differential proteome analysis of human embryonic kidney cell line (HEK-293) following mycophenolic acid treatment</b> .....	<b>24</b>
<b>2.1 Abstract</b> .....	<b>25</b>
<b>2.2 Introduction</b> .....	<b>26</b>
<b>2.3 Materials and Methods</b> .....	<b>27</b>
2.3.1 Reagents.....	27
2.3.2 Cell culture .....	27
2.3.3 Proliferation assay .....	28
2.3.4 Sample preparation for proteome analysis .....	28
2.3.5 2-DE.....	29
2.3.6 Protein visualization, densitometric analysis and in-gel digestion.....	29
2.3.7 Q-TOF LC-MS/MS analysis of protein identification.....	30
2.3.8 Functional classification.....	31
2.3.9 Western blotting .....	31
2.3.10 RNA isolation and cDNA synthesis .....	32

2.3.11 Real-time PCR .....	32
2.3.12 Apoptosis assay .....	33
<b>2.4 Results .....</b>	<b>34</b>
<b>2.5 Discussion .....</b>	<b>40</b>
<b>2.6 Conclusion .....</b>	<b>43</b>
<b>3. Mycophenolic acid mediated disruption of the intestinal epithelial tight junctions.....</b>	<b>44</b>
<b>3.1 Abstract.....</b>	<b>45</b>
<b>3.2 Introduction .....</b>	<b>46</b>
<b>3.3 Materials and methods .....</b>	<b>47</b>
3.3.1 Reagents.....	47
3.3.2 Cell culture .....	48
3.3.3 Lactate dehydrogenase (LDH) measurement .....	48
3.3.4 Determination of caspase 3 activity .....	48
3.3.5 Determination of Trans-epithelial resistance (TER).....	49
3.3.6 FITC-dextran paracellular permeability .....	49
3.3.7 RNA isolation, cDNA synthesis and real-time PCR.....	50
3.3.8 Immunoblotting .....	51
3.3.9 Immunofluorescence microscopy of TJs proteins .....	52
3.3.10 Statistics.....	53
<b>3.4 Results .....</b>	<b>53</b>
3.4.1 MPA altered TER and TJs permeability in a concentration and time dependant manner ..	53
3.4.2 AcMPAG modulation of TER and TJs permeability.....	54
3.4.3 MPA and AcMPAG mediated increase in permeability was not due to cell death/apoptosis .....	55
3.4.4 MPA and AcMPAG increased the expression of MLC2 and MLCK in Caco-2 cells .....	56
3.4.5 MPA and AcMPAG increased MLC2 phosphorylation in Caco-2 cells.....	58
3.4.6 MPA and AcMPAG altered TJ proteins expression and distribution .....	58
3.4.7 MPA and AcMPAG modulation of Caco-2 F-actin.....	60
3.4.8 MPA-mediated increase in MLC phosphorylation through MLCK .....	62
3.4.9 MLCK inhibition partially prevented MPA effects on TER and permeability.....	64

3.4.10 Inhibition of MLCK prevented MPA mediated alteration of TJ proteins .....	65
<b>3.5 Discussion .....</b>	<b>66</b>
<b>3.6 Conclusion.....</b>	<b>70</b>
<b>4. Summary .....</b>	<b>71</b>
<b>5. References .....</b>	<b>75</b>
<b>6. Appendix .....</b>	<b>100</b>
<b>7. Acknowledgements.....</b>	<b>106</b>
<b>8. Curriculum Vitae .....</b>	<b>108</b>

## List of abbreviations

AcMPAG	Acyl glucuronide of mycophenolic acid
ACN	Acetonitrile
BSA	Bovine serum albumin
cAMP	3',5'-cyclic monophosphate
CD	Cytochalasin D
cdc42	Cell division control protein 42 homolog
cDNA	Complementary DNA
C <sub>max</sub>	Maximum plasma concentrations
CRF	Corticotrophin-releasing factor
C <sub>T</sub>	Threshold cycle
CYP	Cytochrome P
DEVD-pNA	Asp-Glu-Val-Asp p-nitroanilide
DMEM	Dulbecco's modified Eagle's medium
DMSO	Dimethyl sulfoxide
DNA	Deoxyribonucleic acid
dNTPs	Deoxyribonucleotides
DSMZ	German collection of microorganisms and cell cultures
DTT	Dithiothreitol
ECL	Enhanced chemiluminescence
EC-MPS	Enteric-coated mycophenolate sodium
EF-2	Elongation factor 2
ELISA	Enzyme linked immunosorbent assay
EPEC	Enteropathogenic <i>Escherichia coli</i>
ER	endoplasmic reticulum
ERK	Extracellular signal regulated kinases
ESI-QTOF-MS	Electro spray ionization time of flight mass spectrometry
F-actin	Filamentous polymers actin
FCS	Fetal calf serum
FD 4	Fluorescein isocyanate-dextran
FDA	United States Food and Drug Administration
FITC	Fluorescein isothiocyanate
g	Gravitational (unit of centrifugation)

GI	Gastrointestinal
GMP	Guanosine monophosphate
GTP	Guanosine triphosphate
H <sub>2</sub> O <sub>2</sub>	Hydrogen peroxide
HDACs	histone deacetylases
HEK-293	Human embryonic kidney-293
hOAT	Human organic anion transporters
HRP	Horse radish peroxidase
IBD	Inflammatory bowel disease
IC <sub>50</sub>	Inhibitory concentration 50
IEF	Iso-electric focusing
IgA	Immunoglobulin-A
IMP	Inosine monophosphate
IMPDH	Inosine monophosphate dehydrogenase
IPG	Immobilised pH gradient
JAMs	Junctional adhesion molecules
kDa	Kilo dalton
LC	Liquid chromatography
LDH	Lactate dehydrogenase
LPS	Lipopolysaccharide
MAGI	MAGUKS with inverted domain structure
MAGUK	Membrane-associated guanylate kinases
MAPK	Mitogen-activated protein kinase
Marvel	MAL-related proteins for vesicle trafficking and membrane link
MC	Mast cells
ML-7	1-5-Iodonaphthalene-1-sulfonyl)-1H-hexahydro-1,4-diazepine hydrochloride
MLC	Myosin light chain
MLCK	Myosin light chain kinase
MLCP	Myosin light chain phosphatase
MMF	Mycophenolate mofetil
MPA	Mycophenolic acid
MPAG	Mycophenolic acid glucuronide
MRP	Multidrug resistant protein



MUPP	Multi-PDZ Domain Protein
NADH	Nicotinamide adenine dinucleotide
NO	Nitric oxide
NSAIDs	Nonsteroidal anti-inflammatory drugs
OD	Optical density
p	Probability
PAGE	Polyacrylamide gel electrophoresis
PAMR	Perijunctional actomyosin ring
P <sub>app</sub>	Apparent permeability
PBS	Phosphate buffer saline
PEG	Polyethylene glycols
PKC	Protein kinase C
pkl	Peak list
PLC	Phospholipase C
PML	Multifocal leukoencephalopathy
PP2A	Protein phosphatase 2A
Prdx1	Peroxiredoxin-1
PVDF	Polyvinylidene fluoride
RNA	Ribonucleic acid
RNase	Ribonuclease
ROCKs	Rho-associated, coiled-coil containing protein kinase
ROS	Reactive oxygen
RT	Reverse transcriptase
SDS	Sodium dodecyl sulfate
SEM	Standard error of the mean
TBS-T	Tris boric acid-tween
TER	Transepithelial electrical resistance
TFA	Trifluoroacetic acid
TJ	Tight junctions
TLR2	Toll-like receptor 2
UGT	Uridine diphosphate-glucuronosyltransferase
VEGF- $\alpha$	Vascular endothelial growth factor alpha
ZONAB	ZO-1-associated nucleic acid-binding protein

# List of Figure

<b>Figure 1.1</b> Chemical structure of MMF, EC-MPS, MPA, and their metabolites, AcMPAG, MPA 7-O-glucoside and 6-o-desmethyl MPA.....	7
<b>Figure 1.2</b> Metabolism of MPA .....	8
<b>Figure 1.3</b> Adverse effects of MPA .....	11
<b>Figure 1.4</b> Intestinal epithelial barrier.....	17
<b>Figure 2.1</b> Inhibition of HEK-293 cells proliferation by MPA treatment.....	36
<b>Figure 2.2</b> Differential protein expression after incubation of HEK-293 cells with MPA.....	36
<b>Figure 2.3</b> Functional classification of regulated proteins .....	37
<b>Figure 2.4</b> Differential expression of Prdx1 and MLC2 by MPA treatment.....	38
<b>Figure 2.5</b> Expression of MLC2 in MMF treated rat kidney lysate and HT-29 cells.....	39
<b>Figure 2.6</b> Measurement of MPA induced caspase-3 activity .....	39
<b>Figure 3.1</b> MPA treatment decreased TER and increased FD4 permeability of Caco-2 cell monolayers...54	
<b>Figure 3.2</b> AcMPAG treatment caused a time dependant decrease in TER and increase in FD4 permeability in Caco-2 cell monolayers.....	55
<b>Figure 3.3</b> Effect of MPA and AcMPAG on cell viability and apoptosis in Caco-2 cells.....	56
<b>Figure 3.4</b> Effect of MPA and AcMPAG on MLC2, MLCK and ROCK expression in Caco-2 cells.....	57
<b>Figure 3.5</b> Effect of MPA and AcMPAG on the phosphorylation of MLC2 in Caco-2 cells.....	58
<b>Figure 3.6</b> Effects of MPA and AcMPAG on ZO-1 and occludin distribution.....	59
<b>Figure 3.7</b> Effect of MPA and AcMPAG on occludin protein expression in Caco-2 cells .....	60
<b>Figure 3.8</b> MPA and AcMPAG-induced remodelling of the F-actin cytoskeleton.....	61
<b>Figure 3.9</b> Effect of ML-7 on MPA-mediated increases in MLC2, MLCK and MLC phosphorylation.....	63
<b>Figure 3.10</b> ML-7 co-treatment reversed the effect of MPA on TER and FD4 permeability .....	64
<b>Figure 3.11</b> ML-7 co-treatment reversed the effect of MPA on distribution of proteins.....	65
<b>Figure 3.12</b> Effect of ML-7 co-treatment with MPA on occludin protein expression in Caco-2 cells.....	66
<b>Figure 4.1</b> A proteomic approach for identification of novel MPA molecular targets .....	73
<b>Figure 4.2</b> Proposed model of MPA mediated TJ disruption .....	74
<b>Figure 5.1</b> A graphical representation of relative abundance (%volume) of all differentially regulated proteins .....	100

## List of Tables

**Table 2.1** Differentially regulated proteins by MPA in HEK-293 cells identified by mass spectrometry .....35

**Table 5.1** MS/MS analysis table of all differentially regulated proteins.....101

# 1. General introduction

## 1.1 Mycophenolic acid

Mycophenolic acid (MPA) is an active fungal agent derived from *Penicillium Brevicopactum* and related fungi. MPA was discovered in 1893 by an Italian physician, Bartolomeo Gosio as an antibiotic against *Bacillus anthracis* (reviewed in [1]) and was named by Alsberg and Black in 1913 [2]. MPA selectively and competitively inhibits inosine monophosphate dehydrogenase (IMPDH), which is a key regulatory enzyme in the *de novo* pathway of purine biosynthesis. IMPDH converts inosine monophosphate (IMP) to guanosine monophosphate (GMP), an important intermediate in the synthesis of DNA, RNA, proteins, and glycoproteins. Inhibition of IMPDH leads to cell cycle arrest in synthesis (S) phase due to the blocking of *de novo* guanosine nucleotide synthesis. MPA exhibits cytotoxic effects on all cell types including its main target, lymphocytic cells [3][4,5]. Lymphocytes presumably utilize a *de novo* pathway for purine biosynthesis while non-lymphocytic cells depend only partially on this pathway, and can utilize a salvage pathway [4]. In the salvage pathway, guanine obtained from the breakdown of nucleic acids is directly converted to guanosine monophosphate and used for purine synthesis [6]. Additionally, MPA has five fold more potent inhibitory action on IMPDH II, an isoform mainly expressed in B & T lymphocytes, than on IMPDH I, which is expressed in all body cells [4]. Consequently, the cytostatic effects of MPA on lymphocytes are greater than on other cell types, which contributes to the prevention of graft rejection, making MPA an especially useful immunosuppressant in transplantation medicine [3,4].

MPA is marketed in two forms: the ester pro-drug mycophenolate mofetil (MMF; CellCept, Roche, Grenzach-Wyhlen, Germany) and enteric-coated mycophenolate sodium (EC-MPS; myfortic®; Novartis Pharma AG, Basel, Switzerland) [7]. MMF gained approval by the United States Food and Drug Administration (FDA) in 1995 for the prevention of renal, cardiac, and hepatic allograft rejection [8,9]. MPA is now the drug of choice in transplantation medicine for the prevention of acute rejection in patients undergoing allogeneic renal, cardiac and liver transplantation [4,10]. Furthermore, MPA has proved to be effective in the treatment of autoimmune

disorders of the eyes and skin as well as in Wegener's granulomatosis and lupus nephritis [11-14], hypertension [15,16] and neuromuscular autoimmune diseases [17,18]. MPA has also been reported to possess anti-viral [19], anti-fungal [20], anti-bacterial [1], anti-tumor [21], and anti-psoriasis [22,23] activities.

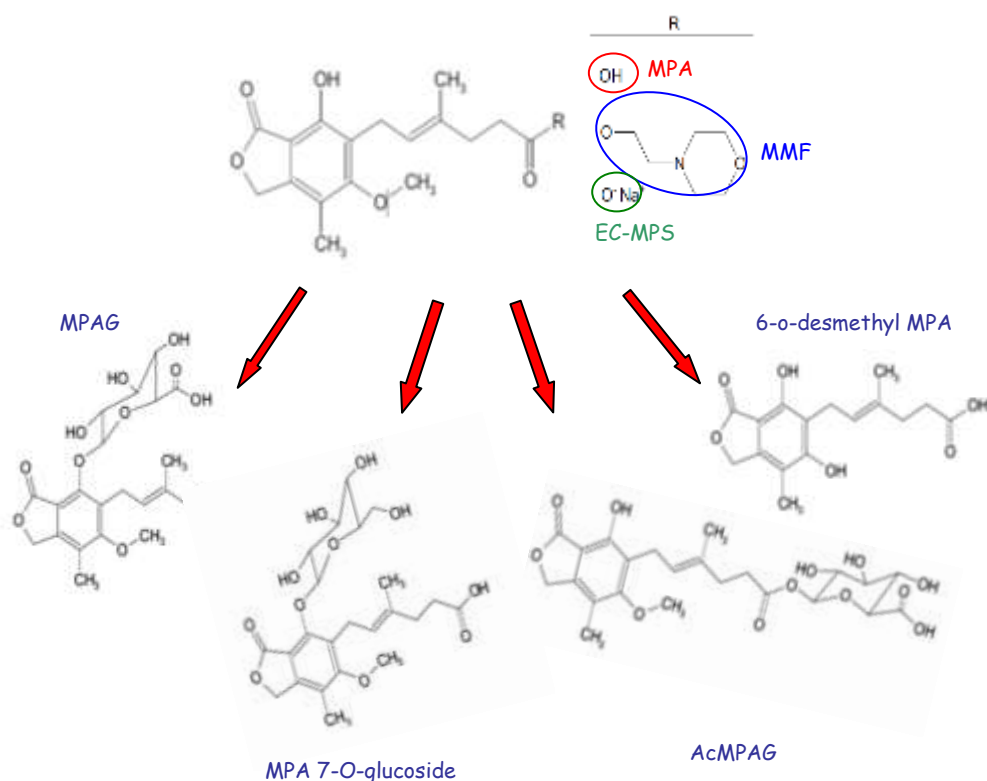


**Figure 1.1: Chemical structure of MMF, EC-MPS, MPA, and their metabolites AcMPAG, MPA 7-O-glucoside, and 6-o-desmethyl MPA.**

### 1.1.1 Metabolism

MMF and EC-MPS is rapidly hydrolyzed by esterases in the gut, blood, liver, and kidney [24]. Maximal MPA plasma concentrations ( $C_{max}$ ) are generally reached within 1-1.5 hr and 1.5-2.5 hr after oral administration of MMF and EC-MPS respectively [7]. EC-MPS is insoluble in the acidic pH of the stomach but highly soluble in the neutral pH of the intestine. This effect is responsible for later peak concentrations seen after EC-MPS administration when compared to MMF [7,25]. Following intravenous administration, MMF is also rapidly hydrolyzed to MPA with  $C_{max}$  achieved within approximately 1.58 hr and with an absorption half life of only a

few minutes [26]. The mean bioavailability of MPA is 81%-94% and 72% following administration of MMF and EC-MPS respectively [7,27], while the mean bioavailability of MPA after oral administration of MMF is estimated to be 94.1% relative to the intravenous route [28]. Trough plasma MPA concentrations are in the range of 0.3-3.4 mg/L [261]. MPA binds extensively (97-99%) to plasma albumin producing free fractions of only <3%. The free fraction of MPA is mainly responsible for the pharmacological effects of MPA [7,24,29,30].

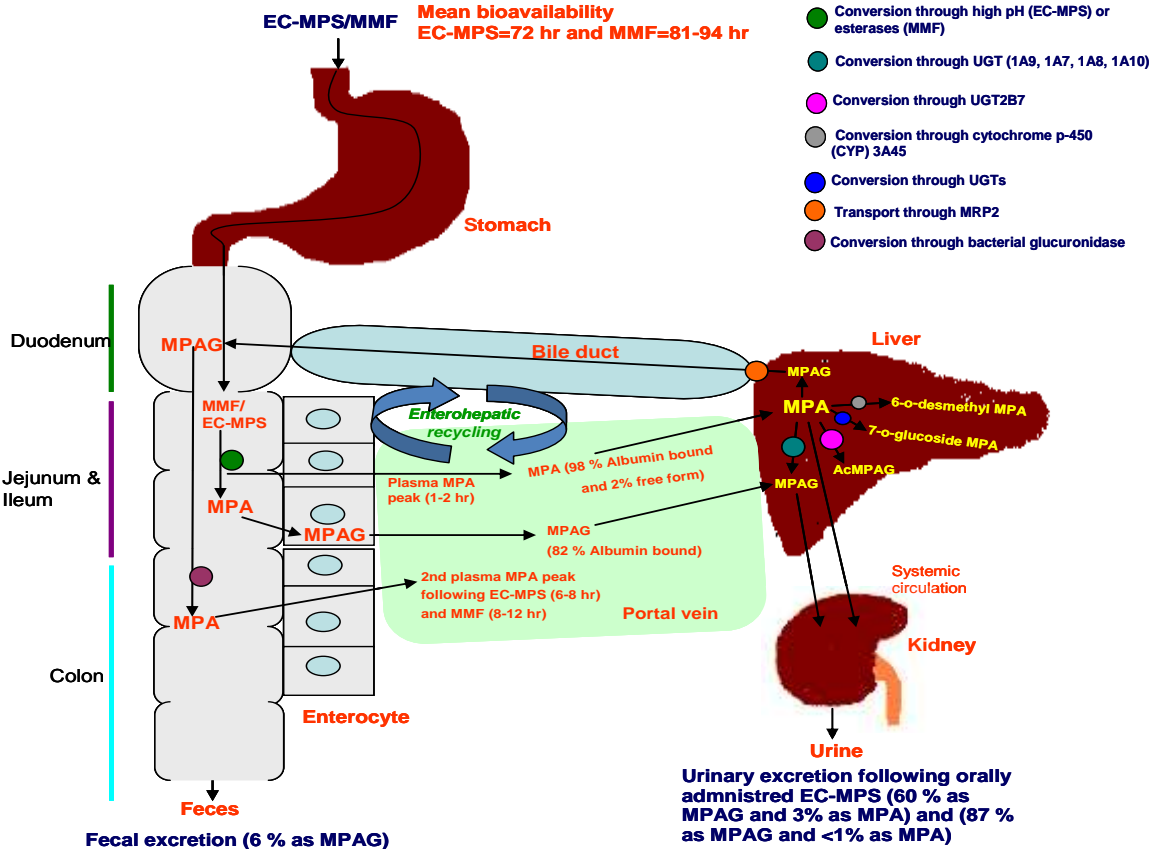


Figure 1.2: Metabolism of MPA.

MMF and EC-MPS are hydrolyzed to their active form MPA in the GI tract. MPA then absorbed and subsequently glucuronated by UGT to MPAG in the hepatocytes. In addition, other metabolites including AcMPAG, MPA 7-O-glucoside, and 6-o-desmethyl MPA are also formed. MPAG is largely excreted into urine by hOATs while some is secreted into bile by MRP, where it is then either excreted into feces or reconverted to MPA by glucuronidases present in gut bacteria and returned to the systemic circulation (enterohepatic recycling).

Like many other xenobiotics, MPA undergoes glucuronidation, which is the major pathway for phase II metabolism for xenobiotics in humans [36]. MPA is conjugated by uridine diphosphate-glucuronosyltransferase (UGT) enzymes to form MPA glucuronide (MPAG) in hepatocytes, kidneys and intestinal mucosa [30,31]. UGT 1A9, UGT1A7, 1A8 and 1A10 are mainly responsible for MPAG formation [32]. Beside MPAG, other minor metabolites of MPA, such as 7-O-glucoside and the active acyl glucuronide of MPA (AcMPAG) are formed by UGT2B7 and miscellaneous UGTs respectively [32,33]. In addition, an oxidation product 6-O-desmethyl MPA is formed by cytochrome P-450 (CYP3A4/5) [34]. The chemical structures of MPA, its pro-drugs, and metabolites are given in Figure 1.1.

MPAG does not exhibit pharmacological activity but is present in 20 to 100-fold higher concentrations than MPA in the blood [24] and achieves its  $C_{max}$  in 1 hr after the MPA  $C_{max}$  [251]. MPAG has a protein binding of 82% and has the capacity to interfere with the MPA-albumin binding. MPAG at high concentrations is known to displace MPA from its albumin binding sites, thus modulating the free fraction of MPA, which is important for the pharmacological activity of MPA [30,35].

AcMPAG, a pharmacologically active metabolite, is believed to be responsible for some of the adverse effects of MPA [33,36,37]. Acyl glucuronides are formed by esterification of carboxylic acid with glucuronic acid [36]. Such acyl glucuronides have been observed for several clinically useful therapeutic drugs including non steroidal anti-inflammatory drugs (NSAIDs) [36]. AcMPAG plasma concentrations are 10-20% of MPA concentrations [75,76]. Mean AcMPAG area under curve (AUC), over 12 hr is generally 10.3% of simultaneous MPA-AUC [75] and AcMPAG reaches its  $C_{max}$  in 1-3 hr following the  $C_{max}$  of MPA {Schutz, 2000 680 /id}.

MPA is eliminated from the body mainly through the kidneys. 93% of the orally administered dose of MMF is excreted in urine and 6% in the feces. MMF is predominantly (87%) excreted as MPAG in the urine and a small amount (<1%) as MPA. Like MMF, orally administered EC-MPS is also excreted maximally through urine, with 60% as MPAG and approximately 3% as MPA 1-7,4,8,9.

A proportion of MPAG is secreted into bile through multidrug resistant protein (MRP) transporters, specifically MRP2 [41]. MPAG then goes into the intestine where gut bacteria deglucuronidate MPAG to reform MPA, which is then reabsorbed back into systemic circulation [24,30]. This reabsorption is responsible for a second peak of MPA concentration detected in plasma 6 to 12 hr and 6 to 8 hr following oral administration of MMF and EC-MPS respectively [45]. This process is known as enterohepatic circulation and accounts for 10 to 60% of total MPA exposure [24,30,31,42]. The mean elimination half-life of MPA is 13 and 13–17 hr following oral administration of MMF and EC-MPS respectively [7,24]. The simplified overview of distribution and metabolism of MPA is shown in Figure 1.2.

### **1.1.2 Cellular and adverse effects of MPA**

MPA causes the depletion of guanosine triphosphate (GTP) pools, which is assumed to be responsible for MPA associated anti-proliferative effects *in vitro* and *in vivo* [43,44]. Nucleotide inhibition leads to G1 cell cycle arrest and thus inhibits cell growth of immune (T and B lymphocytes) and non immune cells (smooth muscle cells, endothelial cells, renal tubular and mesangial cells) in a dose-dependant manner [43,44,46-47]. MPA is also a potent anti-inflammatory agent which inhibits proliferation of immune cells, inhibits pro-inflammatory cytokines such as tumor necrosis factor alpha, interleukin 1 beta, interleukin-17, vascular endothelial growth factor alpha (VEGF- $\alpha$ ), and blocks the migration of leucocytes to inflammation sites [48,49]. MPA has promising effects in reducing myofibroblast infiltration, collagen III deposition and inhibition of the proliferation of both immune (lymphocytes) and non immune (fibroblasts, vascular smooth muscle and tubular) cells which are involved in the development of fibrosis [50-52]. MPA inhibits tumor growth and metastasis through G1-S cell cycle arrest, induction of differentiation in a variety of human tumor cell lines, induces apoptosis, as well as suppress the glycosylation and expression of several adhesion molecules (integrins, ICAM-1, VCAM-1, E-selectin and P-selectin) which promote tumor metastasis [21,53-56].



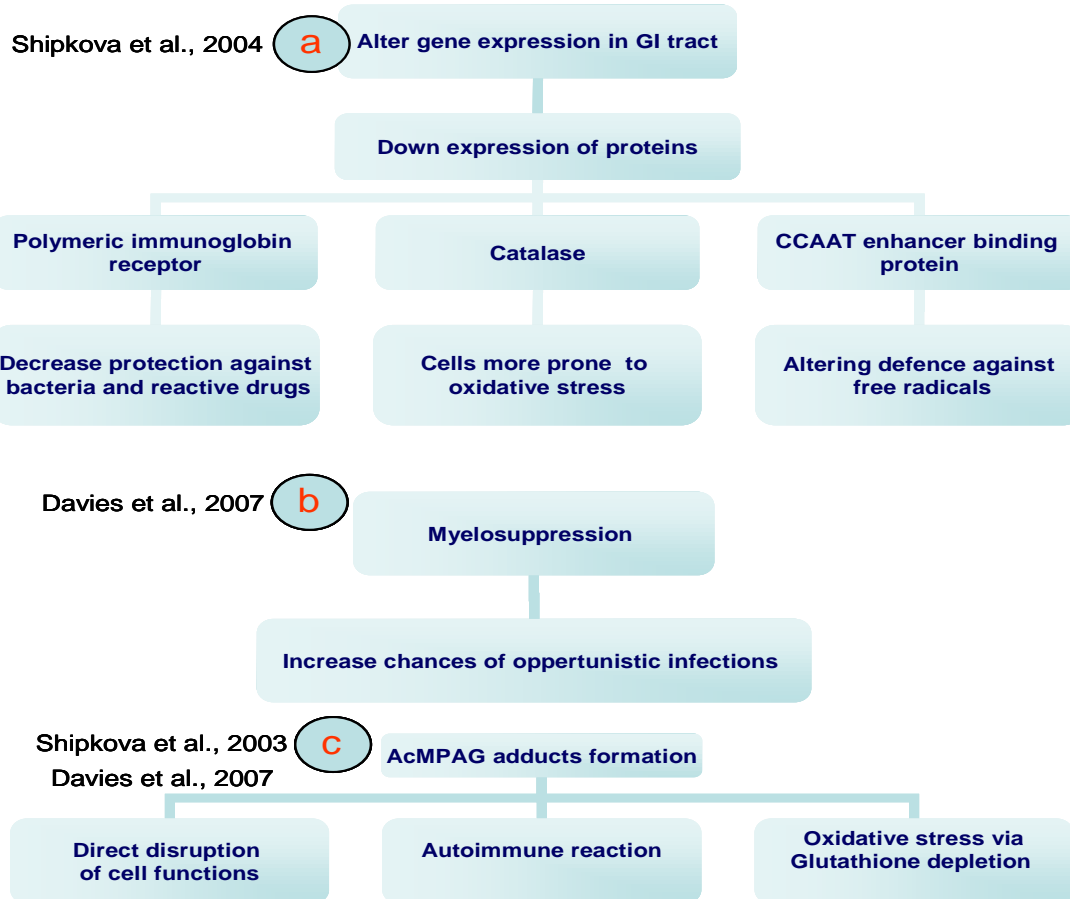


**Figure 1.3: Adverse effects of MPA.**

Various proposed mechanisms of MPA associated side effects are highlighted such as (a) alteration in gene expression making individuals more susceptible to stress [78], (b) immunosuppression leading to opportunistic infections [58], (c) AcMPAG adduct toxicity results in ultrastructural abnormalities, metabolic dysfunction, and oxidative damage [58][36].

MPA is generally a well tolerated immunosuppressive agent and produces less nephrotoxicity compared to other immunosuppressives drugs (reviewed in [57]). GI toxicity is the common adverse effect of MPA, occurs in 20% of renal patients on MMF therapy, and is dose dependant (reviewed in [57]). Symptoms of GI toxicity include diarrhea, abdominal pain, nausea, anorexia, vomiting, [58-60], gastritis, esophagitis, duodenal ulcers, colonic ulceration [60,61], and small intestinal villous atrophy [62,63]. MMF can cause enterocolitis and a Crohn's disease-like colitis syndrome [37,64,65].

In addition to GI tract symptoms MPA can cause genitourinary symptoms such as frequency, urgency, dysuria, sterile pyuria, and hematuria. These symptoms have

been reported to occur during the first year of MPA therapy (reviewed in [2,57]). In addition, MPA can also occasionally produce neurologic disturbances such as weakness, headache, tinnitus and insomnia (reviewed in [66]). Some cases of progressive multifocal leukoencephalopathy (PML) have been reported in patients on MMF therapy. These patients developed clinical features such as hemiparesis, apathy, confusion, cognitive deficiencies, and ataxia [67,68,68]. The occasional skin problems with MPA use include exanthematous eruptions, acne, pedal edema, urticaria, dishydrotic eczema, blistering hand dermatitis, and onycholysis (reviewed in [57,66]).

MPA can cause cardio-respiratory toxicity causing dyspnoea, cough, chest pain, palpitations, hypertension, acute respiratory failure, pulmonary edema, pulmonary fibrosis and pneumonitis [57,69]. Metabolic disturbances are also reported in MMF treated patients. Findings in these patients includes hypercholesterolemia, hypophosphatemia, hypokalemia, hyperkalemia, hyperglycemia (reviewed in [57,66]). There have been reports of mild, dose-related haematologic effects occurring in 5% of patients. Findings include anemia, leucopenia, and thrombocytopenia (reviewed in [2,57]). Pure red cell aplasia (PRCA) has been observed in some patients treated with MPA in combination with other immunosuppressive drugs [70]. An increased incidence of infectious complications occurs in 2% of renal and cardiac transplant patients and in 5% of hepatic transplant patients treated with MPA (reviewed in [57]). Like other immunosuppressive therapies, opportunistic infections occur in up to 40% of transplant patients given MMF (reviewed in [66,71]). Several viral, bacterial and fungal complications have been observed, including infection with *herpes simplex* virus, *herpes zoster* virus, human *herpes virus* type 6, *papillomavirus*, aspergillosis, encephalitis, *streptococcus B* septic shock, recurrent *E.coli* associated epididymitis, pediatric disseminated varicella, candidiasis, cryptococcosis, mucormycosis pneumocystis carinii pneumonia, and intestinal microsporidosis (Reviewed in [3,56,74]).

Diarrhoea is the most common GI adverse effect caused by MPA but the exact mechanism responsible for this have not yet been clearly defined [72]. Several mechanisms have been suggested to be responsible for the adverse events associated with MPA therapy including direct cytotoxic effects on GI cells, release of pro-inflammatory cytokines by AcMPAG [73,74], and formation of AcMPAG protein

adducts [75]. Covalent AcMPAG-protein adducts are formed through two pathways; transacylation and glycation. Transacylation involves direct bounding of an aglycone moiety to the proteins while the glycation mechanism involves intramolecular re-arrangement resulting in a open-chain conjugate with a free aldehyde group which binds with the amino group on various proteins [36,77].

AcMPAG adducts may cause cellular toxicity through a number of proposed mechanisms. These adducts may modify protein structure and thus interfere with normal cell function, or they may activate the immune system resulting in hypersensitivity reactions or autoimmunity. Furthermore, AcMPAG adducts cause oxidative stress via glutathione depletion [58][36]. Previously, it was demonstrated that AcMPAG forms covalent protein adducts in the kidney, liver and intestine of rats treated with MMF [76,77]. The proteins involved are associated with diverse cellular functions. Another study revealed that MMF down-regulates mRNA expression of polymeric immunoglobulin receptor (resulting in decreased protection against invading pathogens and reactive drugs), catalase (cells were more prone to oxidative stress), and CCAAT/enhancer-binding proteins (interference with the defence system against free radicals) [58,78]. The adverse effects of MPA therapy are summarized in Figure 1.3.

## **1.2 Intestinal epithelial barrier**

The mammalian intestine is lined with a single layer of specialized simple columnar epithelium that separates the intestinal lumen from the underlying lamina propria [79,80]. The intestinal lining consists of proliferative crypts, which contain intestinal stem cells, and villi, which contain differentiated specialized cell types such as the absorptive enterocytes, mucous-secreting goblet cells, and hormone-secreting enteroendocrine cells [81] (reviewed in [82]). In addition, there are Paneth cells which are differentiated cells at the bottom of crypts bottom that perform several functions including limiting gut microbial populations by secreting defensins, (antimicrobial peptides) and protecting the intestinal lining from bacterial toxins [80].

The intestinal epithelium represents the major contact between a person and their external environment and covers an extensive surface area of >300 m<sup>2</sup> [83].

Structural components of the intestinal barrier include the unstirred water layer, the hydrophobic mucosal surface, the surface mucous coat, epithelial factors (tight junctions), and endothelial factors [84]. The intestinal epithelium has two vital functions. It selectively filters, allowing the absorption of nutrients, electrolytes, and water from the intestinal lumen into the circulation while it serves as a barrier to prevent luminal pro-inflammatory factors, luminal pathogens and their antigens or toxins from invading the tissues [84-87]. In addition, the stirred water layer plays a role in transport of many nutrients and drugs, especially lipid-soluble compounds [84]. Mucus from goblet cells provides a protective layer against the physical friction, chemical digestion, and adhesion of bacteria. In addition, it also acts as a diffusion barrier [84,88]. The hydrophobicity of the mucosal surface acts as an important barrier to bacterial and other factors within the gut lumen. Many factors such as nonsteroidal anti-inflammatory drugs (NSAIDs), dextran sodium sulfate, trinitrobenzenesulfonic acid, lipopolysaccharide (LPS) and ammonium [89] can decrease this hydrophobicity.

The epithelial layer constitutes the key component of intestinal barrier. It acts as a selectively permeable filter allowing the transport of essential dietary nutrients, electrolytes, and water from the intestinal lumen into the circulation [84,90]. In addition, the intestinal epithelia controls chloride permeability which is responsible for secretion of protective fluids into the intestinal lumen which limits bacterial colonization and entry of toxins into the intestinal cells [91]. Another important function of the intestinal lining is its secretion of local immunoglobulins such as epithelial secretory immunoglobulin-A (IgA) which targets antigens at the mucosal surface, and constitutes a humoral component of the mucosal immune system [92-94].

Permeability of the intestinal epithelium is regulated via transepithelial/transcellular and paracellular pathways. Transcellular transport is an active process and involves transport of water, amino acids, electrolytes, short-chain fatty acids, and sugars across the plasma membrane by specific ion channels and transporters [15,16][95]. Paracellular transport is a passive process which involves the movement of solutes and water across the intercellular space and is regulated by intercellular complexes. Paracellular transport is determined by molecular size or the ionic charge or both and is mainly regulated by tight junctions (TJ) [95,96].

### 1.2.1 Tight junctions

Intestinal epithelial cells are connected to one another by adhesive junctional complexes which serve as a physiological and structural paracellular barrier. Components that constitute the multimolecular junctional complex include desmosomes, adherens junctions, and TJs [97,98]. TJ, the most apical component of the junctional complex are generally considered to be the major barrier to the passage of molecules between adjacent cells and through the intercellular space. The TJ barrier is not absolute but is selectively permeable and is able to discriminate between solutes on the basis of size and charge. TJ complex contains more than forty proteins, having various functions [99]. The structure of TJ was first described with the help of electron microscopy [100]. TJ consist of transmembrane proteins (JAMs, occludin and claudins), adaptors (ZO (type 1-3), MAGI (type 1-3), PAR 3/6, cingulin, PATJ and MUPP1), regulatory proteins (Rab 13, Rab 3b, G proteins, PKC, PP2A and PTEN), and both transcriptional and post-transcriptional regulators (sympleskin, ZONAB, and huASH1). All these proteins interact with each other to form a complex protein network [101,102], responsible for TJ functions including their interaction with F-actin [103]. The basic architecture of TJ is shown in Figure 1.4. All of the TJ proteins listed above play an important role in the structure and function of TJ, but only a brief description of the function of some TJ proteins ( ZO-1, occludin, and claudin), which have been extensively studied in the context of TJ disruption [104] are described below.

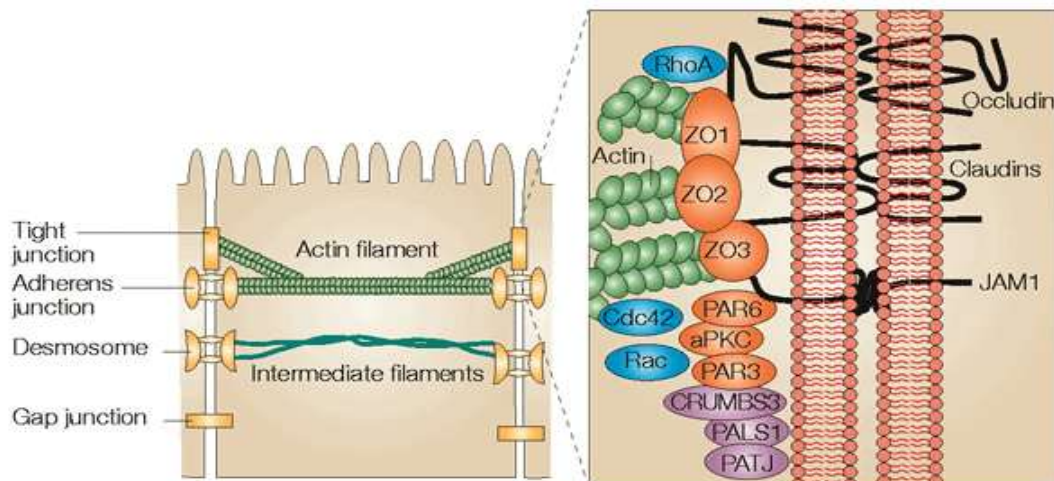
ZO, the first TJ-associated protein to be identified [105], belongs to the membrane associated guanylate kinase family (MAGUK) and contains three N-terminal PDZ repeats, an SH3 domain, and a C-terminal region homologous to guanylate kinases [106]. There are different isoforms of ZO including ZO-1, ZO-2 and ZO-3 with a variety of cellular functions. ZO-1 is a 210-225 KDa peripheral membrane protein and is a major constituent of the cytoplasmic domain of TJ. The C-terminal domain of ZO-1 interacts with other TJ proteins including claudins [107]. ZO-1 is also in close association with actin cytoskeleton responsible for linking transmembrane proteins of the TJ to the actin cytoskeleton that plays a regulatory role in TJ actions. The C-terminal portion of occludin, claudin, ZO-2, and ZO-3 interact closely with the N-terminus of ZO-1. Additionally, the C-terminal half of ZO-1

interacts with F-actin regulating cytoskeleton [107,108]. The expression and distribution of ZO proteins are regulated by myosin light chain kinase (MLCK) and their alteration can lead to defective function of epithelial barriers [109]. The down-regulation and redistribution of ZO-1 has been observed in TJ disruption conditions, such as those involving cytokines [110,111], ethanol [112] and oxidants [113].

Occludin is a 60 KDa protein and was identified as the first among transmembrane TJ proteins in 1993 [114,115]. Occludin is a member of the Marvel (MAL-related proteins for vesicle trafficking and membrane link) domain containing protein family [116]. Occludin has a tetraspan structure that constitutes its extracellular strand within TJ and amino- and carboxy-terminal chains projecting into the cytoplasm [117]. The interactions of occludin with various intracellular TJ proteins, including ZO-1, ZO-2, and ZO-3 have been well documented [118]. Occludin plays an important role in regulating TJ dynamics as demonstrated by the fact that its depletion leads to increases in the permeability of larger-sized molecules shown in both *in vitro* and *in vivo* intestinal models [119]. The down-regulation of occludin proteins, associated with increased permeability has been observed in several inflammatory bowel diseases such as Crohn's disease, ulcerative colitis, and celiac disease [120-122], as well as in animal models of inflammatory bowel disease [123,124]. It has been proposed that a decrease in intestinal occludin expression may be an important mechanism responsible for increased intestinal epithelial TJ permeability. Occludin in epithelial cells is highly phosphorylated on serine and threonine residues and its phosphorylation plays a critical role in the regulation of TJ integrity. Occludin phosphorylation is regulated by the balance between protein kinases (eg. c-Src, PKC $\zeta$ , and PKC $\mu$ 1,) and protein phosphatases (eg. PP2A, PP1, and PTP1B) [125-127]. Occludin has also been reported to be phosphorylated at tyrosine which has been proposed to be implicated in disruption of TJs by various toxins such as hydrogen peroxide and acetylaldehyde [128,129].

Claudins are 20-27 KDa integral membrane TJ proteins that contains four hydrophobic transmembrane domains which have a cytoplasmic N terminus, two extracellular loops, and a C-terminal cytoplasmic domain. The claudin family is a multigene family comprised of at least 24 members [130]. On the basis of their role in controlling permeability, claudins has been divided into two sub-categories,

paracellular barrier forming claudins and paracellular, ion permeability forming claudins. Both are vital for proper and tissue-specific functioning of the TJs; making claudins a critical player in regulation of paracellular function [131,132]. The carboxy terminus of claudins binds to PDZ domains of proteins including those of the ZO proteins [107]. In addition, interaction of claudin-1 with ZO-1 is critical for ZO-1 integration into epithelial TJs [133]. Claudin isotypes 1 to 5 are present in the intestinal cells in various intestinal regions [134,135]. Down-regulation of claudin 1 is believed to be linked to the TJ disruption in inflammatory mucosa by Crohn's disease and ulcerative colitis and is believed to be associated with enhanced paracellular permeability [136]. Claudin 4 down-regulation has also been observed in collagenous colitis, characterized by barrier defects and associated with reduced net  $\text{Na}^+$  and  $\text{Cl}^-$  absorption [137].



Nature Reviews | Microbiology

**Figure 1.4: Intestinal epithelial barrier.**

Schematic diagram of intestinal epithelial cells showing tight junctions (TJ), adherens junctions (AJs), desmosomes and gap junctions. The TJs are positioned at the most apical parts of the plasma membranes of enterocytes, whereas AJs and desmosomes are present mainly at the basal parts of the lateral membranes. TJ and AJ are linked to actin and play an important role in regulation of intestinal permeability (Left panel). The molecular components of epithelial tight junctions (TJs) are outlined (right panel), and consist of transmembrane proteins (occludin, claudins and JAMs), adaptors (ZO (1-3), PAR 6, and PATJ), regulatory proteins (Rac, cdc42, RhoA, and PKC), and other associated proteins. Occludin, claudins and JAMs are linked to the zona occludens, and they are connected to actin forming the main TJ assembly. Adopted from (Aktories K and Barbieri JT 2005, Nat Rev Microbiol) [138].

TJ defects have been described in several patho-physiological conditions such as brain diseases [139,140], pulmonary inflammation, allergic rhinitis [141], obstructive jaundice [142], kidney diseases [143,144], diabetic retinopathy [145], cancers [146], blood-borne metastases [140,147] and bowel diseases [148-150]. Intestinal epithelial barrier dysfunction is a major factor contributing to the predisposition to inflammatory diseases, including food allergy, IBD, and celiac disease. The presence of environmental factors in the intestinal lumen and inappropriate host immune responses are key determinants of the development of IBD [87,148]. In IBD, epithelial barrier function is impaired leading to either diarrhoea because of a leaky flux mechanism or translocation of toxins and macromolecules into intestinal cells causing associated dysfunction [151].

### **1.2.2 Factors modulating intestinal permeability**

Several endogenous molecules such as glucose [153], hormones [154], nucleotides [155], and growth factors [156-158] provide physiological modulation of TJ permeability. In addition, a growing list of pathological agents has been suggested as etiologic factors in several diseases as a result of causing increased mucosal permeability [159]. Dietary components are crucial in the regulation of barrier integrity (reviewed in [160]). Gliadin, a glycoprotein present in wheat, is the key factor in the pathogenesis of celiac disease and is responsible for TJ disruption leading to increased permeability [161]. Several dietary components have been found to increase TJ permeability including: cayenne pepper (*Capsicum frutescens*), paprika (*Capsicum anuum*), galangal (*Alpinia officinarum*), marigold (*Tagetes erecta*), Acer nikoense, and hops (*Humulus lupulus*) (reviewed in [160]). In contrast, black pepper (*Piper nigrum*), green pepper, nutmeg, bay leaf extracts, linden (*Tilia vulgaris*), star anise (*Illicium anisatum*), Arenga engleri, and black tea (*Camellia sinensis*) have been found to decrease paracellular flux and increase transepithelial resistance (TER) (reviewed in [160]).

Pro-inflammatory cytokines have also been proposed as pathophysiological stimuli which trigger several cellular pathways leading to pathological conditions including bowel diseases [110,111,162-166]. For example, TNF $\alpha$  modulates epithelial barrier properties and has a critical role in IBDs [167] and graft-versus-host disease [152]. TNF $\alpha$  up-regulates MLCK which acts as the central player in TNF $\alpha$  induced



barrier loss, both *in vitro* [168] and *in vivo* [150,169]. Additionally, TNF $\alpha$  has also been shown to be involved in the down regulation of apical Na<sup>+</sup>-H<sup>+</sup> exchange, which then is linked to the development of diarrhoea [169,170]. Mast cells (MC) have been reported to regulate intestinal permeability, as suggested by the fact that their degranulation results in blood flow modulation, as well as increased epithelial and endothelial permeability, mucosal secretion, gastrointestinal tract motility, immunologic reactions, and angiogenesis (reviewed in [84] ). Several physiological and pathological conditions have been reported to be associated with MC mediated intestinal permeability including food allergy, irritable bowel syndrome, and after stressful conditions [171,172]. Intracellular mediators including nitric oxide (NO) regulate barrier properties by altering the function of epithelial cells and the GI microcirculation [173]. The activity and synthesis of NO is increased by endotoxin (LPS), cytokines, and ethanol (EtOH), which results in barrier dysfunction via protein oxidation, nitration, S-nitrosylation, cGMP activation, and cellular energy depletion (reviewed in [84]).

Epithelial-microbe interactions are responsible for alterations in the structure and function of the epithelial barrier, regulation of fluid and electrolyte secretion, and modulation of inflammatory signalling (reviewed in [174]). More than 400 microbial species that have a profound impact on gut physiology reside in the gastrointestinal lumen [80]. Pathogenic bacteria, such as *Escherichia coli*, *Klebsiella pneumoniae*, *Streptococcus viridans*, *Clostridium difficile*, *Bacteroides fragilis*, *Vibrio cholerae*, and *Helicobacter pylori*, as well as viruses and parasites (*giardia*) can disrupt the intestinal barrier (reviewed in [84]). Beneficial bacteria:however, such as *Lactobacillus brevis* maintain TJ and reduce intestinal permeability [175]. Psychological stress is another factor responsible for alterations in epithelial barrier physiology (reviewed in [84]). Various parts of brain, brain stem, various CNS afferents, and the neuro-endocrinal system are proposed to be involved in the stress response. During psychological stress corticotrophin-releasing factor (CRF) is released, which triggers the enteric nervous system that causes alterations in gut motility, exocrine and endocrine functions, and the microcirculation (reviewed in [176]). Oxidative stress is caused largely by reactive oxygen (ROS) species such as hydrogen peroxide (H<sub>2</sub>O<sub>2</sub>), nitric oxide, peroxy nitrite and hypochlorous acid which disrupt the epithelial and endothelial barrier function by destabilizing TJs [177].

### 1.2.3 Regulation of TJ structure and function

Regulation of the assembly, disassembly, and maintenance of TJ structure is highly dynamic and is influenced by diverse protein-protein interactions that respond to both extra-cellular and intra-cellular physiological, pharmacological, and pathophysiological stimuli. TJ regulation is controlled by several signalling proteins, including tyrosine kinase,  $Ca^{+2}$ , phospholipase C (PLC), protein kinase C (PKC), calmodulin, mitogen-activated protein kinase (MAPK), MLCK, the Rho family of small GTPases, adenosine, 3',5'-cyclic monophosphate ( $cAMP$ ), and heterotrimeric G proteins [178-182]. Actin has a vital role in the structure and function of TJ. Multiple TJ components interact with the actin cytoskeleton and regulate the permeability of TJs [183,184]. Reorganization of the actin cytoskeleton as a result of interactions between transmembrane proteins and the actomyosin ring [178,183,185,186] and as well as the phosphorylation state of TJ proteins are both critically involved in alterations in TJ physiology [187,188]. Members of the Rho family GTPase (Rac, Rho, and Cdc42) have also been shown to be able to reorganize the actin cytoskeleton and modulate TJ physiology [179,189-191]. Changes in the phosphorylation status of TJ proteins such as ZO, occludin, E-cadherin,  $\beta$ -catenin, and claudins act as a molecular switch that regulates TJ structure and function [125,187,188,192,193].

MLC phosphorylation is an important regulator of barrier function in health and disease [194]. Increased MLC phosphorylation leads to the rearrangement of TJ proteins (ZO-1, occludin, claudin-1 and claudin-4), disruption of perijunctional F-actin, and increases TJ permeability [103,184]. The main pathways associated with MLC phosphorylation are controlled either directly by MLCK activity or indirectly by Rho kinase mediated inhibition of phosphatase [182]. MLCK mediated MLC phosphorylation is sufficient to trigger downstream events necessary for barrier regulation and has a central role in many diseases that are characterized by intestinal barrier dysfunction (reviewed in [170]). Increased MLCK expression or activity has been observed in GI pathology following TNF  $\alpha$  [169], interleukin  $1\beta$  [195,196], lipopolysaccharide [197], and ethanol [112,198] exposure. Similar increased MLCK activity is observed after exposure to virulence factors associated with GI infections with Enteropathogenic *Escherichia coli* (EPEC) [199,200] and

*Helicobacter pylori* [201,202], as well as parasitic diseases like giardiasis [203]. The role of Rho family of small GTPases has been described in the regulation of TJ structure and function including the perijunctional actomyosin ring [194,204]. ROCKs regulate the phosphorylation of MLC by inactivating MLCP (myosin light chain phosphatase), which is involved in decreasing MLC phosphorylation [191]. ROCK inhibition causes the redistribution of F-actin structures and modulates TJ permeability. In addition, ROCK co-localizes with the ZO-1 and its inhibition prevents proper localization of TJ proteins during TJ assembly [204].

PKC is an important member of the serine-threonine kinases family which regulate epithelial barrier structure and function. PKC modulates the expression of subcellular localization and phosphorylation states of TJ proteins which alters barrier dynamics [206]. PKC proteins are also involved in various signal transduction pathways such as the Toll-like receptor 2 (TLR2) pathway. Activation by PKC isoforms results in increases in TER and redistribution of ZO-1 (reviewed in [160]). PKC also interacts with MLCK. PKC phosphorylates MLCK which leads to decreases in MLC phosphorylation, reduces tension on the perijunctional actomyosin ring (PAMR), and increases permeability [207]. The MAPK pathway is a major intracellular signalling pathway involved in cell growth, differentiation, and TJ regulation [208]. Several growth factors, cytokines, and oxidative stresses are involved in the stimulation of the MAPK pathway (reviewed in [160,209]). Members of MAPK have been implicated in modulation of TJ structure and function since extracellular signal regulated kinases (ERK) interact directly with the C-terminal region of occludin to prevent H<sub>2</sub>O<sub>2</sub>-induced disruption of TJ [208].

#### **1.2.4 Caco-2 cells as an *in vitro* model for intestinal epithelial integrity**

A number of both *in vitro* and *in vivo* experimental models are being used to study the integrity of TJs [210-213][214,215]. Caco-2 is one of the most widely used intestine cell models for *in vitro* studies of intestinal barrier functions [211,216,217], intestinal absorption, and toxicity of xenobiotics [216-218]. Caco-2 cells were first generated from the differentiated colon adenocarcinoma of a 72-year old patient

[219]. Caco-2 cells grown in culture usually reach confluency within 3-6 days, a stationary growth phase after 10 days [220], and complete their differentiation within 20 days [221]. Once differentiated these cells exhibit properties similar to enterocytes both structurally, bio-chemically, and functionally including having microvilli, intercellular junctions, nutrient transporters, efflux transporters, and enzymes (alkaline phosphatase, sucrase isomaltase and aminopeptidase) [222,223]. Caco-2 cells also express various transport and metabolizing enzymes such as cytochrome P450 isoforms and UDP-glucuronosyltransferases, sulfotransferases and glutathione-S-transferases [224,225]. Although, most Caco-2 properties resemble those of enterocytes, some differ. Caco-2 cells lack the crypt-villus axis (which is important for *in vivo* transport) and mucus producing goblet cells (leading to a lack of prominent mucus layers [226-228]).

Transepithelial electrical resistance (TER) and paracellular permeability to tracers molecules are two parameters that are commonly used to investigate the integrity and function of the TJ in *in vitro* models such as Caco-2 monolayers [213,229-232]. Usually, TJ barriers limit the ionic diffusion through cell monolayers, which creates a potential difference that is measured as transpithelial resistance (TER). TER has a direct relationship with TJ integrity. The greater the TER, the more intact the TJ [223,233,234]. Paracellular permeability of tracers in cell layers is measured by the diffusion rate of such tracers from apical to basal or vice versa. Paracellular flux is inversely related to TJ integrity (ie. increased paracellular flux suggests TJ disruption [213,233]). A variety of paracellular flux markers are used to investigate the effects of physiological and pathological agents on TJ integrity. The most frequently used paracellular markers include polyethylene glycols (PEG), fluorescein-5 and -6 sulfonic acid [235], inulin [119,236,237], fluorescein isothiocyanate dextrans (FITC-dextran), urea, mannitol, L-glucose [119,237], raffinose [238], atenolol [239] and lucifer yellow [240]. Size, shape, and charge of the solutes used control the permeability properties of any particular paracellular marker [233,241].

### **1.3 Rationale for the proposed research**

Mycophenolic acid is a frequently used immunosuppressive agent and has a wide range of pharmacological actions. The present study was undertaken to identify novel molecular targets of MPA using a comprehensive 2-DE based expression proteomics approach. Whole cell lysates from HEK-293 cells which had been exposed to MPA were resolved by 2-DE, and differentially expressed proteins were identified by QTOF MS/MS analysis. In an attempt to examine effects with possible clinical relevance on a regulated protein, myosin light chain 2 (MLC2), we investigated the effects of MPA on TJ integrity using Caco-2 monolayers as a colonic cell culture model. After employing various physiological assays as well as immunoblotting and immunofluorescence analyses, we found that exposure to therapeutic concentrations of MPA modulated tight junction physiology via MLC2 phosphorylation. The current study may help to understand the etiology of MPA associated adverse intestinal effects.

## **2. Differential proteome analysis of human embryonic kidney cell line (HEK-293) following mycophenolic acid treatment**

Muhammad Qasim<sup>1,2</sup>, Hazir Rahman<sup>1,2</sup>, Michael Oellerich<sup>1</sup>, Abdul R. Asif<sup>1</sup>

1. Department of Clinical Chemistry, University Medical Centre Goettingen, 37075, Goettingen, Germany.

2. Department of Microbiology, Kohat University of Science and Technology, 26000, Kohat, Pakistan.

Published in "*Proteome Science* 2011, **9**:57

## 2.1 Abstract

Mycophenolic acid (MPA) is widely used as a post transplantation medicine to prevent acute organ rejection. In the present study we used proteomics approach to identify proteome alterations in human embryonic kidney cells (HEK-293) after treatment with therapeutic dose of MPA. Following 72 hours MPA treatment, total protein lysates were prepared, resolved by two dimensional gel electrophoresis and differentially expressed proteins were identified by QTOF-MS/MS analysis. Expressional regulations of selected proteins were further validated by real time PCR and Western blotting. The proliferation assay demonstrated that therapeutic MPA concentration causes a dose dependent inhibition of HEK-293 cell proliferation. A significant apoptosis was observed after MPA treatment, as revealed by caspase 3 activity. Proteome analysis showed a total of 12 protein spots exhibiting differential expression after incubation with MPA, of which 7 proteins (complement component 1 Q subcomponent-binding protein, electron transfer flavoprotein subunit beta, cytochrome b-c1 complex subunit, peroxiredoxin 1, thioredoxin domain-containing protein 12, myosin regulatory light chain 2, and profilin 1) showed significant increase in their expression. The expression of 5 proteins (protein SET, stathmin, 40S ribosomal protein S12, histone H2B type 1 A, and histone H2B type 1-C/E/F/G/I) were down-regulated. MPA mainly altered the proteins associated with the cytoskeleton (26%), chromatin structure/dynamics (17%) and energy production/conversion (17%). Both real time PCR and Western blotting confirmed the regulation of myosin regulatory light chain 2 and peroxiredoxin 1 by MPA treatment. Furthermore, HT-29 cells treated with MPA and total kidney cell lysate from MMF treated rats showed similar increased expression of myosin regulatory light chain 2. The emerging use of MPA in diverse pathophysiological conditions demands in-depth studies to understand molecular basis of its therapeutic response. The present study identifies the myosin regulatory light chain 2 and peroxiredoxin 1 along with 10 other proteins showing significant regulation by MPA. Further characterization of these proteins may help to understand the diverse cellular effects of MPA in addition to its immunosuppressive activity.

## 2.2 Introduction

Mycophenolic acid (MPA) is a frequently used immunosuppressant for the prevention of acute rejection in patients undergoing allogeneic renal, cardiac, lung, and liver transplantations [4,10]. MPA is a selective, reversible and uncompetitive inhibitor of inosine monophosphate dehydrogenase (IMPDH), a key regulatory enzyme in the *de novo* pathway of purine synthesis. It exhibits cytotoxic effects on most of the cell types, but exerts greater effects on T and B lymphocytes, thus preventing solid organ rejection [4]. IMPDH inhibition by clinically relevant concentration of MPA results in guanine nucleotide depletion which is associated with G1 cell cycle arrest. MPA also triggers apoptosis by up-regulating pro-apoptotic proteins (p53, p21 and bax) and down-regulating proteins that are important for cell cycle progression, such as bcl-2, survivin p27 and c-myc [242]. IMPDH type II is significantly over-expressed in several tumor cells, for this reason IMPDH could be considered as a potent target for anti-cancer therapy, as well as immunosuppressive chemotherapy [243].

MPA and its metabolites effect most of the cellular functions by influencing biological pathways, like apoptosis [244], immune associated signaling [245] and general cell signaling pathways involving mitogen-activated protein kinases, extracellular-signal regulated kinases, c-Jun N-terminal kinases, p53 and Rho-associated protein kinase [244,246,247]. Collectively, MPA possesses anti-microbial, anti-inflammatory, anti-fibrotic, pro-apoptotic [4], anti-angiogenic, anti-cancerous [248] and anti-oxidant activities [249]. Due to MPA diverse therapeutic activities in the cell, it is also used for the treatment of dermatological diseases, neuromuscular diseases and autoimmune disorders such as lupus [248,250]. Gastrointestinal tract (GIT) complications i.e., diarrhoea, nausea, abdominal pain, vomiting, anorexia, gastritis, intestinal ulceration and small intestinal villous atrophy are common complication for some transplant patients on MPA therapy. Other MPA associated adverse effects are anemia, myelosuppression and risk of opportunistic infections [251]. The exact molecular mechanism of MPA organ toxicity is unknown, but possible mechanisms include direct toxicity by its anti-proliferative effect, opportunistic infections due to myelosuppression and toxicity, and acyl MPA glucuronide (AcMPAG) proteins adduct formation [36,251].



Here we use HEK-293 cell line to uncover cellular protein response to the exposure of clinical dose of MPA. In the present study we used a proteomics based approach to resolve proteins of total cell lysates on two dimensional electrophoresis (2-DE) gels following treatment with DMSO and MPA. The differentially expressed proteins were in-gel tryptic digested and identified by QTOF-MS/MS analysis. Several proteins were identified with modified expression in response to MPA treatment which might be helpful to broaden our understanding regarding the cellular effects of MPA.

## **2.3 Materials and methods**

### **2.3.1 Reagents**

Cell culture media (DMEM and MacCoy's), fetal calf serum (FCS), phosphate buffer saline (PBS), penicillin and streptomycin were purchased from PAA Laboratories, Colbe, Germany. Urea, thiourea, dithiothreitol (DTT), trypsin, trifluoroacetic acid (TFA), sodium carbonate, ammonium bicarbonate, MPA and DMSO were purchased from Sigma-Aldrich, Steiheim, Germany. Acetonitril (ACN) was obtained from Promochem, Wasel, Germany. CHAPS was obtained from AppliChem, Darmstadt, Germany. Ampholytes, protein assay kit and immobilised pH gradient strips (IPG strips) were procured from Bio-Rad, Munich, Germany, while protease and phosphatase inhibitor cocktails were purchased from Roche, Mannheim, Germany. Bromophenol blue and trizma base were obtained from Carl Roth, Karlsruhe, Germany. Sodium dodecyl sulfate (SDS) was obtained from Serva, Heidelberg, Germany. Glycerin, potassium ferricyanide and sodium thiosulfate were purchased from Merck, Darmstadt, Germany and formic acid from BASF, Ludwigshafen, Germany.

### **2.3.2 Cell culture**

HEK-293 and HT-29 cell lines were purchased from German collection of microorganisms and cell cultures (DSMZ), Braunschweig, Germany. The cells were

grown in 75 cm<sup>2</sup> culture flasks (Sarstedt, Nuemberecht, Germany) and maintained in culture at 37°C in 95% humidity, 20% O<sub>2</sub> and 5% CO<sub>2</sub>. DMEM and MacCoy's media supplemented with L-glutamine, 10% fetal calf serum, 100 U/mL penicillin, and 0.1 mg/mL streptomycin was used to grow HEK-293 and HT-29 cells respectively.

### **2.3.3 Proliferation assay**

Briefly, cells were grown in 96 well plates at a density of 3.5 X 10<sup>4</sup> cells/well at least 24 h prior to the start of the experiment. The cells were then incubated with DMSO (control) or 0 to 100 µmol/L MPA for a period of 72 hr. After completion of incubation, proliferation was determined using ELISA based BrdU cell assay (Roche Diagnostics) according to manufacturer's recommendations. Four independent experiments were performed. IC<sub>50</sub> values were calculated by a Grafit software package, version 5 (Erithacus Software, London, UK).

### **2.3.4 Sample preparation for proteome analysis**

The HEK-293 and HT-29 cells were grown for 24 hr followed by treatment with DMSO or MPA (7.5 µmol/L and 10 µmol/L for HEK-293 and HT-29 respectively) for 72 h. Cells were harvested by scraping and were washed three times with ice cold PBS. After washing, cells were pelleted down at 250 x g for 10 min and lysed in a buffer containing 7 mol/L urea, 2 mol/L thiourea, 4% w/v CHAPS, 2% ampholyte pH 3-10 and 1% DTT. The lysates were centrifuged and protein content was measured by Bradford assay [252] using Bio-Rad protein reagent (Bio-Rad, Munich, Germany) according to manufacturer's instructions. Sample aliquots were kept at -80°C until further use. Protein lysate was prepared from 21 days MMF treated adult female Wistar rat's kidney according to the previously reported protocol [253] and were used for Westernblotting.

### **2.3.5 2-DE**

The 2-DE was performed as described by Gorg et al 2000 [254] with some minor modifications. Protein samples of HEK-293 cell (110 µg) were mixed with rehydration buffer (7 mol/L urea, 2 mol/L thiourea, 4% CHAPS, 0.2% ampholyte [pH 3-10], and 0.2% DTT) containing trace amount of bromophenol blue to a total volume of 350 µL. Samples were applied to linear IPG strips [pH 3-10], Bio- Rad) for 1 hr and then covered with mineral oil for passive rehydration overnight at room temperature. Iso-electric focusing (IEF) was performed in Protean IEF cell (Bio-Rad) with a program of 1 h at 100 volts, 1 h at 500 volts, 2 hr at 1000 volts and 8000 volts with a total of 32000 volts-hr. For the second dimension electrophoretic separation, focused strips were equilibrated for 30 min at room temperature in a buffer containing 50 mmol/L Tris-HCL [pH 8.8], 6 mol/L urea, 30% v/v glycerol, 2% SDS and 10 g/L DTT followed by an identical incubation but replacing DTT with 40 g/L iodoacetamide. The proteins in the equilibrated strips were then resolved on the 12.5% SDS-PAGE in a Protean II chamber (Bio-Rad) at 100 V /4°C.

### **2.3.6 Protein visualization, densitometric analysis and in-gel digestion**

Gels were silver stained as described by Blum et al 1987 [255]. After fixation, gels were washed and sensitized. The gels were then incubated in freshly prepared silver nitrate solution (0.2% silver nitrate and 0.026% formaldehyde) for 20 min at room temperature followed by 3 times washes of 20 sec each in distilled water. Gels were placed in developing solution (6% sodium carbonate, 0.018526% formaldehyde and 6% sodium thiosulfate) until standard marker stained completely and adequate spots were visualized. Gels were scanned with a gel Cano scan 8400 (Canon, Tokyo, Japan). Densitometric analysis was done by using Delta 2D software version 3.6 (Decodon GmbH, Gerifswald, Germany) [256]. Spot intensities were first normalized and the relative intensity of each spot was calculated by dividing the intensity of each spot by the sum of all spots intensities on the corresponding gel. Fold change, SD and Student's t test probability were calculated using Microsoft excel software. Spots having at least 1.5 fold expressional changes ( $p < 0.05$ ) were

considered statistically significant. Four independent 2-DE experiments were performed.

Differentially regulated protein spots were excised from the silver stained gel with a clean scalpel blade followed by in-gel digestion according to the method adopted and modified from Shevchenko et al [257]. Briefly, the gel pieces were washed twice in 100 mmol/L ammonium bicarbonate/acetonitrile (1:1, v/v) initially for 10 min and then until all visible dye was removed. The gel pieces were dried using vacuum centrifuge (UNIVAPO 150 H; uniEquip, Matinsried, Germany) followed by reconstitution in the trypsin digestion solution (10 ng/ $\mu$ L in 100 mmol/L ammonium bicarbonate) overnight at 37°C. After incubation the supernatant containing digested peptides was transferred to a tube and 50  $\mu$ L of 0.1% TFA was added followed by sonication for 30 min. After sonication, the supernatant was pooled with the previous one. Two further extractions were collected in the same way using 0.1% TFA in 30% and then 60% ACN. The pooled extracts of peptides were dried in vacuum centrifuge and reconstituted in 0.1% formic acid.

### **2.3.7 Q-TOF LC-MS/MS analysis of protein identification**

The reconstituted peptide samples (1  $\mu$ L) were introduced onto  $\mu$ -precolum<sup>TM</sup> cartridge (C18 pepMap; 300  $\mu$ m x 5 mm; 5  $\mu$ m particle size) and further separated through a C18 pepMap 100 nano- Series<sup>TM</sup> (75  $\mu$ m x 15 cm; 3  $\mu$ m particle size) analytical column (LC Packings, Germering, Germany) using an CapLC autosampler (Waters, Eschborn, Germany). The mobile phase consisted of solution A (0.1% formic acid prepared in 5% ACN) and solution B (0.1% formic acid prepared in 95% ACN). The sample run time was set to 60 min and the flow rate of the pump to 5  $\mu$ L/min. The exponential gradient was initiated at 5 min after loading from 10% to 95% for the period of 50 min. Tip flow rate of 250 nL/min was achieved through a flow splitter. The eluted peptides were injected into a Q-TOF Ultima Global (Micromass, Manchester, UK) mass spectrometer equipped with a nanoflow ESI Z-spray source in positive ion mode. Data was acquired by MassLynx (v 4.0) software and peak list (pkl file) was generated from acquired MS/MS raw data using ProteinLynx Global Server bioinformatics tool (PLGS; v 2.2; Waters, Manchester,

U.K.) under the following settings; Electrospray, centroid 80% with minimum peak width 4 channel, noise reduction 10%, Savitzky-Golay, MSMS, medium deisotoping with 3% threshold, no noise reduction and no smoothing.

The generated pkl files were searched using the online MASCOT (<http://www.matrixscience.com>) algorithm against the SwissProt data base release 15.5 (515203 sequence entries, 181334896 elements). The search criteria was set as follows: enzyme, trypsin; allowance of up to one missed cleavage peptide; mass tolerance  $\pm 0.5$  Da and MS/MS tolerance  $\pm 0.5$  Da; modifications of cysteine carboamidomethylation and methionine oxidation. Proteins were finally identified on the basis of two or more peptides, whose ion scores exceeded the threshold,  $P < 0.05$ , which indicated the 95% confidence level for these matched peptides. To ensure accurate identification, protein spots were digested from more than two gels and analyzed with MS. Proteins were considered as identified if the threshold was exceeded and the protein spot possessed the correct molecular weight and pI value of the corresponding spot on 2-DE.

### **2.3.8 Functional classification**

Biological function annotations for all of the identified proteins were done by KOGnitor (<http://www.ncbi.nlm.nih.gov/COG/grace/kognitor.html>) [258].

### **2.3.9 Western blotting**

Proteins were separated on 12.5% SDS-PAGE and blotted onto PVDF membrane (ImmobilonP, Millipore) using semidry Trans-Blot<sup>®</sup> SD cell system (Bio-Rad, Munich, Germany) for 30 min at 15 V in a blotting buffer (192 mmol/L glycine, 20% methanol, 25 mmol/L Tris [pH 8.3]). The membranes were blocked with 5% (w/v) skimmed milk repared in TBS-T buffer (50 mmol/L Tris-HCl [pH 7.5], 200 mmol/L NaCl, 0.05% Tween 20) for 1 hr at room temperature and washed twice with TBS-T buffer. The membranes were incubated with 1:1000 mouse anti Prdx1 antibody (Abcam, Cambridge, MA), 1:1000 rabbit anti MLC2 (Cell Signaling Technology, Inc., Danvers, MA) and 1:1000 mouse anti beta tubulin (Biovender,

Czech Republic) overnight at 4°C, followed by washes with TBS-T buffer. Membranes were further incubated with appropriate HRP-conjugated secondary antibodies for 1 hr at room temperature. The signals on the blots were detected by using ECL system (GE Healthcare) according to manufacturer's instructions. Signal intensities from each Western blot were quantified by using Lab Image software, version 2.71 (Leipzig, Germany).  $\beta$  tubulin was used as a loading control and at least four independent experiments were performed.

### **2.3.10 RNA isolation and cDNA synthesis**

RNA was extracted using Trizol reagent (Invitrogen, Carlsbad, CA) according to manufacturer's recommendations. Briefly, cells were scraped, washed and then homogenized in Trizol reagent. RNA was separated by chloroform/isopropanol precipitation method. The concentration of RNA was determined by the GeneQuant II RNA/DNA calculator (Pharmacia Biotech, Freiburg, Germany). The RNA quality was verified at OD<sub>260</sub>/OD<sub>280</sub> nm ratios and subsequent electrophoretically on 1% agarose gels using ethidium bromide staining. The cDNAs were synthesized from 2  $\mu$ g total RNA in a 30  $\mu$ L reaction mix containing 1X reverse transcriptase (RT) PCR buffer (10 mmol/L Tris-HCL [pH 8.3], 15 mmol/L KCl, 0.6 mmol/L MgCl<sub>2</sub>), 0.5 mmol/L of dNTPs mix, 1 U/ $\mu$ L RNase inhibitor and 13.3 U/ $\mu$ L M-MLV RT enzyme. The RT reaction was performed in a thermocycler (Biometra, Goettingen, Germany) at 42°C for 1 hr. cDNA was stored at -70°C until use.

### **2.3.11 Real-time PCR**

Relative quantitative PCR were carried out using the LightCycler instrument (Roche Diagnostic Systems, NJ, USA). The primers for the human Prdx1 (forward 5'-TGGGGTCTTAAAGGCTGATG-3' and reverse 5'-TCCCCATGTTTGTCAGTGAA -3'), human MLC2 (forward 5'- CAGGAGTTCAAAGAGGCCTTCAAC -3' and reverse 5'-CTGTACAGCTCATCCACTTCCTCA -3') and elongation factor 2 (forward 5'-GACATCACCAAGGGTGTGCAG-3' and reverse 5'-GCGGTCAGCACACTGGCATA-3) were designed by the Primer3 software (<http://frodo.wi.mit.edu>) [259]. The total volume of 20  $\mu$ L PCR contained 1  $\mu$ L of cDNA solution, 2  $\mu$ L of 10X PCR buffer

(Invitrogen), 2  $\mu$ L Syber green, 1  $\mu$ L BSA, 1  $\mu$ L DMSO, 0.25  $\mu$ L of each primer (Eurofins MWG-Biotech, Ebersberg, Germany), 2.0 mmol/L  $MgCl_2$ , 0.2 mmol/L dNTPs mix and 0.15 U/ $\mu$ L PAN Script DNA polymerase (PAN Biotech, Aidenbach, Germany). The amplification conditions for Prdx1 and MLC2 were: initial denaturation 30 sec at 95°C and repeated cycles of denaturation (95°C for 1 sec), primer annealing (55°C for 5 sec), elongation (72°C for 10 sec), and fluorescence reading at 82 °C. For elongation factor 2 (EF-2) PCR conditions were similar to Prdx1 except for primer fluorescence reading which was measured at 88°C.

The relative expression of Prdx1 and MLC2 mRNA in the treated samples was determined as a fold increase compared with control samples using the comparative threshold cycle ( $C_T$ ) method  $2^{-\Delta\Delta C_T}$  ( $\Delta\Delta C_T = \Delta C_{\text{target genes}} - \Delta C_{\text{reference gene}}$ ) [260]. EF-2 was used as the internal control gene. Experiments were performed four times. Statistical difference (p value) in mRNA expression level between MPA and DMSO samples were calculated using the Mann-Whitney U test. The PCR product was run on a 1% ethidium bromide-agarose gel to confirm the presence of desired specific amplified product.

### **2.3.12 Apoptosis assay**

The caspase 3 activity was measured using CaspACE™ Assay kit (Promega Corporation, WI, USA) according to the manufacturer's protocol. Cells were treated with DMSO and MPA for 72 hr, harvested and briefly suspended in lysis buffer. Proteins were extracted and quantified by Bradford method [252]. Briefly, 70  $\mu$ g of protein lysate were mixed with reaction mixtures containing colorimetric substrate peptides specific for caspase 3 (DEVD-pNA) and then incubated at room temperature for overnight. The absorbance of the cleaved *p*-nitroanilide from the substrate DEVD-pNA was measured at 405 nm using EL808 microplate reader (Bio-Tek instruments, VT, USA). Five independent experiments were performed.

## 2.4 Results

In the present study the alteration in the cellular proteome by the MPA treatment was investigated using HEK-293 as cell culture model. Incubation of HEK-293 cells with MPA followed a dose dependent inhibition of cell proliferation (Figure 2.1). The  $IC_{50}$  concentration (7.5  $\mu$ mol/L or 2.4 mg/L) of MPA was selected as standard dose for further analysis, which is within the therapeutic range (0.3 to 3.4 mg/L) [261]. Cells were treated with MPA and DMSO (as vehicle) for 3 days, and total cell lysates were prepared. Total protein extracts of MPA and DMSO treated cells were separated by 2-DE using pH 3-10 linear IPG strips and visualized by silver stain. The protein spots which showed  $\geq \pm 1.5$  fold change ( $p < 0.05$  using Student's t test) as compared to DMSO treated controls were considered as differentially expressed proteins. Statistical analysis showed that a total of 12 proteins exhibited significantly altered expression due to MPA treatment (Table 2.1). The altered expression pattern of the HEK-293 proteins by MPA is shown in Figure 2.2.

Among 12 regulated proteins spot under MPA treatment, 7 proteins were significantly up-regulated and 5 proteins showed down-regulated expression. The up-regulated spots under MPA treatment were identified as complement component 1Q subcomponent binding protein (C1q), electron transfer flavoprotein subunit beta, cytochrome b-c1 complex subunit, thioredoxin domain-containing protein 12, myosin regulatory light chain 2 (MLC2), peroxiredoxin1 (Prdx1) and profilin 1. Five proteins, which showed down-regulated expression, were identified as protein SET, stathmin, 40S ribosomal protein S12, histone H2B type 1-A, and histone H2B type 1-C/E/F/G/I. A bar diagram, showing relative abundance (% Vol), SD and statistical significance of all the significantly regulated protein is provided as figure 5.1. Figure 2.2 shows an exemplary gel of DMSO (vehicle) and MPA with marked regulated proteins. The extent of regulation in protein expression with predicted and actual pI, as well as molecular masses with their SwissProt accession numbers are provided in Table 2.1 and MS/MS spectral information is provided in the figure 5.2.



**Table 2.1. Differentially regulated proteins by MPA in HEK-293 cells identified by mass spectrometry**

Spot No	Acc	M <sub>t</sub> /M <sub>o</sub> (kDa)	Score	pI <sub>t</sub> / pI <sub>o</sub>	Pep	Protein name	Function By KOGnitor NCBI	Expression change (in folds)
6	Q01105	33.4/37.0	154	4.23/4.14	3	Protein SET	Replication, recombination and repair	1.86*↓
9	Q07021	31.3/31.0	141	4.74/4.5	3	Complement component 1 Q subcomponent- binding protein, mitochondrial	Defense mechanisms	1.58*↑
14	P38117	27.8/25.5	181	8.24/9.18	6	Electron transfer flavoprotein subunit beta	Energy production and conversion	1.54*↑
15	P47985	29.6/25.0	112	8.51/7.081	6	Cytochrome b-c1 complex subunit Rieske, mitochondrial	Energy production and conversion	3.71***↑
18	Q06830	22.0/21.0	64	8.27/8.14	2	Peroxiredoxin-1	Posttranslational modification, protein turnover, chaperones	1.71***↑
22	P16949	17.2/15.8	56	5.76/6.32	3	Stathmin	General function prediction only	1.50**↓
23	O95881	19.1/16.0	123	5.24/5.89	4	Thioredoxin domain- containing protein 12	Cytoskeleton	1.95*↑
24	O14950	19.7/16.0	195	4.71/5.32	4	Myosin regulatory light chain MRLC2	Cytoskeleton	3.41*↑
27	Q96A08	14.1/14.5	51	10.31/7.0	2	Histone H2B type 1-A	Chromatin structure and dynamics	1.90*↓
28	P62807	13.8/14.2	250	10.31/6.51	9	Histone H2B type 1- C/E/F/G/I	Chromatin structure and dynamics	1.58*↓
31	P25398	14.5/13.0	89	6.81/7.10	3	40S ribosomal protein S12	Translation, ribosomal structure and biogenesis	2.44*↓
34	P07737	15.0/13.5	142	8.44/9.07	6	Profilin-1	Cytoskeleton	1.51***↑

Acc: Accession number; Mt: theoretical molecular mass; Mo: observed molecular mass; pI<sub>t</sub>: theoretical isoelectric point; pI<sub>o</sub>: observed isoelectric point; pep: number of peptides sequenced for identification; Score: Peptide mass fingerprint probability score as defined by Mascot ([www.matrixscience.com](http://www.matrixscience.com)). Individual ions score >42 indicate identity or extensive homology (p < 0.05); ↓: down-regulated; ↑ up-regulated; \*p < 0.05, \*\*p < 0.005. Molecular function determined from the online protein reference database KOGnitor NCBI. (<http://www.ncbi.nlm.nih.gov/COG/grace/kognitor.html>).

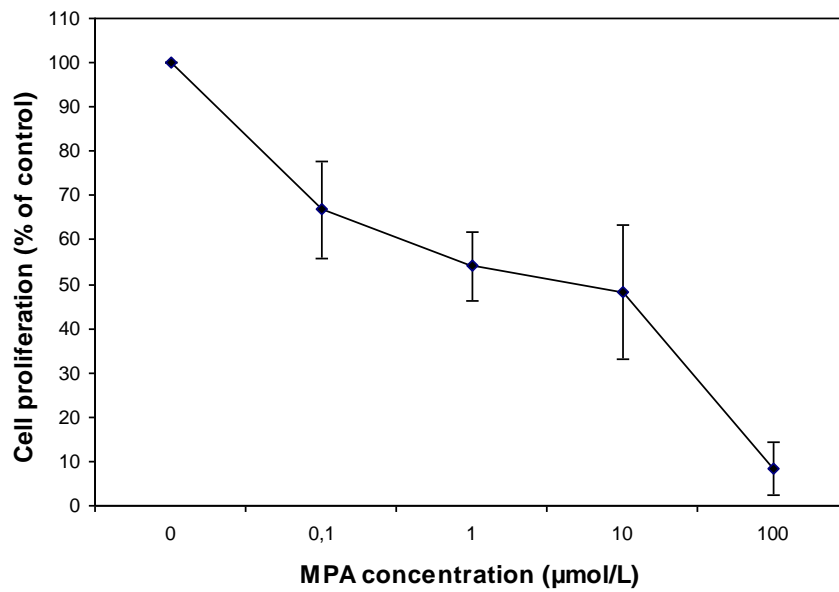


**Figure 2.1: Inhibition of HEK-293 cells proliferation by MPA treatment.**

The cell proliferation was determined after 72 hr of treatment with different doses of MPA (0–100 µmol/L) using BrdU colorimetric based method. Results are shown as percentage of control (DMSO treated) and represent four independent experiments.

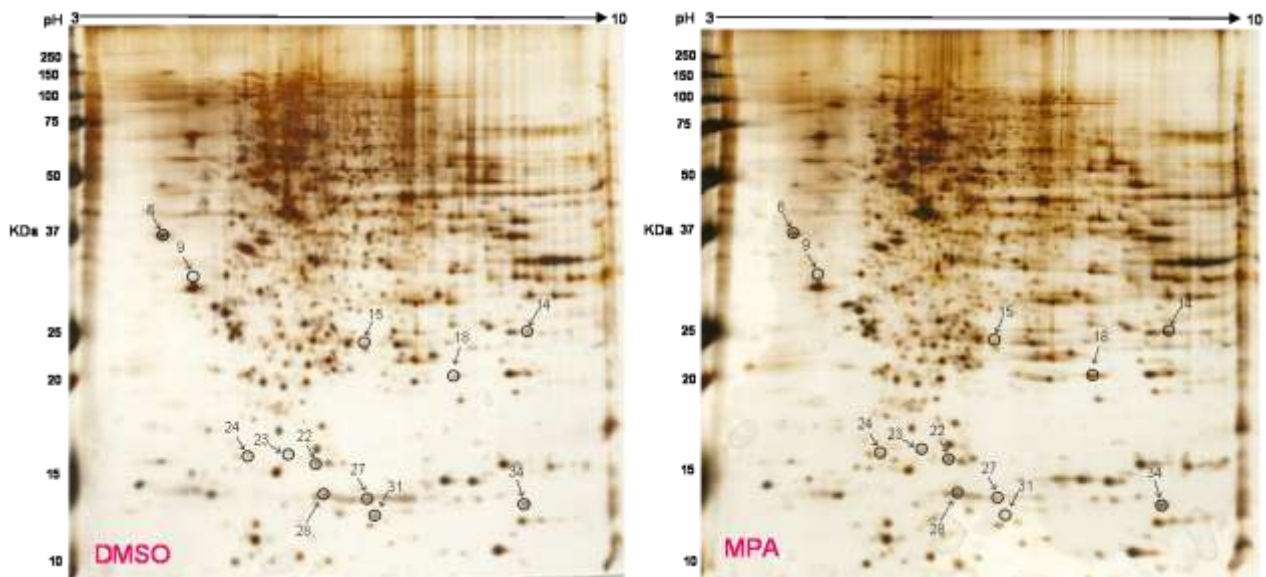


**Figure 2.2: Differential protein expression after incubation of HEK-293 cells with MPA.**

Total protein lysate from DMSO and MPA treated cells was separated by 2-D gel electrophoresis and silver stained. Encircled differentially regulated proteins spots were identified using Q-TOF MS/MS analysis. The figure shows exemplary 2-DE gels of DMSO and MPA treated HEK-293 cells.

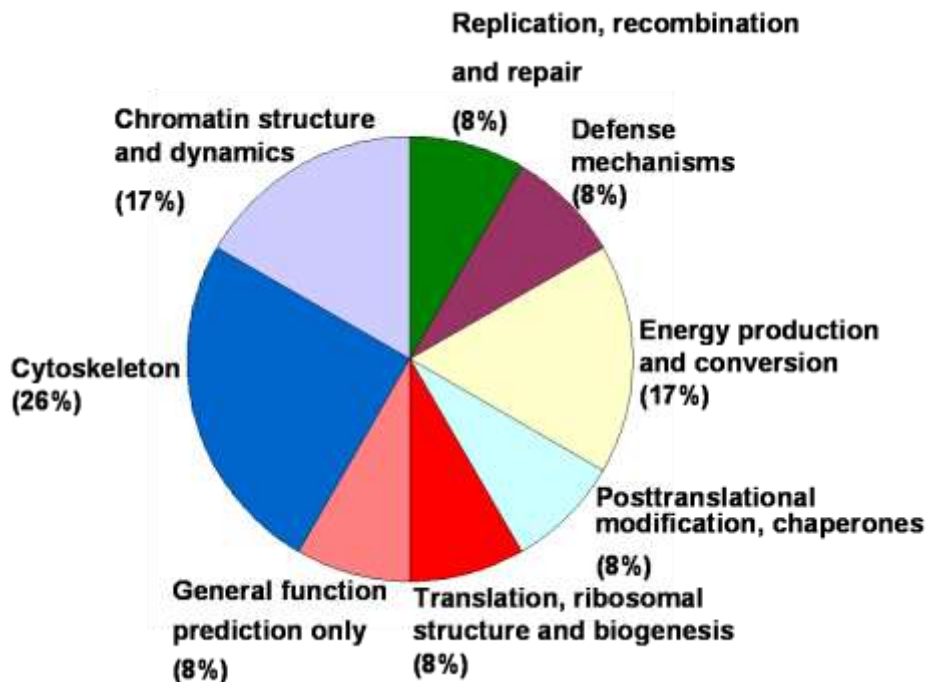


**Figure 2.3: Functional classification of regulated proteins.**

Biological functions were assigned using online KOGnitor NCBI. (<http://www.ncbi.nlm.nih.gov/COG/grace/kognitor.html>) software.

Functional classification of differentially regulated proteins was done using KOGnitor, an online biological function annotation tool [258]. The proteins altered by MPA treatment belong to various categories i.e., cytoskeleton (26%), chromatin structure/dynamics and energy production/conversion (17% each) (Figure 2.3). Gels spot diagram of two selected protein spots (MLC2 and Prdx1) in 4 biological replicates are shown in Figure 2.4a

To validate the 2-DE results, the expression of MLC2 and Prdx1 were confirmed by Western blotting and real time PCR analysis. Expression of Prdx1 and MLC2 were up-regulated at both transcriptional (Figure 2.4b) and protein level (Figure 2.4c). Specifically, MPA increased MLC2 protein (Mean fold: +1.78,  $p < 0.005$ ,  $n = 4$ , Western blotting) and mRNA expression (Mean fold: +2.25,  $p < 0.05$ ,  $n = 4$ , real time PCR). Prdx1 expression was also up-regulated, both at protein level (Mean fold: +2.73,  $p < 0.005$ ,  $n = 4$ ) and mRNA level (Mean fold: +1.93,  $p < 0.05$ ,  $n = 4$ ). To check whether over-expression of MLC2 following MPA treatment is only HEK-293 cells specific, we determined MLC2 expression in total protein lysate prepared from kidney of MMF (pro-drug of MPA) treated rats (Figure 2.5a) and MPA treated HT-29

cells (Figure 2.5b). MLC2 expression was increased both in kidney total protein lysate and HT-29 cells by (Mean fold: +2.57,  $p < 0.005$ ,  $n = 4$ ) and (Mean fold: +1.95,  $p < 0.005$ ,  $n = 4$ ) respectively.

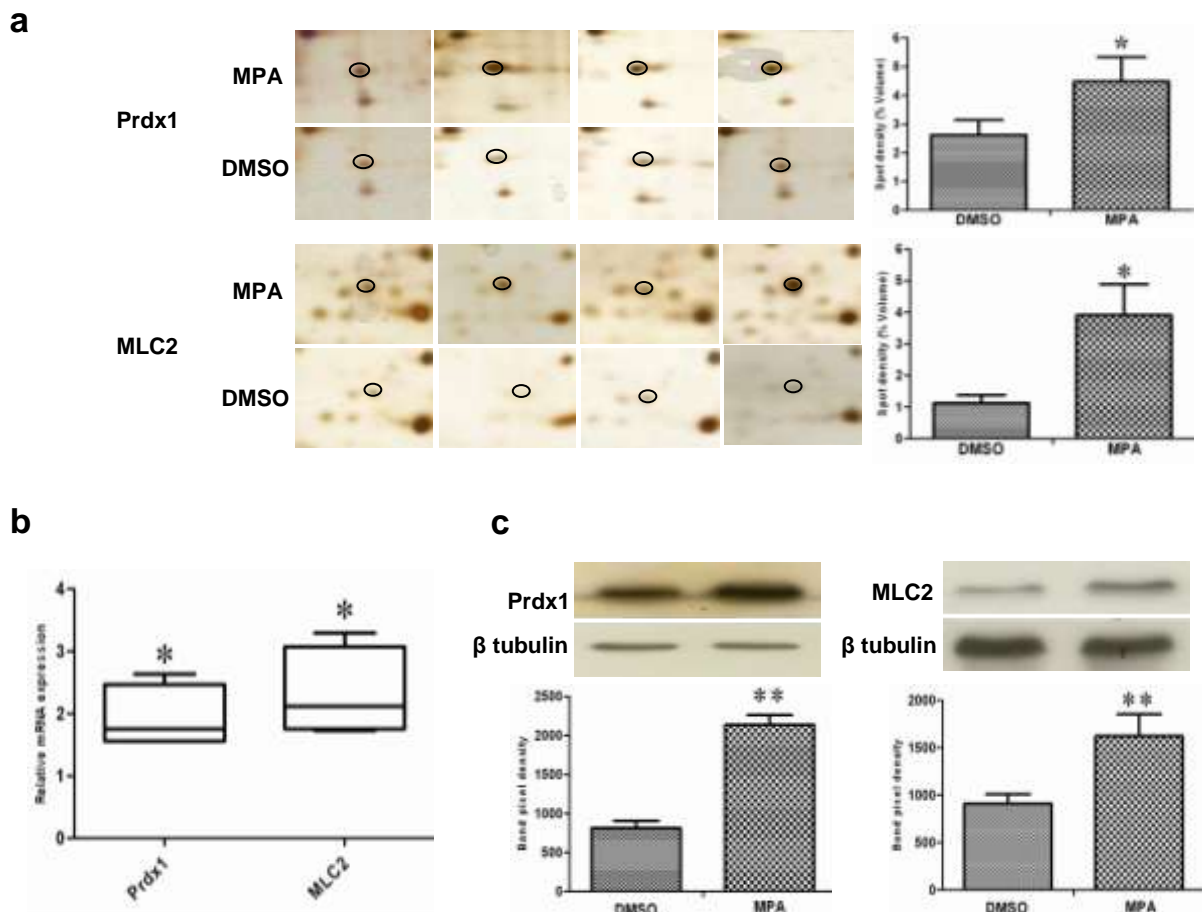


**Figure 2.4: Differential expression of Prdx1 and MLC2 by MPA treatment.**

(a) Selected areas in the silver stained gels showing differential expression of Prdx1 and MLC2. Delta 2D software was used for densitometric analysis. The quantification of the level of expression (% volume) in MPA treated cells and control cells (DMSO) is illustrated as a bar chart with the mean and SD of four separate experiments ( $*p < 0.05$ ). (b) Expression patterns of Prdx1 and MLC2 genes determined by real-time PCR. The relative expression of Prdx1 and MLC2 mRNA in the treated samples was determined as a fold change compared with control samples using the comparative threshold cycle ( $C_T$ ) method ( $2^{-\Delta\Delta C_T}$ ) as described in materials and methods part. Results shown are representative of four independent experiments. EF-2 was used to normalize the values. The boxes represent range in variation statistics and the lines across the boxes represent the medians and the whiskers extend to the highest and lowest values. Significance was calculated using the Mann-Whitney-U test ( $*p < 0.05$ ) (c) Effect of MPA treatment on Prdx1 and MLC2 protein expression. Protein extracts from MPA and DMSO treated cells were Western blotted using specific antibodies against Prdx1 and MLC2. Densitometric analysis was done using Lab image version 2.71 software.  $\beta$  tubulin signal was used to control the equal protein load. The experiments were repeated four times and error bars represent  $\pm$  SD ( $**p < 0.005$ ).

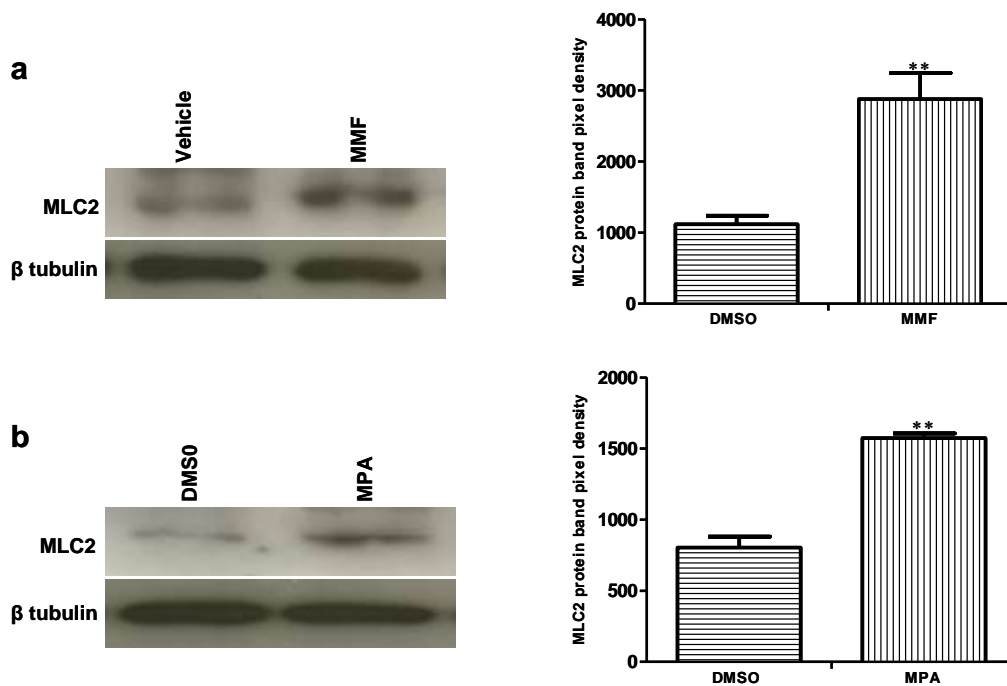


**Figure 2.5: Expression of MLC2 in MMF treated rat kidney lysate and HT-29 cells.**

Protein lysate was prepared and immunoblotted for MLC2 as described in method section.  $\beta$  tubulin was used to show equal protein load. Lab image software was used for quantification of protein bands. Four independent experiments were performed and results presented as mean  $\pm$  SD (\*\* $p < 0.005$ ).

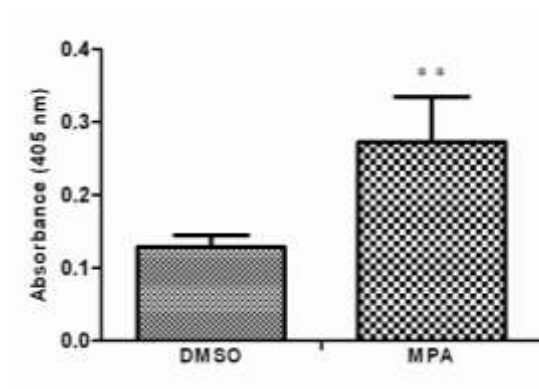


**Figure 2.6: Measurement of MPA induced caspase-3 activity.**

Cells were treated with MPA and DMSO for 72 hr. Protein extracts from each was measured for caspase-3 activity. Five independent experiments were performed and results presented as mean absorbance  $\pm$  SD (\*\* $p < 0.005$ ).

To demonstrate the effect of MPA on cell apoptosis, caspase-3 activity (apoptosis marker) was determined using a commercially available colorimetric assay. There was a significant difference in caspase-3 activity between MPA and DMSO treatment groups. MPA increased mean absorbance by 2 fold ( $p < 0.005$ ,  $n = 5$ ) as compared to DMSO treated cells. The results from caspase-3 assay revealed that MPA treated cells exhibit more apoptosis than cells treated with DMSO alone (Figure 2.6).

## 2.5 Discussion

We have used a 2-DE and mass spectrometric based proteomics approach to develop a better understanding of the influence of MPA therapeutic dose on the proteome in HEK-293 cells. HEK-293 cells are widely used cell culture model to study the mechanisms of drug action, investigating drug targets and molecular aspects of xenobiotic toxicity [262-264]. The regulated proteins are found to be involved in diverse functions including apoptosis and cell signaling mechanism. Apoptosis assay showed that MPA has a pro-apoptotic role in HEK-293 cell line, a property which makes it a drug with potential anti-tumor activities. MLC2 is an important myosin regulatory subunit, which regulates smooth muscle and nonmuscle cells contractile activity [265]. MLC2 displayed an increased expression by MPA treatment. It is already reported that MPA influences the cellular cytoskeletal architecture via modulating mesangial actin reorganization by activating actin polymerization and inhibiting actin-depolymerization [266,267]. Phosphorylation of MLC2 causes significant changes in the physiological dynamics of actin cytoskeleton, leading to barrier defects in intestine [184], heart [268] and lungs [269]. However, it remains unclear if such cytoskeleton reorganization in different organs may lead to a completely different outcome, for example in intestine, diarrhoea is associated with MPA therapy in some patients [251]. In the present study, we observed that MLC2 over-expression is not limited to a specific cell type (i.e. HEK-293) but was reproducible in MMF treated rat kidney and in MPA treated HT-29 cells protein lysates.

We observed an increase Prdx1 expression by MPA treatment, both at gene and protein level. Prdx1 is a cytoplasmic stress-inducible anti-oxidant enzyme and a major member of peroxiredoxin family [270]. Cells deficient in Prdx1 have increased sensitivity to oxidative DNA damage [271]. Prdx1 along with its anti-oxidant activity also possesses anti-inflammatory and anti-atherogenic effects [272]. Oxidative stress contributes to the pathophysiology of diverse clinical conditions, including ischemia-reperfusion mediated post transplantation graft injuries [273]. Prdx1 expression was also reported to be up-regulated in human gingival fibroblasts by cyclosporine A (another commonly used immunosuppressive drug) treatment [274]. MPA has previously been reported to diminish oxidative injuries and induce anti-oxidant effects by preventing the production of reactive oxygen species [249]. Furthermore, MPA exerts lesser oxidative stress in renal transplant patients, as compared to everolimus, cyclosporine and other calcineurin inhibitors [275,276].

Prdx1 contribute to the inhibition of tumorigenesis through PTEN/Akt pathway [277] and its lower expression in the tumor indicated high tumor proliferation, increased metastasis and could be used as cancer biomarker [278]. Prdx1 is also involved in ageing process as Prdx1-deficient mice have a shortened lifespan and other malignancies [271]. Anti-tumor drugs like histone deacetylase inhibitors (HDACs) activate Prdx1, a tumor suppressor, which leads to apoptosis [279]. Previously it was observed that MPA also inhibit histone deacetylases (HDACs) [21]. A further investigation is needed to gain a deeper insight into the Prdx1 regulation by MPA through HDACs inhibition interaction with Prdx1 and its role in anti-tumor activities.

Profilin 1, another cytoskeletal protein was up-regulated by MPA treatment. Profilins are widely distributed actin binding proteins [280], involved in actin filament dynamics and several signaling pathways [281]. Profilin 1 over-expression has been reported to cause cell proliferation inhibition, apoptosis induction and tumor suppression [282]. Whether MPA via profilin over-expression exerts extended anti-proliferative or anti-tumor activities requires further investigation. Stathmin was down regulated by MPA. Stathmin is a 19 kDa cytoplasmic protein, which plays an important role in the regulation of the microtubule cytoskeleton. Stathmin regulates microtubule turnover by promoting microtubules depolymerization and hydrolyze

guanosine triphosphate (GTP) from terminal tubulin, preventing polymerization of tubulin heterodimers [283]. Previously, our group demonstrated that AcMPAG alters tubulin polymerization in a concentration-dependent manner [284]. Furthermore, stathmin repression stabilizes microtubules, inhibits angiogenesis [285] and suppress tumors [286].

Thioredoxin domain-containing protein 12, also known as endoplasmic reticulum resident protein 18 (ERp18) is ubiquitous in mammalian cells and acts as a disulfide isomerase in the endoplasmic reticulum (ER). It provides defense against oxidative stress, refolds disulfide-containing proteins, and regulates transcription factors [287]. ERp18 expressional up-regulation might cause cell adoptivity in response to MPA induced ER stress. SET protein was down-expressed by MPA. SET, a major cellular serine threonine phosphatase is a potent inhibitor of protein phosphatase 2A (PP2A) activity [288] and a negative regulator of histone acetylation [289], thus involved in cell growth and signaling cascades [290]. PP2A expression induced by down-regulation of SET leads to the apoptosis and growth suppression [291],

MPA triggers nuclear stress and causes disruption of the nucleus, leading to the activation of p53, which may initiate cell cycle arrest and apoptosis [292]. In the present study histone H2B was down-regulated by MPA treatment, which is a major component of eukaryotic nucleosome core. Post translational modification such as methylation, acetylation, phosphorylation and ubiquitination of histone proteins alter transcription, DNA replication, and DNA repair [293,294]. Previous data showed that MPA mediated down-regulation of HDAC2 which might relate with potential epigenetic regulations [21]. The microarray analysis of mononuclear cells treated with AcMPAG (a metabolite of MPA) showed down-regulation of histones in a previous study by our group [295].

MPA affects ribosomal machinery by decreasing intracellular guanine nucleotide level, depending on dosage and cell type, resulting in global reduction of RNA synthesis [292]. Other studies suggested that guanine nucleotide depletion by IMPDH leads to a decrease in pre-ribosomal RNA synthesis, nuclear disruption, and p53 activation [296]. Disorganization of nuclear and ribosomal biogenesis is suggested to be an effective therapeutic target in cancers [297]. We observed a



down-regulation of 40S ribosomal protein S12 by MPA, which might be due to the altered ribosome biogenesis. The proapoptotic stimuli including chemotherapeutic agents induced a dose-dependent increase in the expression of the cytochrome c proteins [298].

In the present study we also observed up-regulation of cytochrome b-c I complex by MPA which suggests a possible role of MPA in the regulation of energy metabolism. Complement component 1 Q subcomponent-binding protein (C1q), a component of complement system involved in the clearance of apoptotic cells was up-regulated by MPA. C1q binds to surface blebs of apoptotic cells, which follows subsequent phagocytosis [299]. C1q deficiency leads to a significant decline in the clearance of apoptotic cells in both C1q- and C4-deficient mice, causing glomerulonephritis [300]. MPA causes cellular apoptosis and cells might utilize C1q over-expression to clear the apoptotic cells.

## **2.6 Conclusion**

This investigation identifies proteins related to diverse cellular functions which altered their expression by MPA treatment; many of which are reported for the first time in this context. The expression of Prdx1 (involved in apoptosis) and MLC2 (protein important for epithelial barrier integrity) were observed to be regulated at RNA and protein level. Further investigations of the regulated proteins will provide new insights into the cellular pathways influenced by MPA therapy and could help in more rational use of MPA in transplantation medicine.

### **3. Mycophenolic acid mediated disruption of the intestinal epithelial tight junctions**

Muhammad Qasim<sup>1,2</sup>, Hazir Rahman<sup>1,2</sup>, Raees Ahmed<sup>3</sup>, Michael Oellerich<sup>1</sup>, Abdul R. Asif<sup>1</sup>

1. Department of Clinical Chemistry, University Medical Centre Goettingen, 37075, Goettingen, Germany.

2. Department of Microbiology, Kohat University of Science and Technology, 26000, Kohat, Pakistan.

3. Institute for Applied Science and Clinical Trials GmbH - IFS, Georg-August University Goettingen, 37075, Goettingen, Germany.

Submitted

### 3.1 Abstract

Gastrointestinal toxicity is a common adverse effect of mycophenolic acid (MPA) treatment in solid organ transplantation patients, through poorly understood mechanisms. Phosphorylation of myosin light chain 2 (MLC2) is associated with epithelial tight junction modulation which leads to defective epithelial barrier function, and has been implicated in gastrointestinal diseases. The aim of this study was to investigate whether MPA could induce epithelial barrier permeability via MLC2 regulation. Human colonic cells (Caco-2) monolayers were exposed to therapeutic concentrations of MPA, and MLC2 and myosin light chain kinase (MLCK) expression were analysed using PCR and immunoblotting. Permeability was assessed by measuring transepithelial resistance (TER) and the flux of paracellular permeability marker FITC-dextran across the epithelial monolayers. MPA increased the expression of both MLC2 and MLCK at both the transcriptional and translational levels. In addition, the amount of phosphorylated MLC2 was increased after MPA treatment. Confocal immunofluorescence analysis showed disrupted distribution of tight junction proteins (ZO-1 and occludin) after MPA treatment. This MPA mediated tight junction disruption was not due to apoptosis or cell death. AcMPAG, a reactive metabolite of MPA, also showed similar effects on TER and TJ proteins expression and distribution. Additionally ML-7, a specific inhibitor of MLCK was able to reverse both the MPA mediated decrease in TER and the increase in FITC-dextran influx, suggesting a modulating role of MPA on intestinal epithelial barrier permeability via MLCK activity. These results suggest that MPA induced alterations in MLC phosphorylation may have a role in the patho-physiology of intestinal epithelial barrier disruption and may be responsible for the adverse effects of MPA on the intestine.

## 3.2 Introduction

The tight junctions (TJs) are intercellular, multifunctional complexes present in the epithelial and endothelial cells which form the paracellular diffusion barrier [97,100]. This barrier contributes to the regulation of epithelial permeability and intramembrane diffusion of ions and solutes through the paracellular space [301-303]. TJs are comprised of transmembrane (occludin, claudins and junctional adhesion molecules) and peripheral membrane proteins (zonula occludins [ZO-1], membrane-associated guanylate kinase, and the Ras-related protein Rab13). These proteins interact with each other to form a complex protein network [304]. Various intestinal and non-intestinal disorders including inflammatory bowel disease, celiac disease, and diarrhoeal infections are characterized by barrier dysfunction which is thought to play a crucial role in their pathogenesis [303].

Mycophenolic acid (MPA) is the active agent in the two currently commercially available formulations: the MPA ester mycophenolate mofetil (MMF) and the enteric-coated salt mycophenolate sodium (EC-MS) [7]. After oral ingestion, MPA is liberated in the gastrointestinal tract, absorbed and metabolized in the liver to form MPA glucuronide (MPAG) and two other metabolites, 7-O-glucoside and acyl glucuronide (AcMPAG). AcMPAG is pharmacologically active and believed to be responsible for some MPA associated GI tract adverse effects [30]. MPA is an immunosuppressant which is frequently used for the prevention of acute transplant rejection. MPA is also used for the treatment of non-transplant, autoimmune, renal, rheumatological, gastrointestinal, ophthalmological, dermatological and neurological diseases [250].

Several immunosuppressive drugs including MPA used in solid organ transplantation lead to diarrhoea [305]. Various possible aetiologies of this diarrhoea have been described including infectious agents, drug reactions, metabolic alterations, and surgical complications. MPA has been claimed to account for 50% of all drug induced post-transplantation diarrhoea [306], while 20% of total MPA complications involve the GI tract [307,308]. GI symptoms similar to those seen with Crohn's disease and enterocolitis are also observed in patients receiving MPA therapy [65,309-312]. The underlying mechanisms of MPA induced GI toxicity remain unclear; however, several hypotheses exist including direct toxicity as a

result of its anti-proliferative effects, myelosuppression induced opportunistic infections, variations in local immune response, and AcMPAG adduct toxicity [36,251,305].

Several GI associated abnormalities, including inflammatory bowel disease (Crohn's disease and ulcerative colitis), and Graft versus host disease are characterized by epithelial barrier defects which contribute to increased intestinal permeability [313]. The effects of MPA or its metabolites on cell junction biophysical properties including paracellular permeability, and the regulation of TJ proteins, especially in relation to intestinal barrier defects, have not been well studied. Studies were conducted to explore the molecular effects of MPA and its active AcMPAG metabolite on gut integrity via possible effects on TJs. We used Caco-2 cell monolayers as *in vitro* model of intestinal epithelia [314] and incubated them with therapeutic concentrations (3.1 mg/L, or 10  $\mu$ mol/L) of MPA and (10  $\mu$ mol/L) AcMPAG. Trans-epithelial resistance (TER) measurements, paracellular influx assays, immunoblotting and immunofluorescence analyses were then conducted to evaluate integrity of the TJs complex. We hypothesized that MPA may modulate the TJs by altering expression and distribution of crucial TJs proteins.

### **3.3 Materials and methods**

#### **3.3.1 Reagents**

Reagents (and their sources) included: agarose (Gibco BRL, Paisley, UK), Magnesium chloride ( $MgCl_2$ ), M-MLV RT enzyme and 5X buffer (Invitrogen, Karlsruhe, Germany), deoxynucleotide triphosphate (dNTP) (Roche, Mannheim, Germany), Ribonuclease (RNAase) inhibitor (Promega, Mannheim, Germany), MPA, fluorescein isocyanate-dextran 4 KDa (FD4), 1-5-Iodonaphthalene-1-sulfonyl)-1H-hexahydro-1,4-diazepine hydrochloride (ML-7) and cytochalasin (CD) (Sigma-Aldrich, Mannheim, Germany) and PCR primers (Eurofins, Ebersberg, Germany). AcMPAG was a kind gift from Roche (Roche, Mannheim, Germany).

### **3.3.2 Cell culture**

The human colon adenocarcinoma cell line (Caco-2) was purchased from DSMZ (German collection of microorganisms and cell cultures, Braunschweig, Germany). Tissue culture media ingredients were obtained from PAA Laboratories (Pasching, Austria). Cells were grown in Dulbecco's modified Eagle's medium (DMEM) (4.5 g/L glucose) supplemented with 10% heat-inactivated fetal calf serum, 2 mmol/L glutamine, 50 IU/mL penicillin, 50 mg/mL streptomycin and non-essential amino acid supplement (1% v/v) under conditions of 37°C, 5% CO<sub>2</sub> and 90% relative humidity. The Caco-2 cells were allowed to grow for 21 days of post-confluence to form differentiated and polarised monolayer growth [315]. The culture medium was changed every second day.

### **3.3.3 Lactate dehydrogenase (LDH) measurement**

LDH measurements were performed using a commercially available LDH measurement kit (Roche, Mannheim, Germany) according to the manufacturer's instructions. This assay is based on the principle that LDH catalyzes the conversion of NADH (substrate) to NAD and the rate of this conversion is directly proportional to LDH activity. Briefly, cells were incubated in DMSO, 10 µmol/L MPA or 10 µmol/L AcMPAG for 72 hr. Following incubation, supernatant medium was collected, centrifuged for 5 min at 15,700 x g at 4°C and LDH was measured photometrically using a Hitachi analyzer (Roche, Mannheim, Germany). The experiments were repeated at least four times and values were represented as mean IU/L ± SEM.

### **3.3.4 Determination of caspase 3 activity**

Cell were treated with DMSO, 10 µmol/L MPA or 10 µmol/L AcMPAG for 72 hr and the caspase specific activity was measured using CaspACE™ Assay kits (Promega, WI, USA) as previously described [316]. Briefly, cell proteins (70 µg) were mixed with reaction mixtures containing the colorimetric substrate Ac-DEVD-p-nitroaniline (Ac-DEVD-pNA). The pNA released from Ac-DEVD-pNA due to caspase

activity was measured at a wavelength of 405 nm using a EL808 microplate reader (Bio-Tek instruments, VT, USA). Caspase 3 specific activity (CSA) in the cell extract was measured using the standard formula (CSA = pmol pNA liberated per hour/  $\mu\text{g}$  protein). Five independent experiments were performed and results were expressed as mean pmol pNA liberated per hour/  $\mu\text{g}$  protein.

### **3.3.5 Determination of trans-epithelial resistance (TER)**

TER was measured as previously described [317]. Briefly, cells were seeded on polyester transwell inserts (6.5 mm diameter, 0.4  $\mu\text{m}$  pore size, 0.33  $\text{cm}^2$  growth area, Corning Costar Corporation, NY, USA) at  $2.0 \times 10^5$  cells/well and grown for 21 days post-confluence. Cells were treated with DMSO, 10  $\mu\text{mol/L}$  MPA, 10  $\mu\text{mol/L}$  AcMPAG or CD (10  $\mu\text{mol/L}$ ) for 72 hr or pre-treated with ML-7 (10 $\mu\text{mol/L}$ ) for 1 hr followed by 72 hr treatment of MPA (10  $\mu\text{mol/L}$ ) after cells developed into a differentiated and polarised monolayer. TER was measured using an EVOM voltohmmeter with a STX2 electrode (WPI, FL, USA). For epithelial resistance measurements, both the apical and basolateral sides of the epithelia were bathed in cell culture medium. Resistance (TER) =  $[\text{RC}-\text{RE}] \times \text{A}$ ; where RC is resistance of the cells ( $\Omega$ ); RE is resistance of the blank ( $\Omega$ ); and A is surface area of the membrane insert ( $\text{cm}^2$ ). TER was calculated as  $\Omega \cdot \text{cm}^2$  for at least four consecutive measurements.

### **3.3.6 FITC-dextran paracellular permeability**

Epithelial permeability was assessed using a previously reported method [318,319]. Briefly, Caco-2 cells were grown into monolayers and treated as described above. Following treatment, cells were rinsed with PBS and incubated in Hank's balanced salt solution containing 1mg/mL FITC-dextran 4 kD (FD4) solution for 2 hr. Permeability marker flux was assessed by taking 100  $\mu\text{L}$  from the basolateral chamber. Fluorescent signal was measured using a Lambda fluoro 320 fluorescence plate reader (MWG Biotech, Ebersberg, Germany) using 492 nm excitation and 520 nm emission filters. FD4 concentrations were determined using standard curves

generated by serial dilution of FD4. Fluxes were calculated using the apparent permeability coefficient ( $P_{app}$ ) equation:  $P_{app} = \Delta C_A / \Delta t * V_A / A * C_L$ , where  $P_{app}$  is the apparent permeability (cm/s),  $\Delta C_A$  is the change of FD4 concentration,  $A$  is the surface area of the membrane (cm<sup>2</sup>),  $\Delta t$  is the change of time,  $V_A$  is the volume of the abluminal medium, and  $C_L$  is the initial concentration in the luminal chamber.

### 3.3.7 RNA isolation, cDNA synthesis and real-time PCR

Total cellular RNA was extracted using the acid guanidinium-phenol-chloroform method (Trizol reagent; Invitrogen, CA) according to manufacturer's recommendations. Briefly, Caco-2 monolayers were scraped into Trizol reagent, homogenized, and RNA was extracted using chloroform/isopropanol precipitation. The precipitated RNA was dissolved in sterile water and stored at -80°C until analysis. RNA concentration was determined with the GeneQuant II RNA/DNA calculator (Pharmacia Biotech, Freiburg, Germany) and quality was verified by OD<sub>260</sub>/OD<sub>280</sub> nm ratios and subsequent electrophoresis in 1.5% agarose gels using ethidium bromide staining. cDNA was synthesized from 2 µg total RNA in a 30 µL reaction mix containing 1x RT-PCR buffer (10 mmol/L Tris-HCL [pH 8.3], 15 mmol/L KCl, 0.6 mmol/L MgCl<sub>2</sub>), 0.5 µmol/L of each dNTP, 1 U/µL RNase inhibitor and 13.3 U/µL M-MLV RT enzyme. The RT reactions were performed in a thermocycler (Biometra, Goettingen, Germany) at 75°C for 5 min, and then 42°C for 1 hr. cDNA was stored at -80°C until use.

Primers for real time PCR were selected using the online Primer 3 software [320]. The primers used in this study were as follows: MLC2 (forward 5'-CAGGAGTTCAAAGAGGCCTTCAAC-3', reverse 5'-CTGTACAGCTCATCCACTTCCTCA-3'); MLCK (forward 5'-CAACAGGGTCACCAACCAGC-3', reverse 5'-GCCTTG CAGGTG TACTTGGC-3'); ROCK (forward 5'-GTGAAGGTGATTGGTAGAGGTGC-3', reverse 5'-CCACCAGGCATGTATTCCATCAC-3') and elongation factor 2 (forward 5'-GACATACCAAGGGTGTGCAG-3', reverse 5'-GCGGTCAGCACACTGGCATA-3). Relative quantitative PCR was carried out using the LightCycler instrument (Roche, Mannheim, Germany). The total PCR volume of 20 µL contained 1 µL of cDNA solution, 2 µL of 10X PCR buffer (Invitrogen, Darmstadt, Germany), 2 µL syber



green, 1  $\mu$ L BSA, 1  $\mu$ L DMSO, 0.25  $\mu$ L of each primer (Eurofins MWG-Biotech AG, Ebersberg, Germany), 2.0 mmol/L  $MgCl_2$ , 0.2 mmol/L of each dNTP, and 0.15 U/ $\mu$ L PAN Script DNA polymerase (PAN Biotech, Aidenbach, Germany). Amplification conditions were set to: MLC2 (initial denaturation 30 sec at 95°C, repeated cycles of denaturation at 95°C, for 1 sec, primer annealing at 55°C for 5 sec, elongation at 72°C for 10 sec, and fluorescence reading at 82°C), MLCK (initial denaturation for 30 sec at 95°C and repeated cycles of denaturation at 95°C for 1 sec, primer annealing at 60°C for 5 sec, elongation at 72°C for 10 sec, and fluorescence reading at 82°C). ROCK (initial denaturation for 30 sec at 95°C and repeated cycles of denaturation at 95°C for 1 sec, primer annealing at 60°C for 5 sec, elongation at 72°C for 10 sec, and fluorescence reading at 80°C), elongation factor 2 (EF-2) (initial denaturation for 30 sec at 95°C, repeated cycles of denaturation at 95°C, for 1 sec, primer annealing (55°C, 5 sec), elongation (72°C, 10 sec), and fluorescence reading at 88°C). For each sample, real-time PCR reactions were performed in quadruplicate. RNA relative expression was calculated as fold change using the comparative threshold cycle ( $C_T$ ) method ( $2^{-\Delta C_T}$ ) [260] with EF-2 used as the internal control gene. The relative expression of mRNA in the treated samples was determined as a fold increase compared with control samples. The PCR product was run on 1.5% agarose gel electrophoresis to confirm the specificity of the amplified product.

### 3.3.8 Immunoblotting

Protein lysates were separated by SDS-PAGE and blotted onto PVDF (Immobilon, Millipore, MA, USA) using the Trans-Blot SD cell system (Bio-rad, Munich, Germany) for 30 min at 15 V in a blotting buffer (192 mmol/L glycine, 20% methanol, and 25 mmol/L tris [pH 8.3]). The membranes were blocked with 5% (w/v) milk in TBS-T buffer (50 mmol/L TrisHCl [pH 7.5], 200 mmol/L NaCl, 0.05% Tween 20) for 1 hr at room temperature followed by washing twice in TBS-T for 5 min. The membranes were incubated with a 1: 500 dilution of a mouse monoclonal anti-MLC antibody (Sigma, Mannheim, Germany), 1: 10000 dilution of mouse monoclonal anti-MLCK antibody (Sigma, Mannheim, Germany), 1: 1000 rabbit anti-phospho MLC antibody (Cell Signaling, Beverly, USA), 1  $\mu$ g/mL rabbit anti-ZO-1, 0.5  $\mu$ g/mL mouse anti-occludin (Zymed, CA, USA), or 1: 5000 anti- $\beta$  actin (Sigma, Mannheim,

Germany) in 5% BSA in TBS-T overnight at 4°C. Following washing in TBS-T, membranes were then incubated with appropriate HRP-conjugated secondary antibodies (Bio-rad, Munich, Germany). The membranes were washed with PBS and prepared for enhanced chemiluminescence (GE, Buckinghamshire, UK) according to the manufacturer's instructions. Developed membranes were then exposed to hyperfilm-ECL (GE, Buckinghamshire, UK). The films were scanned and protein band densities were quantified with the Lab Image software, version 2.71 (Kapelan, Leipzig, Germany).

### **3.3.9 Immunofluorescence microscopy of TJ proteins**

Cell monolayers were grown on Lab-Tek™ eight chamber slides (Nunc, Naperville, IL, USA) and treated as indicated above. Cells were immunolabelled as previously described [321] with some modifications. Briefly, cells were rinsed with PBS and fixed in 3.7% formaldehyde at room temperature for 20 min. Cell monolayers were then rinsed in PBS and permeabilized in 0.2% Triton X-100 for 7 min at room temperature. Cells were rinsed in PBS followed by blocking with 1% bovine serum albumin (BSA) for 30 min at room temperature. Cells were incubated with 3 µg/mL anti-rabbit ZO-1 and 2 µg/mL anti-mouse occludin (Zymed, San Francisco, USA) overnight at 4°C. After washing with PBS, cells were incubated with anti-rabbit IgG conjugated to Alexa 488 and anti-mouse IgG conjugated to cydye 3 (Molecular Probes, Eugene, OR, USA) in 1% BSA for 1 hr at room temperature. For F actin localization cells were incubated in 0.33 µg/mL of FITC-conjugated phalloidin (Sigma-Aldrich, St. Louis, USA) in PBS for 30 min as described previously [322]. Cells were also incubated with Hoechst dye (10 µg/mL in PBS) (Molecular Probes, Eugene, USA) for 10 minutes to stain nuclei. After washing with PBS, cells were mounted using the Dako fluorescence mounting medium (Dako, Carpintera, USA) and stored at 4°C in the dark until analyzed. The fluorescence was visualized using Axiovert 200M confocal microscope (Carl Zeiss, Jena, Germany). All of the fluorescent labelling experiments were repeated four times to ensure reproducibility.

### 3.3.10 Statistics

The data are presented as sample means with error bars indicating the standard error of the mean. The p value was calculated using a Student's *t* test and a p value <0.05 was considered statistically significant

## 3.4 Results

### 3.4.1 MPA altered TER and TJs permeability in a concentration and time dependant manner

In the present study, the effect of MPA on Caco-2 TJ integrity was determined by measuring TER and epithelial permeability to the paracellular marker FD4. To assess the influence of MPA treatment on TER, cells were incubated with different concentrations of MPA (5-100  $\mu\text{mol/L}$ ) for up to 72 hr. DMSO did not have any significant effect on TER of polarised Caco-2 cell monolayers. Increasing concentrations of MPA exhibited concentration- and time-dependant decreases in Caco-2 TER (Figure 3.1a). The mean cell monolayer TER decreased from 190.4 to 181.5, 190.8 to 147.5 and 193.1 to 120.4  $\Omega\cdot\text{cm}^2$  after 5, 10 and 50  $\mu\text{mol/L}$  MPA treatment respectively. The maximal decrease in Caco-2 TER was observed at 100  $\mu\text{mol/L}$  MPA concentration ( $86 \pm 0.7 \Omega\cdot\text{cm}^2$ ). The decrease in Caco-2 TER increased with time between 12 hr and 72 hr (Figure 3.1a).

Similarly, MPA was associated with a concentration-dependent increase in Caco-2 paracellular permeability to FD4 (Figure 3.1b). FD4 permeability analysis following 72 hr MPA treatment showed a concentration-dependant increase in FD4 influx. The FD4 influx from the apical to the basolateral chamber was increased 1.5, 2.7, 4.6 and 7.9 fold after incubation with 5, 10, 50 and 100  $\mu\text{mol/L}$  MPA concentrations respectively (Figure 3.1b).

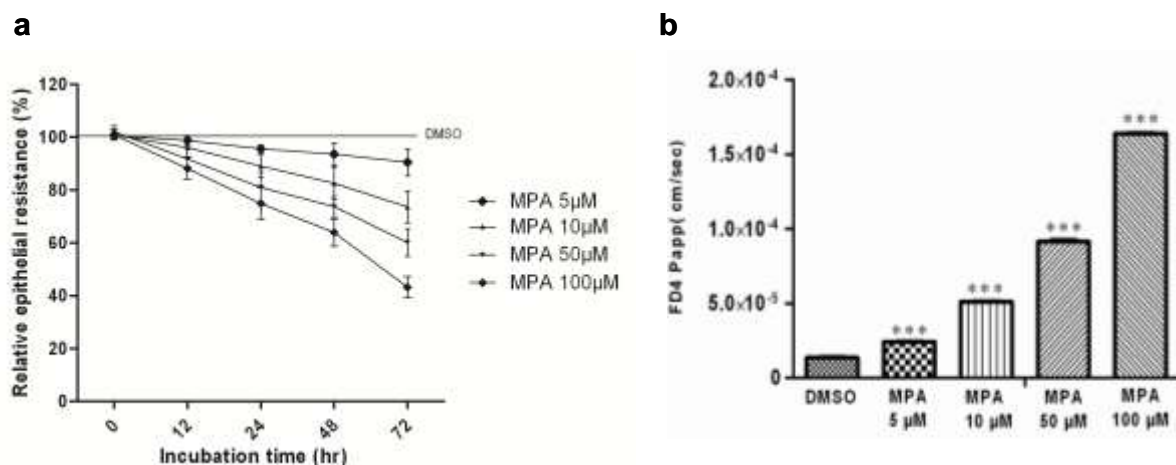


**Figure 3.1: MPA treatment decreased TER and increased FD4 permeability of Caco-2 cell monolayers.**

Caco-2 cells were cultured on filter inserts and grown for 21 days post-confluence to form differentiated monolayers. (a) Caco-2 cells were treated with MPA (5-100  $\mu\text{M}$ ) for 0-72 hr. MPA concentration and time dependent decrease in TER were observed. Graph shows TER ( $\Omega\cdot\text{cm}^2$ ) vs. time (hr) with means  $\pm$  SEM from four independent experiments. (b) Paracellular flux of FD4. Values are means of apparent permeability for FD4 (cm/sec) which is the amount of apical FD4 crossing the insert membrane per  $\text{cm}^2$  per sec. Bars show SEM and \*\*\*= $p < 0.0005$ .

### 3.4.2 AcMPAG modulation of TER and TJs permeability

To determine whether AcMPAG, a reactive metabolite of MPA, influenced the TER and FD4 influx, we incubated Caco-2 cells with AcMPAG (10  $\mu\text{mol/L}$ ). A time dependant decrease in TER (0 hr: 101.1%, 12 hr: 94.2%, 24 hr: 86.5%, 48 hr: 74.4%, 72 hr: 67.1% relative to the DMSO control) (Figure 3.2a) was observed after incubation with AcMPAG. FD4 influx analysis from apical to basal chamber showed that AcMPAG exhibited a mean 2.78 fold increase in FD4 permeability (Figure 3.2b).

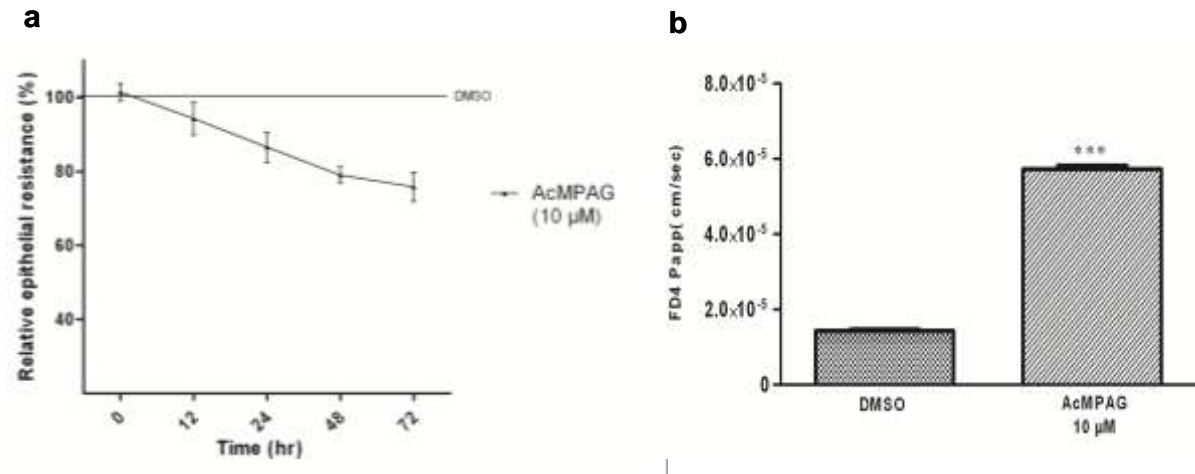


**Figure 3.2: AcMPAG treatment caused a time dependant decrease in TER and increase in FD4 permeability in Caco-2 cell monolayers.**

Caco-2 cells were grown for 21 days post-confluence and treated with AcMPAG (10 μM) for 72 hr following which TER (a) and FD4 influx (b) were determined. Values are means ± SEM of four independent experiments. \*\*\*=p< 0.0005.

### **3.4.3 MPA and AcMPAG mediated increase in permeability was not due to cell death/apoptosis**

To determine whether MPA or AcMPAG induced decreases in TER and increased FD4 permeability were due to TJs regulation and not due to the cell death, the LDH release from the treated cells was determined. LDH measurement has previously been used as an indicator of cell death [112]. Exposure to 10 μmol/L MPA and 10 μmol/L AcMPAG for up to 72 hr did not result in any significant increase in LDH release from the Caco-2 cells (Figure 3.3a). Furthermore, caspase 3 activity was measured to check the effect of MPA or AcMPAG on cell apoptosis. Neither 10 μmol/L MPA nor 10 μmol/L AcMPAG exposure for 72 hr caused any significant apoptosis as compared to DMSO (vehicle) (Figure 3.3b). These findings suggest that the TJs disruption caused by MPA/AcMPAG was not associated with cell death or apoptosis.

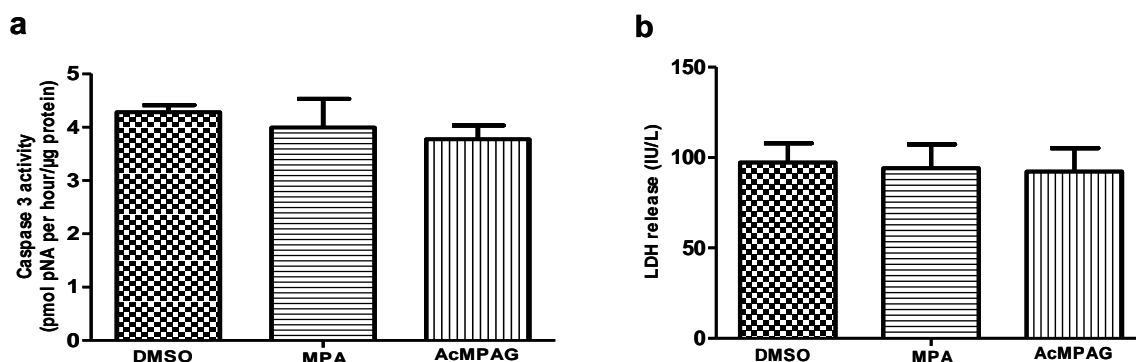


**Figure 3.3: Effect of MPA and AcMPAG on apoptosis and cell viability in Caco-2 cells.**

Caco-2 were grown for 21 days post-confluence and treated with MPA or AcMPAG for 72 hr. (a) Apoptosis was determined by measuring the caspase-3 activity in cell lysates using CaspACE™ Assay kits. Caspase 3 activity is expressed as pmol/hr/μg (b) Cell viability was assessed by measuring the lactate dehydrogenase (LDH) release in the culture media. Data represent IU/L LDH released into the media. Values are presented as the mean ± SEM; of four independent experiments and the significance was determined by Student's t-test.

### 3.4.4 MPA and AcMPAG increased the expression of MLC2 and MLCK in Caco-2 cells

In a previous study we reported that MPA increased the total MLC2 in HEK-293 cells [323]. Additionally we observed up-regulation of MLCK and ROCK expression by MPA in HEK-293 and HT-29 cells (data not shown). In view of these findings, we investigated regulation of MLC2 expression and MLCK in Caco-2 cells. MLCK is involved in the regulation of barrier function through the phosphorylation of MLC2 in response to diverse stimuli [153,324]. In line with the previous findings [323], MPA treatment increased the expression of MLC2 at both the mRNA (1.5 fold increase) and protein level (1.47 fold increase) in Caco-2 cells (Figure 3.4a and Figure 3.4b). AcMPAG (10 μmol/L) exposure for 72 hr, however, increased MLC2 protein expression (1.68 fold increase) without any significant change in mRNA expression. MLCK expression was also up-regulated by MPA (10 μmol/L) at the mRNA (1.9 fold) and protein level (2.1 fold). AcMPAG also increased the expression of MLCK at the mRNA (1.3 fold increase) and protein (1.7 fold increase) level. ROCK expression was significantly regulated by MPA (1.53 fold increase) while AcMPAG had no significant effect (Figure 3.4 a).

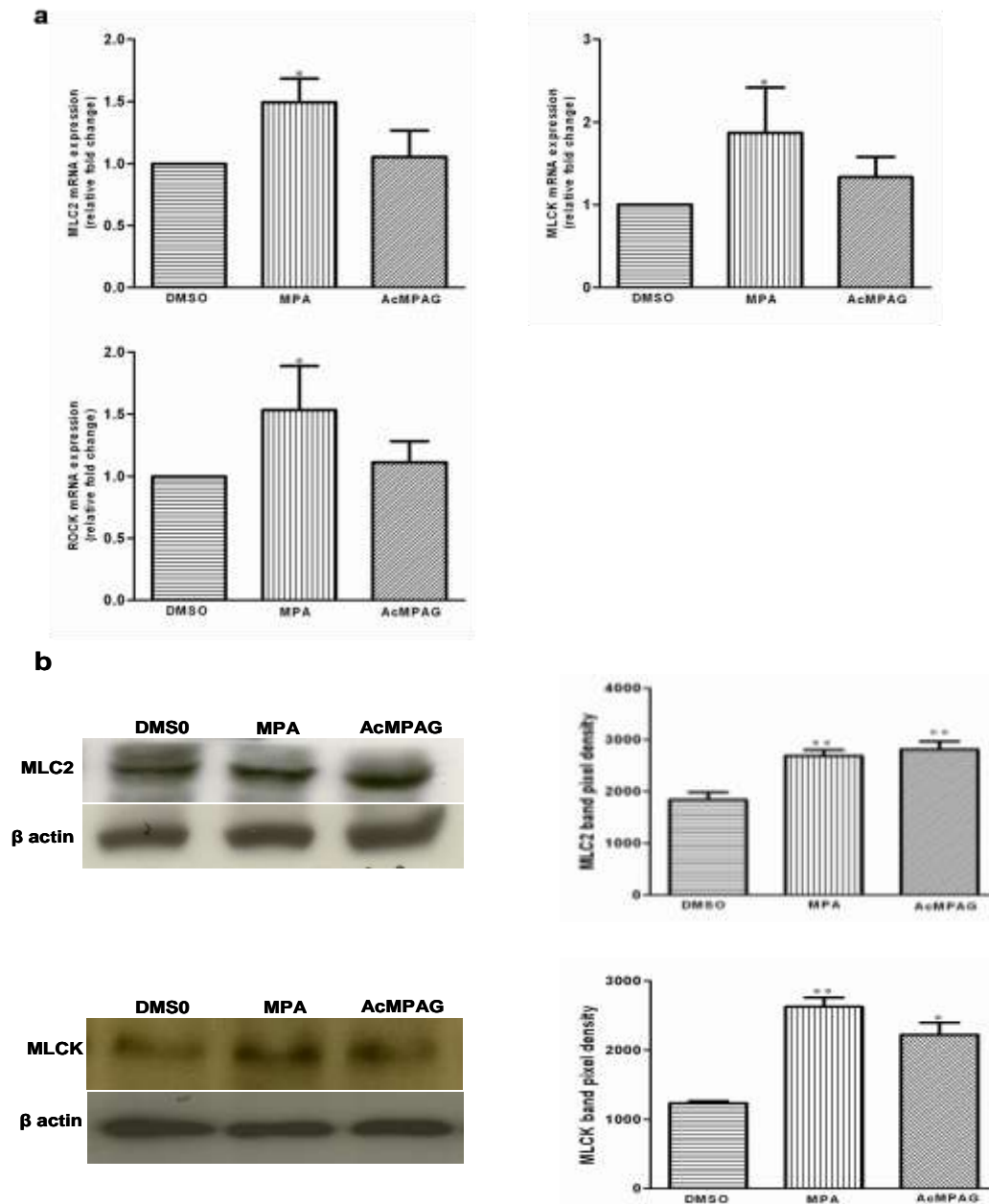


**Figure 3.4: Effect of MPA and AcMPAG on MLC2, MLCK and ROCK expression in Caco-2 cells.**

Caco-2 monolayers (21 days post-confluence) were incubated with DMSO (vehicle), MPA (10  $\mu$ mol/L) or AcMPAG (10  $\mu$ mol/L) for 72 hr. (a) mRNA expression analysis for MLC2, MLCK and ROCK. Total RNA was extracted, reverse transcribed and subjected to real time PCR analysis. EF-2 was used as a house keeping gene and the relative mRNA expression of MLC2, MLCK, and ROCK in the MPA, AcMPAG and DMSO (vehicle) treated samples was determined using the comparative threshold cycle ( $C_T$ ) method ( $2^{-\Delta\Delta C_T}$ ) as described in material and methods. Data indicate the mean of four independent experiments  $\pm$  SEM. (b) Immunoblot analyses for MLC2 and MLCK. Whole cell lysates were resolved on 1DE and immunoblotted using MLC2 and MLCK specific antibodies.  $\beta$  actin was used as a control for an equal amount of protein load. Densitometric analysis was done using the Lab image software. The data represent mean relative intensities  $\pm$  SEM from four independent immunoblots. \* $p < 0.05$  and \*\* $p < 0.005$  significance relative to DMSO.

### 3.4.5 MPA and AcMPAG increased MLC2 phosphorylation in Caco-2 cells

MLC phosphorylation has been extensively studied with regard to tight junction regulation and has been reported to be required for increased paracellular permeability [153,184]. To determine whether MPA and AcMPAG caused any defect in the epithelial barrier through phosphorylation of MLC2, we checked the phosphorylation of MLC2 using specific phospho-MLC2 antibody. MPA and AcMPAG treatment (10  $\mu\text{mol/L}$  each) for 72 hr increased the expression of phospho-MLC2 by 2.8 and 2.3 fold respectively (Figure 3.5).

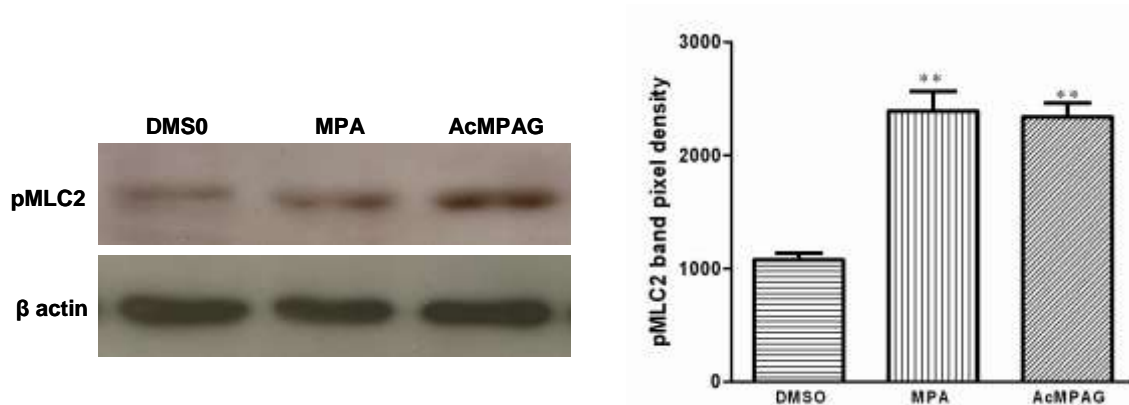


**Figure 3.5: Effect of MPA and AcMPAG on the phosphorylation of MLC2 in Caco-2 cells.**

Caco-2 monolayers (21 days post-confluent) were incubated with either vehicle (DMSO), MPA or AcMPAG (10  $\mu\text{mol/L}$  each) for 72 hr. Whole cell lysates were resolved on 1DE and immunoblotting was performed using a specific phospho-MLC2 antibody.  $\beta$  actin was used as a loading control for equal amount of protein load. Densitometric analyses were done using the Lab image software. The representative data are average of relative intensities  $\pm$  SEM from four independent immunoblot. \*\*= $p < 0.005$ .

### 3.4.6 MPA and AcMPAG altered TJ proteins expression and distribution

The modulatory effect of MPA on TJs proteins, ZO-1 and occludin was investigated by immunofluorescent labelling. Changes in the distribution and expression of occludin and ZO-1 can be used as the markers for determination of TJs disruption which has been implicated in several GI tract diseases [147,325].



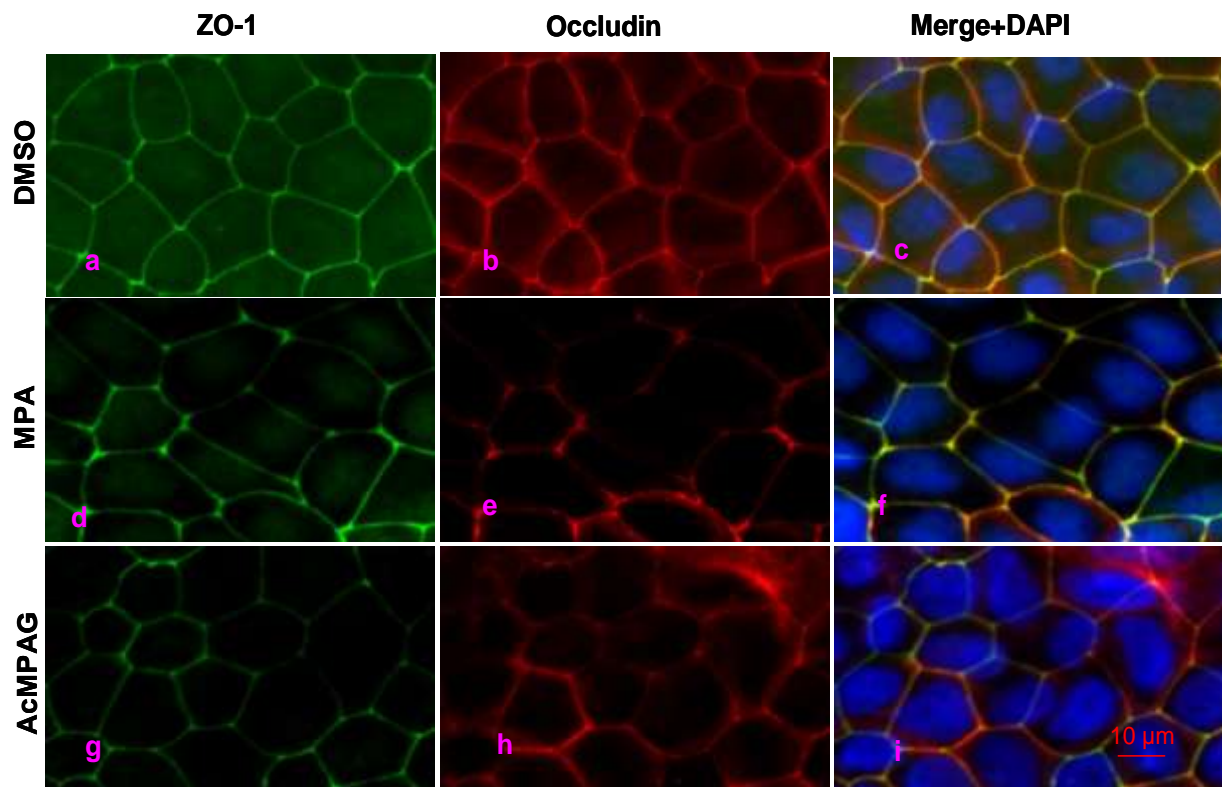


**Figure 3.6: Effects of MPA and AcMPAG on ZO-1 and occludin distribution.**

Caco-2 cells were grown for 21 days post-confluence and treated with DMSO (vehicle), MPA or AcMPAG for 72 hr. Cells were fixed, permeated, and stained for ZO-1 and occludin, as described in materials and methods section. Figure shows the distribution of ZO-1 and occludin in Caco-2 cells exposed to DMSO (vehicle) (a, b, and c), 10  $\mu\text{mol/L}$  MPA (d, e, and f) alone, 10  $\mu\text{mol/L}$  AcMPAG (g, h, and i). Cells were double stained for ZO-1 (a, d, g) and occludin (b, e, h). An overlay (ZO-1, occludin, DAPI) is shown in the right panel (c, f, i). Corresponding proteins were detected with secondary antibodies conjugated with either FITC 488 (green; ZO-1) or cydye 3 (red; occludin). DAPI (blue; nuclei) was used to stain nuclei. Images were examined using confocal microscopy. Images presented are representative images of 5 independent experiments.

Confocal analyses of ZO-1 and occludin distribution showed uniform and continuous staining at the plasma membrane in control cells (DMSO) (Fig 3.6 (a-c)). MPA and AcMPAG treatment (10  $\mu\text{mol/L}$ ) for 72 hr led to redistribution of ZO-1 and occludin proteins. The most prominent features were disappearance of staining at the cellular periphery, with aggregation and paracellular openings between the adjacent cells (MPA: Figure 3.6 (d-f), AcMPAG: Figure 3.6 (g-i)). These microscopic alterations at the apical cellular borders correlated with the amount of increased TJ permeability (Figure 3.1 and Figure 3.2) observed.

We further investigated whether MPA or AcMPAG quantitatively altered the expression of TJs proteins in Caco-2 cells. Immunoblot analysis showed that 10  $\mu\text{mol/L}$  of both MPA and AcMPAG decreased the expression of occludin by 2.1 and 2.7 fold respectively (Figure 3.7). These expressional changes are consistent with the immunostaining of occludin protein which also revealed disappearance and redistribution of occludin protein from the membranes (Figure 3.6).

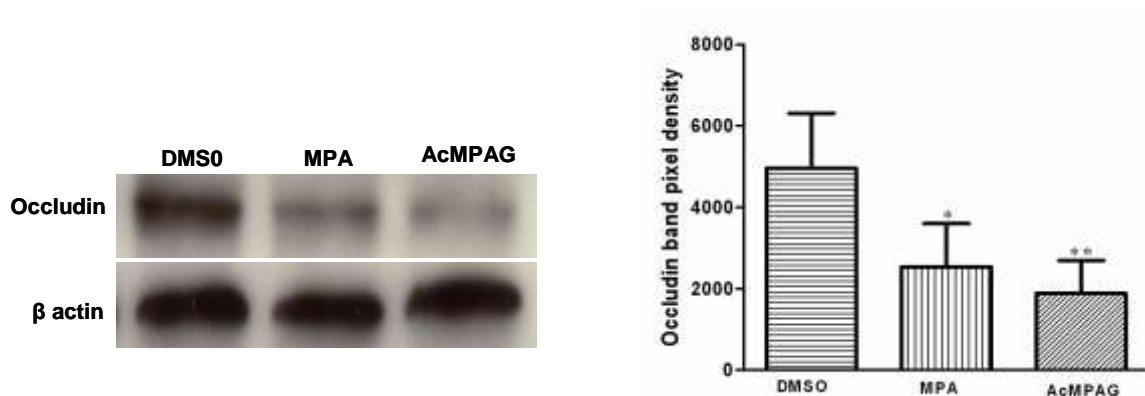


**Figure 3.7: Effect of MPA and AcMPAG on occludin protein expression in Caco-2 cells.**

Cells were grown to 21 days post-confluency and then treated for 72 hr with DMSO (vehicle), MPA or AcMPAG (10  $\mu\text{mol/L}$  each). Whole cell lysates were extracted, separated on 1-DE and occludin detected using specific antibody as mentioned in the methods section. Four independent experiments were carried out and results represent mean  $\pm$  SEM. \*= $P < 0.05$ , \*\*= $P < 0.05$ .

### 3.4.7 MPA and AcMPAG modulation of Caco-2 F-actin

The perijunctional ring of F-actin is the fundamental unit of the actin cytoskeleton that supports the tight junction and thus plays an important role in barrier regulation [326]. Structural alterations of the F-actin-based cytoskeleton are used to detect changes in actin and tight junctions [327,328].

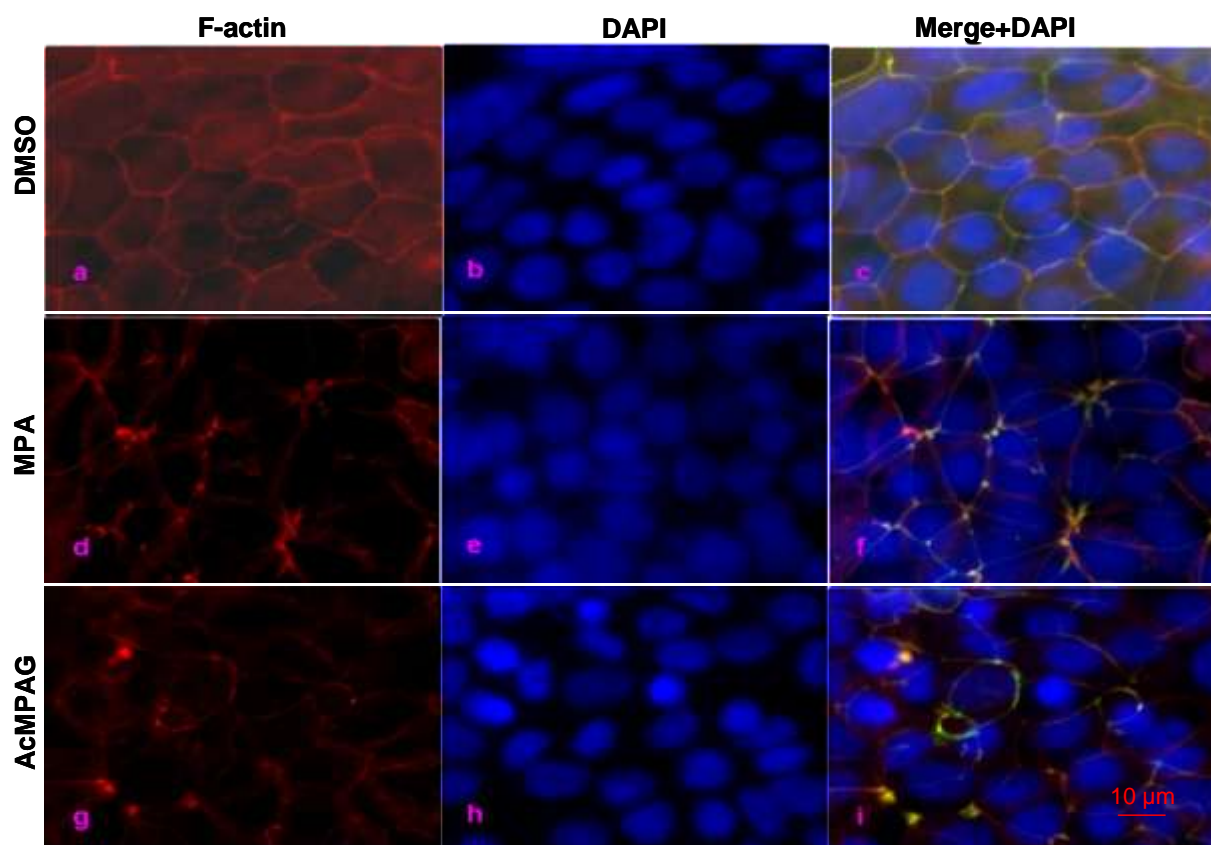


**Figure 3.8: MPA and AcMPAG-induced remodelling of the F-actin cytoskeleton.**

Caco-2 cells grown to 21 days post-confluence followed by 72 hr treatment with DMSO (a, b), 10  $\mu\text{mol/L}$  MPA (c, d) and 10  $\mu\text{mol/L}$  AcMPAG (e, f). Cells were fixed, permeated, and F-actin was stained with FITC-phalloidin (red) and nuclei were stained with DAPI (blue), as described in methods section. Fluorescence images were obtained using Axiovert 200M confocal microscope. Images are representative of 4 independent experiments.

To investigate whether MPA or AcMPAG mediated colonic epithelial barrier disruption was associated with structural modulation of the F-actin cytoskeleton, we stained Caco-2 cells with FITC-labelled phalloidin, a commonly used fluorescent marker for F- actin [322,328]. In the vehicle control (DMSO) cell monolayers, the F-actin cytoskeleton was uniformly organized as shown in figure 3.8 (a-c). Following 72 hr exposure to 10  $\mu\text{mol/L}$  of either MPA (Figure 3.8 d-f) or AcMPAG (Figure 3.8 g-i), the uniform distribution of actin staining in epithelial cells appeared disrupted and was marked by randomly distributed dense patches of staining, which suggest disruption of the actin cytoskeleton as a possible mechanism for the alterations in the TJs by MPA and AcMPAG.

### **3.4.8 MPA-mediated increase in MLC phosphorylation through MLCK**

To analyze for the possible involvement of MLCK in the MPA mediated TJs disruption, we determined the effect of MPA on total protein expression of MLC2, MLCK, and phospho-expression of MLC2 in the presence of ML-7 (Figure 3.9). ML-7 acts as a selective antagonist of MLCK by competing for its ATP-binding site and reverses the effects of agents involved in TJs disruptions [328]. Previously it was reported that ML-7 had no significant effect on total MLC2 and MLCK expression and that ML-7 mainly affects the phosphorylation of MLC2 by decreasing the activity of MLCK [112]. In the present study, expressional analysis showed that MPA treatment in the presence of ML-7 did not alter total MLC2 and MLCK expression, which was observed after MPA treatment alone. Additionally, we observed that the presence of ML-7 in the medium was able to reverse the effect of MPA on MLC2 phosphorylation (Figure 3.9). To further validate these results, cells were incubated with CD which is an actin-disrupting drug that has previously been reported to increase MLC2 phosphorylation [329]. Our results also showed that CD increased phospho-MLC2 expression; which is consistent with the previous report [329].

In the present study, expressional analysis showed that MPA treatment in the presence of ML-7 did not alter total MLC2 and MLCK expression, which was observed after MPA treatment alone. Additionally, we observed that the presence of ML-7 in the medium was able to reverse the effect of MPA on MLC2 phosphorylation (Figure 3.9). To further validate these results, cells were incubated with CD which is an actin-disrupting drug that has previously been reported to increase MLC2 phosphorylation [329]. Our results also showed that CD increased phospho-MLC2 expression; which is consistent with the previous report [329].

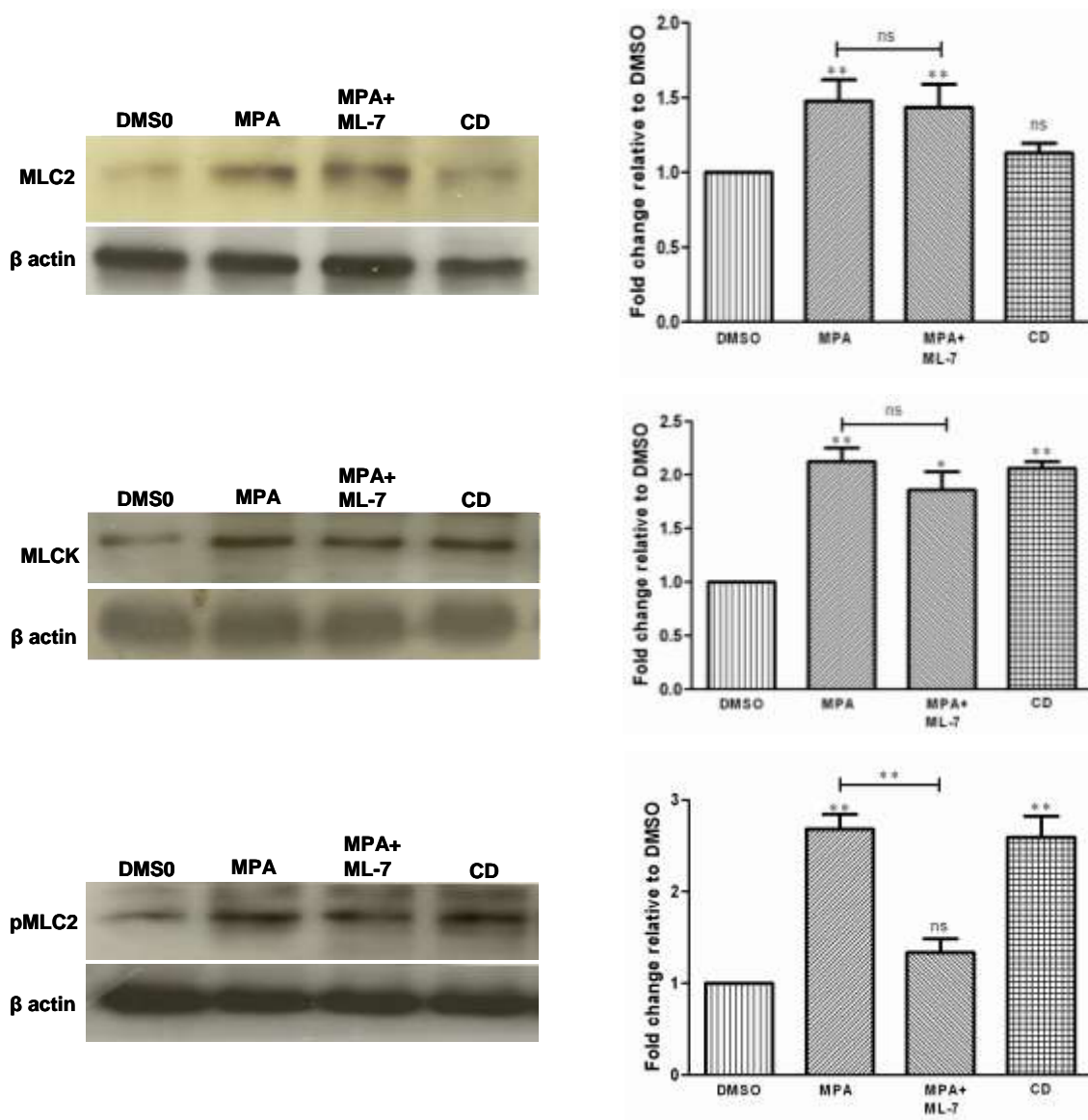


**Figure 3.9: Effect of ML-7 on MPA-mediated increases in MLC2, MLCK and MLC phosphorylation.**

Caco-2 monolayers (21 days post-confluent) were incubated with either vehicle (DMSO), MPA, MPA+ML-7, or CD for 72 hr. Total cell proteins were isolated and equal amount of protein was loaded resolved on 1DE. Expression was analysed by immunoblot analysis using antibodies against MLC2, MLCK and p-MLC2. Beta actin was used as a control for an equal amount of protein load. Bands were quantified using the Lab image software. The data represent the mean of 4 independent experiments  $\pm$  SEM. \*= $p < 0.05$ , \*\*= $p < 0.005$ .

### 3.4.9 MLCK inhibition partially prevented MPA effects on TER and permeability

To investigate whether MPA mediated TJs alteration is through effects on MLCK, we pre-treated Caco-2 monolayers with ML-7 for 1 hr and then co-incubated them with (10  $\mu\text{mol/L}$ ) MPA for the indicated time periods. It was previously reported that ML-7 prevents TJs disrupting agent mediated decreases in TER and increases the permeability via inhibition of MLCK [153,328]. Co-treatment with ML-7 and MPA resulted in a significant higher TER as compared to cells treated with MPA alone. Similarly, apical to basal FD4 influx was also reduced in cells co-treated with MPA and ML-7 (Figure 3.10). CD was previously reported to decrease TER and increase permeability [330]. In the following experiments, similar to MPA, CD treated cells showed significant decreases in TER and increases in FD4 influx (Figure 3.10). These findings suggest that the MPA-induced increases in Caco-2 TJ permeability are at least partly the result of a mechanism closely associated with MLCK expression and activity.

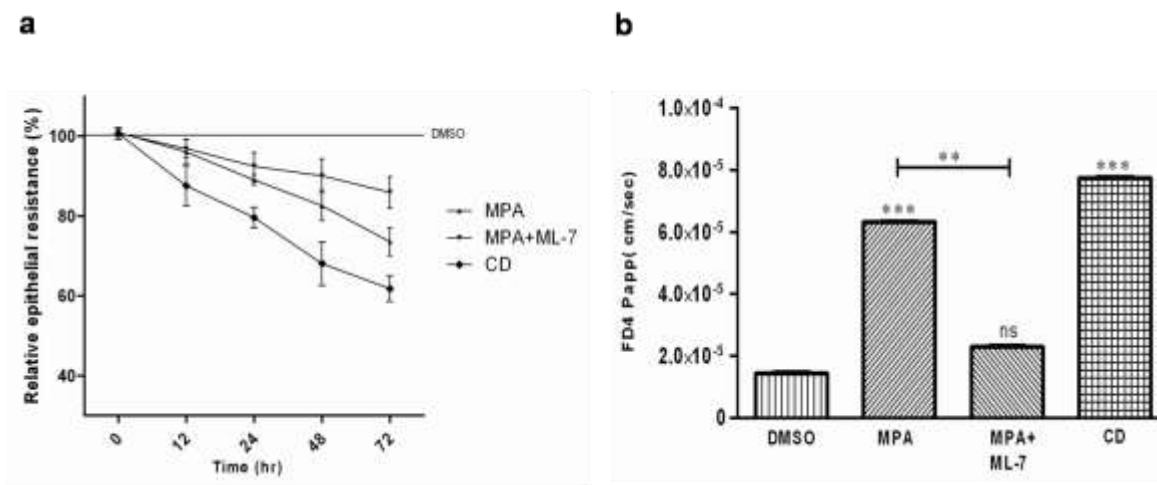


**Figure 3.10: ML-7 co-treatment reversed the effect of MPA on TER and permeability.**

Cells were grown to 21 days post-confluence and incubated with MPA or MPA+ML-7, or CD for 72 hr. The effects on (a) TER and (b) FD-4 influx were measured as described in the methods section. ML-7 a specific MLCK inhibitor prevented both the MPA-mediated increase in FD 4 paracellular diffusion and the decreases in TER. Data are the mean  $\pm$  SEM of at least four independent experiments. \*\*= $p < 0.005$ , \*\*\*= $p < 0.0005$ .

### 3.4.10 Inhibition of MLCK prevented MPA mediated alteration of TJ proteins

We examined the involvement of MLCK in MPA mediated TJs regulation using immunofluorescence methods. Previously it was reported that the redistribution of TJs proteins by TJs disrupting agents can be reversed by inhibiting MLCK [215,331,332]. Immunofluorescence localization of occludin and ZO-1 showed that ML-7 could partly prevent redistribution of ZO-1 and occludin induced by MPA exposure (Figure 3.11 d-f) when compared to cells treated with MPA alone (Figure 3.11 a-c).

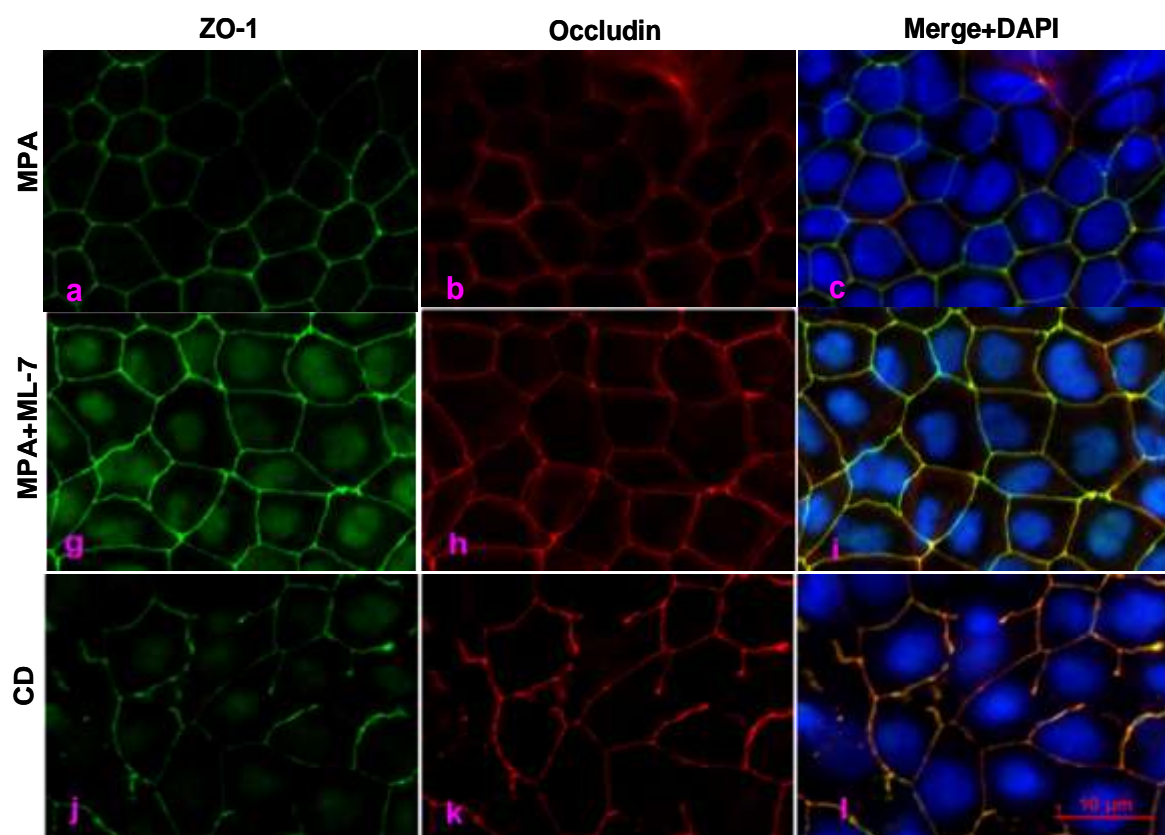


**Figure 3.11: ML-7 co-treatment reversed the effect of MPA on distribution of TJs proteins.**

Cells following 21 days post-confluency were treated with MPA, and CD or pre-treated with ML-7 followed by MPA treatment. Cells were labelled with florescent antibodies specific for ZO-1 and occludin. Figure shows ZO-1 (a, g, j), occludin (b, h, k) and an overlay of ZO-1 and occludin along with DAPI stained nuclei (c, i, l). Four independent experiments were performed.

ML-7 co-treatment induced reassembly of the ZO-1 and occludin at the cellular borders with reclosure of the paracellular gaps (Figure 3.11 g-i). The MPA induced disruption of TJs proteins distribution was prevented by an MLCK inhibitor (ML-7), indicating that the downstream alteration of TJs proteins is dependent on MLCK

activation. In contrast, CD, like MPA, disrupts the distribution of ZO-1 and occludin as shown by disappearance of these proteins from the paracellular membrane (Figure 3.11 j-l)

We also performed immunoblot analysis for occludin protein expression. Results showed that ML-7 was able to reverse the effect of MPA on occludin expression by increasing its expression by 1.92 fold as compared to cells treated with MPA alone. CD treatment showed a 3.2 fold decrease in occludin protein as compared to DMSO control (Figure 3.12).

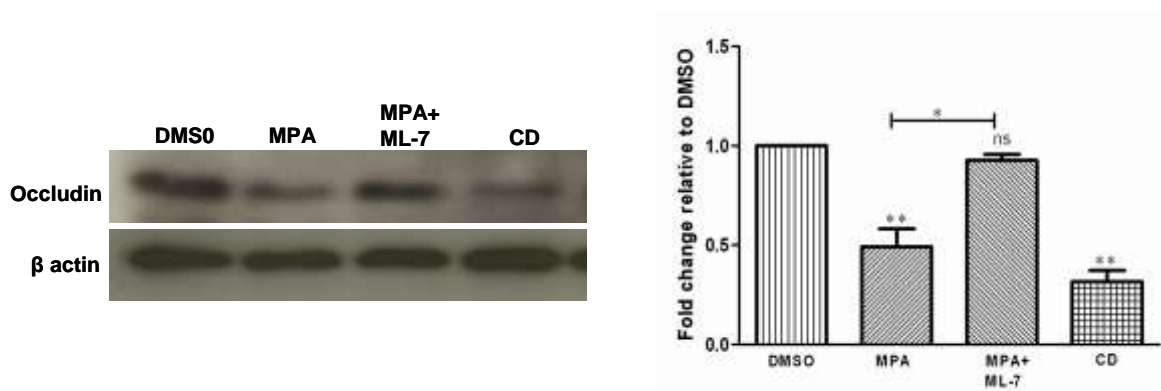


**Figure 3.12: Effect of ML-7 co-treatment with MPA on occludin protein expression in Caco-2 cells.**

Caco-2 cell monolayers following 21 days post-confluency were incubated with DMSO, MPA (10  $\mu$ mol/L), MPA (10  $\mu$ mol/L) +ML-7 (10  $\mu$ mol/L) or CD (10  $\mu$ mol/L) for 72 hr. Protein extracts were immunoblotted for occludin and  $\beta$ -actin. Densitometric measurement was done with the Lab image software. Values are means  $\pm$  SEM (n = 4).

### 3.5 Discussion

Intestinal cells form a crucial physical and functional barrier, which regulates the movement of water, electrolytes, nutrients, and xenobiotics [333]. The gastrointestinal tract is directly involved in the metabolism and transport of various endogenous and exogenous compounds [334]. Several intestinal diseases are characterized by barrier dysfunction including inflammatory bowel disease, graft versus host disease, and infectious enterocolitis (reviewed in [335]). It has been previously reported that epithelial barrier defects lead to increased intestinal



permeability and the development of diarrhoea in human patients with bowel diseases [336] and in mouse models [337].

MPA associated gastrointestinal adverse effects are a major concern in transplantation medicine and diarrhoea is the most frequent unwanted clinical outcome following treatment with MPA regimes [338]. Previous reports showed that MPA is associated with gastrointestinal mucosal injury [60,65,311,339,340]. The effect of therapeutic concentrations of MPA on the gastrointestinal epithelial barrier is not well described. Diverse physiological and pathophysiological stimuli cause intestinal barrier dysfunction, regulated via several pathways such as those involving protein kinase C, protein kinase A, MLCK, Rho-kinase, mitogen-activated protein kinases, and phosphoinositide 3-kinase. Disturbances in these pathways can all lead to the alteration in TJs protein expression and distribution [181,303]. In a previous study, we observed a significant increase in the MLC2 expression in HEK-293 cells following MPA exposure [323]. MLC2 phosphorylation via MLCK and/or ROCK has been implicated in several barrier disorders [329].

To better understand the possible mechanism of MPA mediated TJs regulation, we used Caco-2 monolayers as a colonic model [341]. The present study demonstrates for the first time in vitro that MPA, at non-toxic and therapeutic concentrations produces a significant modulation of intestinal epithelial barrier function in Caco-2 cells. The Caco-2 cell line is widely used as an in vitro intestinal barrier cell model, which exhibits a well differentiated brush border, TJs and intestinal proteins [341,342]. MPA exposure increased TJs permeability and impaired TJ proteins (ZO-1 and occludin) expression and distribution. On the other hand, the MPA concentrations used did not cause significant apoptosis or cell death, suggesting that the effects of MPA on GI barrier function are the result of a non-cytotoxic mechanism.

Previously it was shown that MLCK activity in Caco-2 cells triggers a series of molecular processes such as induction of MLC phosphorylation, myosin-Mg<sup>2+</sup>-ATPase activation, and perijunctional actin-myosin interaction which are responsible for actin filament disruption leading to Caco-2 epithelial barrier opening [328]. Several agents increase MLCK mediated MLC2 phosphorylation which disrupts tight junction proteins, leading to the increased TJs permeability implicated in barrier associated

diseases [184]. We investigated the possible disruptive role of MPA on epithelial barrier permeability and attempted to link this effect with MLCK-induced MLC-2 phosphorylation.

To demonstrate the effect of MPA and one of its active metabolites, AcMPAG, on barrier properties of this colonic model, Caco-2 cells were exposed to non-cytotoxic concentrations of MPA (10  $\mu\text{mol/L}$ ) and AcMPAG (10  $\mu\text{mol/L}$ ) followed by measurements of TER and influx of markers. Determination of TER and influx of permeability markers are widely used techniques to assess the integrity and permeability of monolayers [343] because TJs disruption can be reflected by the reduction in TER and the increase in influx of permeability markers [335].

Our data revealed that MPA and AcMPAG increased Caco-2 cell monolayer permeability as shown by decreases in TER and increases in FD4 influx (Fig 1). These findings are in agreement with another report on the effects of MMF (an ester prodrug of MPA) on the barrier function of small bowel and distal colon of Wistar rats [344].

TJs proteins, ZO-1, and occludin are protein markers which are widely used to investigate TJs integrity [184,345]. These proteins maintain structure and function of TJs integrity which are vital for normal intestinal architecture [97,148]. The disturbance in the distribution and expression of these proteins has been observed in intestinal barrier disorders [150,313]. In the present study, we investigated the effect of MPA and AcMPAG on the distribution and expression of ZO-1 and occludin. We found that exposure of Caco-2 monolayers (21-days post-confluency) to therapeutic, non-cytotoxic concentrations of MPA and AcMPAG for 72 hr led to a decrease in the expression of occludin proteins, as evidenced by Western blot analysis (Figure 3.7). Under normal conditions ZO-1 and occludin are generally present at the pericellular boundary, and distributed homogeneously, presenting a characteristic feature of intact TJs structure. Disruption and redistribution of TJs proteins has been reported previously in several studies that suggested that alteration in these proteins can lead to hyperpermeability [184,346]. MLCK mediated MLC-2 phosphorylation (involved in modulation of ZO-1 and occludin morphologically and biochemically) can induce an increase in TJs permeability [184,184].

Furthermore, we also demonstrated that MPA and AcMPAG exposure changed the distribution of ZO-1 and occludin proteins, as revealed by a discontinuous pattern of immunofluorescent staining of these TJ proteins (Figure 3.5). To investigate whether MLCK was involved in MPA modulation of TJs, we used a specific MLCK inhibitor, ML-7 which is a selective antagonist of MLCK [347]. Previously it was reported that inhibition of MLCK mediated MLC phosphorylation by ML-7 can prevent or reverse TJ barrier losses induced by several agents such as TNF $\alpha$ , Cytochalasin B, and ethanol [112,153,328,348]. To investigate the effect of MPA on MLCK activity, we pre-incubated cell monolayers with ML-7 followed by MPA exposure. Results showed that ML-7 could at least partially reverse the MPA mediated decrease in TER as well as the increase in FD4 influx. Additionally, ML-7 was able to prevent the MPA induced redistribution and decrease in expression of ZO-1 and occludin proteins.

Treatment with CD, a known stimulant of MLCK and actin-depolymerising agent [329] which was used as positive control for the effects of MPA treatment, also showed a decrease in TER and increase in paracellular flux (Figure 3.10). Previously, it was reported that CD was able to increase MLCK activity and MLC2 phosphorylation [329], which our results confirmed. In addition, we found that CD was able to alter the expression and distribution of TJ proteins which is consistent with results of a previous study of CD treated epithelial cells [349]. These results showed that both CD and MPA decreased TER and disrupted the actin cytoskeleton. The present study revealed that inhibition of MLCK activity by ML-7 significantly prevented the MPA mediated increase in MLC2 phosphorylation with no significant effect on total MLCK and MLC2 expression.

MLC2 phosphorylation has a key role in maintaining TJ integrity by regulating actomyosin contraction [153]. Several pathways were described previously which regulate the phosphorylation of MLC2; among them Rho-kinase and MLCK signalling are widely studied in the context of barrier defects [191]. MLCK is involved in the regulation of barrier function by phosphorylation of MLC2 in response to diverse stimuli [153,324]. ML-7 via MLCK inhibition prevents the disruption of both occludin and actin, which demonstrates the importance of MLCK activity in TJ physiology [350]. Our results suggest that increases in MLCK might be responsible for the MPA induced redistribution of ZO-1 and occludin in Caco-2 monolayers.

### **3.6 Conclusion**

The present study indicates that MPA and its active AcMPAG metabolite at therapeutic concentrations produce functional alterations in TJs of Caco-2 cells resulting in abnormal TJs permeability, and redistribution of TJs proteins including disturbance and displacement of F-actin. These data suggest that MPA mediated increases in permeability required increased MLCK activity which could be reversed by ML-7. While requiring further investigation, MLCK inhibition by ML-7 significantly reduced the effect of MPA exposure on TJs disruption, thus suggesting a pivotal role of MLCK in regulating TJs barrier properties. These findings provide new insights into the mechanism by which therapeutic use of MPA may alter intestinal epithelial barrier functions and suggest mechanisms which may be responsible for some of the GI adverse effects associated with MPA.

## 4. Summary

Mycophenolic acid (MPA) is a potent inhibitor of inosine monophosphate dehydrogenase (IMPDH), a key regulator of purine biosynthesis. MPA is frequently used as an immunosuppressant drug to prevent acute graft rejection for kidney, liver and lung transplantation. The use of MPA is associated with GI toxicity which is a problem to the patients, and a challenge for clinicians. The present study was undertaken to identify novel molecular targets of MPA using a proteomics approach (Figure 4.1). Two dimensional gel electrophoresis (2-DE) and mass spectrometry were used to identify proteome alterations in human embryonic cells (HEK-293) following exposure to therapeutic concentrations of MPA. Cells were treated for 72 hours, and total cell lysate was resolved by 2-DE followed by QTOF-MS/MS analysis of all identified differentially regulated proteins. A total of 12 proteins were differentially regulated in HEK-293 cells following exposure to MPA. Among these, 7 proteins were up-regulated (complement component 1 Q subcomponent-binding protein, electron transfer flavoprotein subunit beta, cytochrome b-c1 complex subunit, peroxiredoxin 1, thioredoxin domain-containing protein 12, myosin regulatory light chain 2, and profilin 1), while 5 proteins were down-regulated (protein SET, stathmin, 40S ribosomal protein S12, histone H2B type 1 A, and histone H2B type 1-C/E/F/G/I). Functional annotation tool analysis showed that MPA modulated proteins were mainly involved in the cytoskeleton (26%), chromatin structure/dynamics (17%), and energy production/conversion (17%). Considering both putative functions and their clinical significance, peroxiredoxin-1 (Prdx-1) and myosin light chain 2 (MLC2) were selected for Western blot and real time PCR analysis. Both proteins showed up-regulation at mRNA as well as at protein level following MPA exposure.

MLC2 is known to be involved in several functions including tight junctions (TJ) regulation. Epithelial barrier disruption by phosphorylation of MLC2 has been implicated in several bowel diseases. Since MPA treatment often causes diarrhea when used clinically, we hypothesized that MPA regulated epithelial TJ by modulation of MLC2. To test this hypothesis, we investigated the effect of MPA on the expression of MLC2 in two colonic cell lines, HT-29 and Caco-2. Increased MLC2 expression was observed in both cell lines following MPA exposure. These findings suggest that the increase in MLC2 expression after exposure to MPA is not a cell specific effect. Moreover, we observed similar up-regulation of MLC2 expression in

whole cell lysates prepared from MMF treated rats, which implies that MPA has similar effects both *in vitro* and *in vivo*.

We then used Caco-2 cells grown for 21 days post confluence to develop polarize monolayers to conduct physiological, expressional and microscopic analysis to establish the possible role of MPA in disruption of TJ (Figure 4.1). MPA exposure caused a time and dose dependent decreases in transepithelial resistance (TER), and increases in the FITC-dextran 4 KDa (FD4) paracellular influx in these Caco-2 monolayers. In addition, we found that AcMPAG (a pharmacologically active metabolite of MPA) was also able to cause decreases in TER and increases in FD4 influx. These MPA and AcMPAG mediated increases in permeability were not due to cellular toxicity, as shown by the fact that no significant apoptosis or cell death was observed. In MPA and AcMPAG treated cells, we also found altered expression and distribution of TJ proteins (ZO-1 and occludin).

Since MLC phosphorylation is a key modulator of TJ disruption; we investigated whether MPA also increased MLC2 phosphorylation. Using immunoblot analysis we found that MPA significantly increased MLC2 phosphorylation. We then investigated whether MPA mediated increases in MLC2 phosphorylation was through effects on MLCK. Immunoblot analysis revealed that MPA increased MLCK expression both at mRNA and protein levels. To further confirm that MLCK was the key player in MPA mediated MLC2 phosphorylation and its associated TJ disruption, we pre-incubated cells with ML-7 (a specific MLCK inhibitor), and observed that ML-7 was able to partially prevent the MPA mediated increase in MLC2 phosphorylation. Furthermore, we found that ML-7 partially reversed MPA mediated decreases in TER, and increases in FD4 paracellular influx. ML-7 also prevented the MPA associated disruption of the distribution and expression of TJ proteins (Figure 4.2). These findings suggest that MPA may regulate TJ function via MLCK-driven MLC2 phosphorylation. However, these results do not exclude the possibility that other pathways may also be involved in MPA induced regulation of TJ function.

Taking together findings of the present studies showed that therapeutic concentrations of MPA can modulate the expression of important proteins which are crucial for various cellular functions. MPA may modulate epithelial TJ integrity via MLC2 phosphorylation. These findings will be helpful to understand the molecular mechanisms of MPA-induced proteome alterations, including proteins that are

involved in disruption of TJ. Further studies are needed to clarify the mechanism(s) and consequences of MPA mediated disruption of TJs, especially in *in vivo* models, to know whether these TJ barrier changes are responsible for the GI adverse events associated with MPA treatment.

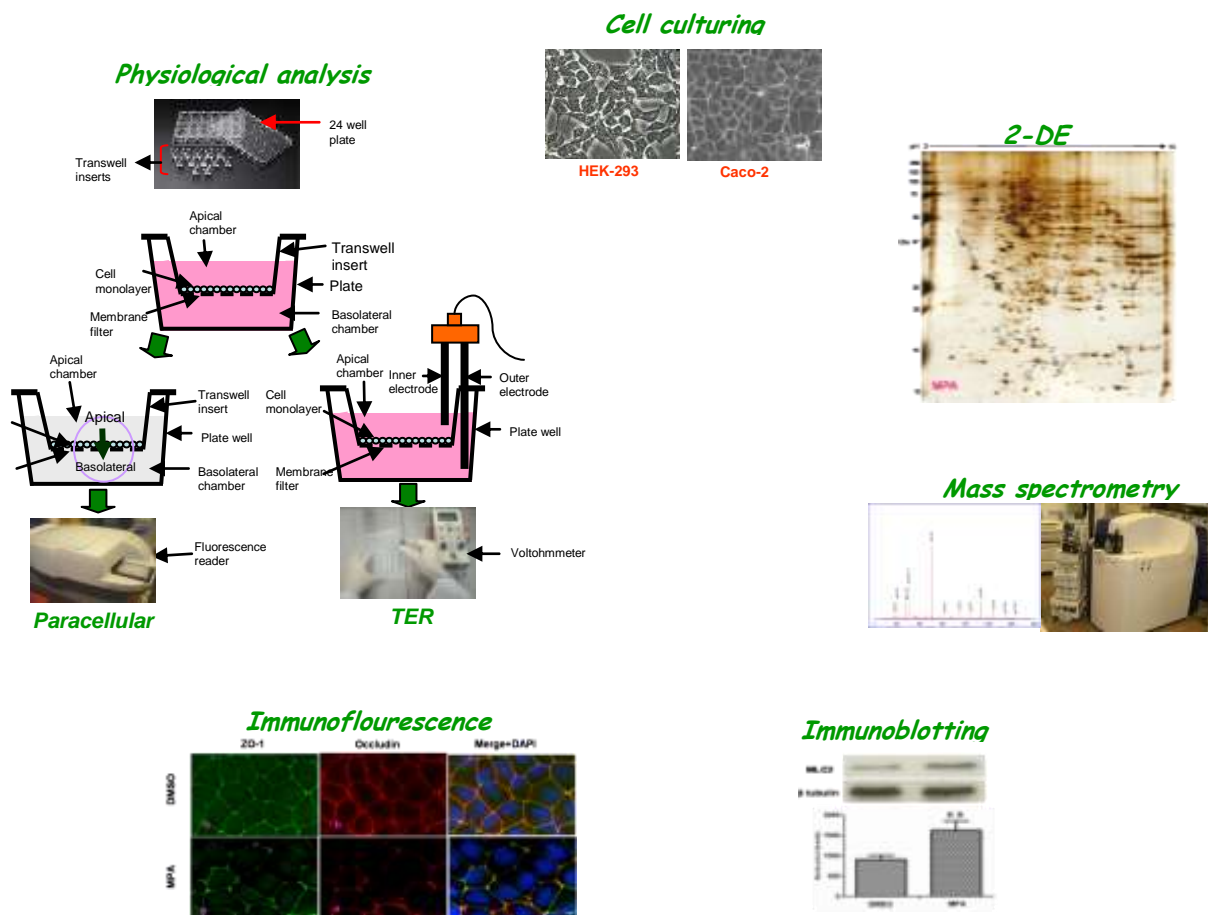


**Figure 4.1: A proteomic approach for identification of novel MPA molecular targets.**

HEK-293 cells were cultured, treated with MPA, whole cell lysates was resolved using 2-DE, and silver stained. Protein spots were densitometrically analysed and differentially expressed proteins were subjected to in-gel digestion and identified by QTOF-MS/MS. The up-regulation of MLC2 by MPA was further confirmed by immunoblot analysis. The functional involvement of MLC2 in MPA mediated barrier defects was determined by physiological assays such as TER and paracellular influx of FITC-dextran using Caco-2 cells monolayers. In addition, the expression and distribution of TJ proteins (ZO-1 and occludin) were also investigated using immunoblotting and immunofluorescence microscopy.

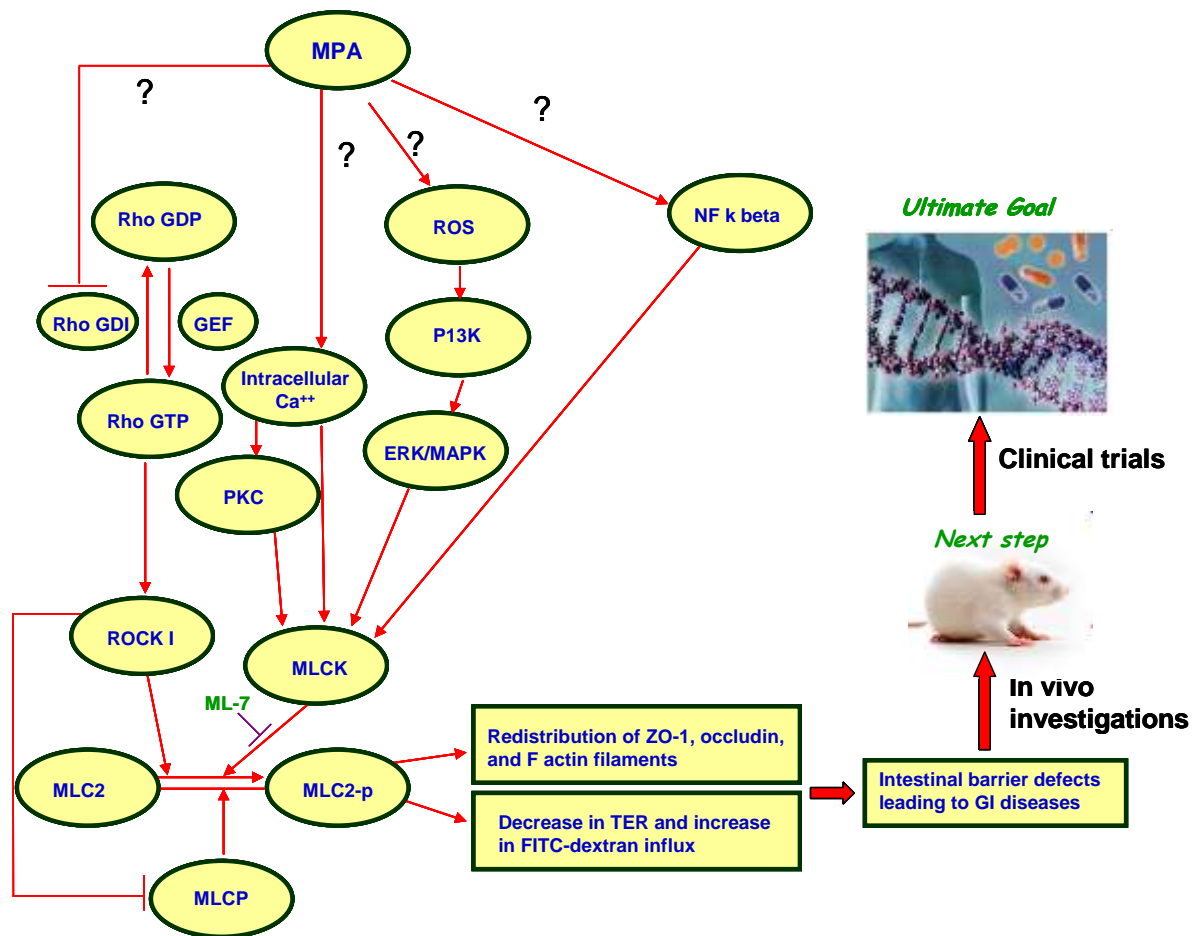


**Figure 4.2: Proposed model of MPA mediated TJ disruption.**

MPA increased MLCK-mediated MLC2 phosphorylation in Caco-2 cell monolayers. MLC2 phosphorylation altered the expression and distribution of TJ proteins (ZO-1 and occludin) that have been identified as a key factor in the development of barrier defects seen in several intestinal diseases. MLC2 phosphorylation also alters the distribution of F actin filaments and the associated TJ disruption results in decreases in TER and increases in paracellular influx. In the present study we observed that MPA disrupted TJ, was associated with increased MLCK expression, and MLC2 phosphorylation. We therefore propose that MPA associated TJ disturbance is dependant on MLCK-driven MLC phosphorylation that leads to decreased expression and redistribution of TJ proteins. Pre-treatment with ML-7 (a specific inhibitor of MLCK) partially prevented the MPA mediated increase in MLC2 phosphorylation, disturbance of TJ proteins, and increase in permeability. We hypothesized that the observed increase in paracellular permeability following MPA treatment is due to TJ disruption caused by MLC2 phosphorylation, which mediates alterations in the expression and distribution of TJ proteins.



## 5. References

1. Bentley R: Mycophenolic Acid: a one hundred year odyssey from antibiotic to immunosuppressant. *Chem Rev* 2000, 100: 3801-3826.
2. Kitchin JE, Pomeranz MK, Pak G, Washenik K, Shupack JL: Rediscovering mycophenolic acid: a review of its mechanism, side effects, and potential uses. *J Am Acad Dermatol* 1997, 37: 445-449.
3. Eugui EM, Almquist SJ, Muller CD, Allison AC: Lymphocyte-selective cytostatic and immunosuppressive effects of mycophenolic acid in vitro: role of deoxyguanosine nucleotide depletion. *Scand J Immunol* 1991, 33: 161-173.
4. Allison AC, Eugui EM: Mycophenolate mofetil and its mechanisms of action. *Immunopharmacology* 2000, 47: 85-118.
5. Sintchak MD, Fleming MA, Futer O, Raybuck SA, Chambers SP, Caron PR et al.: Structure and mechanism of inosine monophosphate dehydrogenase in complex with the immunosuppressant mycophenolic acid. *Cell* 1996, 85: 921-930.
6. Kinsella AR, Smith D, Pickard M: Resistance to chemotherapeutic antimetabolites: a function of salvage pathway involvement and cellular response to DNA damage. *Br J Cancer* 1997, 75: 935-945.
7. Newbold N, Riley B, Hardinger K: A Review of Enteric-coated Mycophenolate Sodium for Renal Transplant Immunosuppression. *Clinical Medicine: Therapeutics* 2009, 1: 927-933.
8. Srinivas TR, Kaplan B, Meier-Kriesche HU: Mycophenolate mofetil in solid-organ transplantation. *Expert Opin Pharmacother* 2003, 4: 2325-2345.
9. Abraham EP: The effect of mycophenolic acid on the growth of *Staphylococcus aureus* in heart broth. *Biochem J* 1945, 39: 398-408.
10. van Hest RM, van GT, Vulto AG, Mathot RA: Population pharmacokinetics of mycophenolic acid in renal transplant recipients. *Clin Pharmacokinet* 2005, 44: 1083-1096.
11. Nowack R, Göbel U, Klooker P, Hergesell O, Andrassy K, van der Woude FJ: Mycophenolate Mofetil for Maintenance Therapy of Wegener's Granulomatosis and Microscopic Polyangiitis: A Pilot Study in 11 Patients with Renal Involvement. *Journal of the American Society of Nephrology* 1999, 10: 1965-1971.
12. Schanz S, Ulmer A, Rassner G, Fierlbeck G: Successful treatment of subacute cutaneous lupus erythematosus with mycophenolate mofetil. *British Journal of Dermatology* 2002, 147: 174-178.
13. Larkin G, Lightman S: Mycophenolate mofetil: A useful immunosuppressive in inflammatory eye disease. *Ophthalmology* 1999, 106: 370-374.

14. Enk AH, Knop J: Treatment of pemphigus vulgaris with mycophenolate mofetil. *The Lancet* 1997, 350: 494.
15. Herrera J, Ferrebuz A, MacGregor EG, Rodriguez-Iturbe B: Mycophenolate mofetil treatment improves hypertension in patients with psoriasis and rheumatoid arthritis. *J Am Soc Nephrol* 2006, 17: S218-S225.
16. Suzuki C, Takahashi M, Morimoto H, Izawa A, Ise H, Hongo M et al.: Mycophenolate mofetil attenuates pulmonary arterial hypertension in rats. *Biochem Biophys Res Commun* 2006, 349: 781-788.
17. Chaudhry V, Cornblath DR, Griffin JW, O'Brien R, Drachman DB: Mycophenolate mofetil: A safe and promising immunosuppressant in neuromuscular diseases. *Neurology* 2001, 56: 94-96.
18. Schneider-Gold C, Hartung HP, Gold R: Mycophenolate mofetil and tacrolimus: New therapeutic options in neuroimmunological diseases. *Muscle & Nerve* 2006, 34: 284-291.
19. Sebastian L, Madhusudana SN, Ravi V, Desai A: Mycophenolic acid inhibits replication of Japanese encephalitis virus. *Chemotherapy* 2011, 57: 56-61.
20. Nicoletti R, De SM, De SS, Trincone A, Marziano F: Antagonism against *Rhizoctonia solani* and fungitoxic metabolite production by some *Penicillium* isolates. *Mycopathologia* 2004, 158: 465-474.
21. Domhan S, Muschal S, Schwager C, Morath C, Wirkner U, Ansorge W et al.: Molecular mechanisms of the antiangiogenic and antitumor effects of mycophenolic acid. *Mol Cancer Ther* 2008, 7: 1656-1668.
22. Akhyani M, Chams-Davatchi C, Hemami MR, Fateh S: Efficacy and safety of mycophenolate mofetil vs. methotrexate for the treatment of chronic plaque psoriasis. *J Eur Acad Dermatol Venereol* 2010, 24: 1447-1451.
23. Zwerner J., Fiorentino D.: Mycophenolate mofetil. *Dermatologic Therapy* 2007, 20: 229-238.
24. Staatz CE, Tett SE: Clinical Pharmacokinetics and Pharmacodynamics of Mycophenolate in Solid Organ Transplant Recipients. *Clinical Pharmacokinetics* 2007, 46: 13-58.
25. Arns W, Breuer S, Choudhury S, Taccard G, Lee J, Binder V et al.: Enteric-coated mycophenolate sodium delivers bioequivalent MPA exposure compared with mycophenolate mofetil. *Clinical Transplantation* 2005, 19: 199-206.
26. Pescovitz M, Conti D, Dunn J, Gonwa T, Halloran P, Sollinger H et al.: Intravenous mycophenolate mofetil: safety, tolerability, and pharmacokinetics. *Clinical Transplantation* 2000, 14: 179-188.
27. Rupprecht K, Schmidt C, Raspé A, Schweda F, Shipkova M, Fischer W et al.: Bioavailability of Mycophenolate Mofetil and Enteric-Coated Mycophenolate Sodium Is Differentially Affected by Pantoprazole in Healthy Volunteers. *The Journal of Clinical Pharmacology* 2009, 49: 1196-1201.

28. Bullingham R, Monroe S, Nicholls A, Hale M: Pharmacokinetics and bioavailability of mycophenolate mofetil in healthy subjects after single-dose oral and intravenous administration. *The Journal of Clinical Pharmacology* 1996, 36: 315-324.
29. Cox VC, Ensom MH: Mycophenolate mofetil for solid organ transplantation: does the evidence support the need for clinical pharmacokinetic monitoring? *Ther Drug Monit* 2003, 25: 137-157.
30. Bullingham RE, Nicholls AJ, Kamm BR: Clinical pharmacokinetics of mycophenolate mofetil. *Clin Pharmacokinet* 1998, 34: 425-455.
31. Shipkova M, Strassburg CP, Braun F, Streit F, Grone HJ, Armstrong VW et al.: Glucuronide and glucoside conjugation of mycophenolic acid by human liver, kidney and intestinal microsomes. *Br J Pharmacol* 2001, 132: 1027-1034.
32. Picard N, Ratanasavanh D, Prémaud A, Le Meur Y, Marquet P: Identification of the udp-glucuronosyltransferase isoforms involved in mycophenolic acid phase ii metabolism. *Drug Metabolism and Disposition* 2005, 33: 139-146.
33. Shipkova M, Armstrong VW, Wieland E, Niedmann PD, Schutz E, Brenner-Weiss G et al.: Identification of glucoside and carboxyl-linked glucuronide conjugates of mycophenolic acid in plasma of transplant recipients treated with mycophenolate mofetil. *Br J Pharmacol* 1999, 126: 1075-1082.
34. Picard N, Cresteil T, Prémaud A, Marquet P: Characterization of a Phase 1 Metabolite of Mycophenolic Acid Produced by CYP3A4/5. *Therapeutic Drug Monitoring* 2004, 26.
35. Nowak I, Shaw LM: Mycophenolic acid binding to human serum albumin: characterization and relation to pharmacodynamics. *Clinical Chemistry* 1995, 41: 1011-1017.
36. Shipkova M, Armstrong VW, Oellerich M, Wieland E: Acyl glucuronide drug metabolites: toxicological and analytical implications. *Ther Drug Monit* 2003, 25: 1-16.
37. Maes BD, Dalle I, Geboes K, Oellerich M, Armstrong VW, Evenepoel P et al.: Erosive enterocolitis in mycophenolate mofetil-treated renal-transplant recipients with persistent afebrile diarrhea. *Transplantation* 2003, 75: 665-672.
38. Takekuma Y, Kakiuchi H, Yamazaki K, Miyauchi S, Kikukawa T, Kamo N et al.: Difference between pharmacokinetics of mycophenolic acid (MPA) in rats and that in humans is caused by different affinities of MRP2 to a glucuronized form. *J Pharm Pharm Sci* 2007, 10: 71-85.
39. Bullingham R, Monroe S, Nicholls A, Hale M: Pharmacokinetics and bioavailability of mycophenolate mofetil in healthy subjects after single-dose oral and intravenous administration. *J Clin Pharmacol* 1996, 36: 315-324.
40. Fulton B, Markham A: Mycophenolate Mofetil: A Review of its Pharmacodynamic and Pharmacokinetic Properties and Clinical Efficacy in Renal Transplantation. *Drugs* 1996, 51.
41. Hesselink DA, Van Hest RM, Mathot RAA, Bonthuis F, Weimar W, De Bruin RWF et al.: Cyclosporine Interacts with Mycophenolic Acid by Inhibiting the Multidrug

Resistance-Associated Protein 2. *American Journal of Transplantation* 2005, 5: 987-994.

42. Arns W, Breuer S, Choudhury S, Taccard G, Lee J, Binder V et al.: Enteric-coated mycophenolate sodium delivers bioequivalent MPA exposure compared with mycophenolate mofetil. *Clin Transplantation* 2005, 19: 199-206.
43. Morath C, Reuter H, Simon V, Krautkramer E, Muranyi W, Schwenger V et al.: Effects of mycophenolic acid on human fibroblast proliferation, migration and adhesion in vitro and in vivo. *Am J Transplant* 2008, 8: 1786-1797.
44. Morath C, Zeier M: Review of the antiproliferative properties of mycophenolate mofetil in non-immune cells. *Int J Clin Pharmacol Ther* 2003, 41: 465-469.
45. Manitpisitkul W, Lee S, Cooper M: Mycophenolic acid agents: is enteric coating the answer? *Transplant Research and Risk Management* 2011, 3: 45-53.
46. Baer PC, Gauer S, Hauser IA, Scherberich JE, Geiger H: Effects of mycophenolic acid on human renal proximal and distal tubular cells in vitro. *Nephrol Dial Transplant* 2000, 15: 184-190.
47. Mohacsi PJ, Tuller D, Hulliger B, Wijngaard PL: Different inhibitory effects of immunosuppressive drugs on human and rat aortic smooth muscle and endothelial cell proliferation stimulated by platelet-derived growth factor or endothelial cell growth factor. *J Heart Lung Transplant* 1997, 16: 484-492.
48. Monguilhott DE, Mendes de Cordova CM, Frode TS: Evidence of an anti-inflammatory effect of mycophenolate mofetil in a murine model of pleurisy. *Exp Lung Res* 2011.
49. Allison AC, Eugui EM: Purine metabolism and immunosuppressive effects of mycophenolate mofetil (MMF). *Clin Transplant* 1996, 10: 77-84.
50. Morath C, Schwenger V, Beimler J, Mehrabi A, Schmidt J, Zeier M et al.: Antifibrotic actions of mycophenolic acid. *Clin Transplant* 2006, 20 Suppl 17: 25-29.
51. Brandhorst G, Brehmer F, Petrova DT, Gross O, Miosge N, Armstrong VW et al.: Mycophenolic acid predose concentrations and renal function in a mouse model for progressive renal fibrosis. *Ther Drug Monit* 2010, 32: 73-78.
52. Petrova DT, Brandhorst G, Brehmer F, Gross O, Oellerich M, Armstrong VW: Mycophenolic acid displays IMPDH-dependent and IMPDH-independent effects on renal fibroblast proliferation and function. *Ther Drug Monit* 2010, 32: 405-412.
53. Tressler RJ, Garvin LJ, Slate DL: Anti-tumor activity of mycophenolate mofetil against human and mouse tumors in vivo. *Int J Cancer* 1994, 57: 568-573.
54. Koehl GE, Wagner F, Stoeltzing O, Lang SA, Steinbauer M, Schlitt HJ et al.: Mycophenolate mofetil inhibits tumor growth and angiogenesis in vitro but has variable antitumor effects in vivo, possibly related to bioavailability. *Transplantation* 2007, 83: 607-614.

55. Floryk D, Huberman E: Mycophenolic acid-induced replication arrest, differentiation markers and cell death of androgen-independent prostate cancer cells DU145. *Cancer Lett* 2006, 231: 20-29.
56. Leckel K, Beecken WD, Jonas D, Oppermann E, Coman MC, Beck KF et al.: The immunosuppressive drug mycophenolate mofetil impairs the adhesion capacity of gastrointestinal tumour cells. *Clin Exp Immunol* 2003, 134: 238-245.
57. Orvis AK, Wesson SK, Breza TS, Church AA, Mitchell CL, Watkins SW: Mycophenolate mofetil in dermatology. *Journal of the American Academy of Dermatology* 2009, 60: 183-199.
58. Davies NM, Grinyo J, Heading R, Maes B, Meier-Kriesche HU, Oellerich M: Gastrointestinal side effects of mycophenolic acid in renal transplant patients: a reappraisal. *Nephrol Dial Transplant* 2007, 22: 2440-2448.
59. Jacqz-Aigrain E, Khan Shaghaghi E, Baudouin V, Popon M, Zhang D, Maisin A et al.: Pharmacokinetics and tolerance of mycophenolate mofetil in renal transplant children. *Pediatric Nephrology* 2000, 14: 95-99.
60. Nguyen T, Park JY, Scudiere JR, Montgomery E: Mycophenolic acid (cellcept and myfortic) induced injury of the upper GI tract. *Am J Surg Pathol* 2009, 33: 1355-1363.
61. McDiarmid SV: Mycophenolate mofetil in liver transplantation. *Clin Transplant* 1996, 10: 140-145.
62. Ducloux D, Ottignon Y, Semhoun-Ducloux S, Labbe S, Saint-Hillier Y, Miguet JP et al.: Mycophenolate mofetil-induced villous atrophy. *Transplantation* 1998, 66: 1115-1116.
63. Kamar N, Faure P, Dupuis E, Cointault O, Joseph-Hein K, Durand D et al.: Villous atrophy induced by mycophenolate mofetil in renal-transplant patients. *Transpl Int* 2004, 17: 463-467.
64. Dost D, van Leerdam ME, van Dekken H, Weimar W, Kuipers EJ, Bijl AH et al.: Crohn's-like enterocolitis associated with mycophenolic acid treatment. *Gut* 2008, 57: 1330.
65. Phatak UP, Seo-Mayer P, Jain D, Selbst M, Husain S, Pashankar DS: Mycophenolate mofetil-induced colitis in children. *J Clin Gastroenterol* 2009, 43: 967-969.
66. Mydlarski PR: Mycophenolate mofetil: a dermatologic perspective. *Skin Therapy Lett* 2005, 10: 1-6.
67. Roche Laboratories Inc.: Important changes in the CellCept® (mycophenolate mofetil) prescribing information: reports of progressive multifocal leukoencephalopathy (PML) in patients treated with CellCept. [http://www.rocheusa.com/products/cellcept/CellceptLetterPML\\_May2008.pdf](http://www.rocheusa.com/products/cellcept/CellceptLetterPML_May2008.pdf) 2008, Accessed March 1, 2009.
68. Neff RT, Hurst FP, Falta EM, Bohlen EM, Lentine KL, Dharnidharka VR et al.: Progressive Multifocal Leukoencephalopathy and Use of Mycophenolate Mofetil After Kidney Transplantation. *Transplantation* 2008, 86.

69. Gross DC, Sasaki TM, Buick MK, Light JA: Acute Respiratory Failure and Pulmonary Fibrosis Secondary To Administration of Mycophenolate Mofetil. *Transplantation* 1997, 64: 1607-9.
70. Roche Laboratories Inc: Important Changes in the CellCept® (mycophenolate mofetil) Prescribing Information - Reports of Pure Red Cell Aplasia (PRCA) in Patients Treated with CellCept . [http://www.genec.com/gene/products/information/cellcept/pdf/DM009\\_Dear\\_Doctor\\_Letter.pdf](http://www.genec.com/gene/products/information/cellcept/pdf/DM009_Dear_Doctor_Letter.pdf) 2009.
71. Pelletier RP, Akin B, Henry ML, Bumgardner GL, Elkhammas EA, Rajab A et al.: The impact of mycophenolate mofetil dosing patterns on clinical outcome after renal transplantation. *Clinical Transplantation* 2003, 17: 200-205.
72. Xia Z, Jun C, Hao C, Bing C, Min S, Jie X: The occurrence of diarrhea not related to the pharmacokinetics of MPA and its metabolites in liver transplant patients. *European Journal of Clinical Pharmacology* 2010, 66: 671-679.
73. Wieland E, Shipkova M, Schellhaas U, Schutz E, Niedmann PD, Armstrong VW et al.: Induction of cytokine release by the acyl glucuronide of mycophenolic acid: a link to side effects? *Clin Biochem* 2000, 33: 107-113.
74. Dost D, van Leerdam ME, van DH, Weimar W, Kuipers EJ, Bijl AH et al.: Crohn's-like enterocolitis associated with mycophenolic acid treatment. *Gut* 2008, 57: 1330.
75. Shipkova M, Armstrong VW, Weber L, Niedmann PD, Wieland E, Haley J et al.: Pharmacokinetics and protein adduct formation of the pharmacologically active acyl glucuronide metabolite of mycophenolic acid in pediatric renal transplant recipients. *The Drug Monit* 2002, 24: 390-399.
76. Asif AR, Armstrong VW, Voland A, Wieland E, Oellerich M, Shipkova M: Proteins identified as targets of the acyl glucuronide metabolite of mycophenolic acid in kidney tissue from mycophenolate mofetil treated rats. *Biochimie* 2007, 89: 393-402.
77. Shipkova M, Beck H, Voland A, Armstrong VW, Grone HJ, Oellerich M et al.: Identification of protein targets for mycophenolic acid acyl glucuronide in rat liver and colon tissue. *Proteomics* 2004, 4: 2728-2738.
78. Shipkova M, Spielbauer B, Voland A, Grone HJ, Armstrong VW, Oellerich M et al.: cDNA microarray analysis reveals new candidate genes possibly linked to side effects under mycophenolate mofetil therapy. *Transplantation* 2004, 78: 1145-1152.
79. Blikslager AT, Moeser AJ, Gookin JL, Jones SL, Odle J: Restoration of Barrier Function in Injured Intestinal Mucosa. *Physiological Reviews* 2007, 87: 545-564.
80. Turner HL, Turner JR: Good fences make good neighbors: Gastrointestinal mucosal structure. *Gut Microbes* 2010, 1: 22-29.
81. Sherwood L: Human physiology: from cells to system. 7th edition. Publisher: Yolanda Cossio 2010.
82. van der Flier LG, Clevers H: Stem Cells, Self-Renewal, and Differentiation in the Intestinal Epithelium. *Annual Review of Physiology* 2009, 71: 241-260.

83. Müller C, Autenrieth I, Peschel A: Intestinal epithelial barrier and mucosal immunity. *Cellular and Molecular Life Sciences* 2005, 62: 1297-1307.
84. Farhadi Ashk, Banan Ali, Fields Jere, Keshavarzian Ali: Intestinal barrier: An interface between health and disease. *Journal of Gastroenterology and Hepatology* 2003, 18: 479-497.
85. Müller C, Autenrieth I, Peschel A: Intestinal epithelial barrier and mucosal immunity. *Cellular and Molecular Life Sciences* 2005, 62: 1297-1307.
86. Bliklager AT, Moeser AJ, Gookin JL, Jones SL, Odle J: Restoration of barrier function in injured intestinal mucosa. *Physiol Rev* 2007, 87: 545-564.
87. Groschwitz KR, Hogan SP: Intestinal barrier function: molecular regulation and disease pathogenesis. *J Allergy Clin Immunol* 2009, 124: 3-20.
88. Smithson KW, Millar DB, Jacobs LR, Gray GM: Intestinal diffusion barrier: unstirred water layer or membrane surface mucous coat? *Science* 1981, 214: 1241-1244.
89. Qin X, Caputo FJ, Xu DZ, Deitch EA: Hydrophobicity of Mucosal Surface and Its Relationship To Gut Barrier Function. *Shock* 2008, 29.
90. Kunzelmann K, Mall M: Electrolyte transport in the mammalian colon: mechanisms and implications for disease. *Physiol Rev* 2002, 82: 245-289.
91. Barrett KE, Keely SJ: Chloride Secretion by the Intestinal Epithelium: Molecular Basis and Regulatory Aspects. *Annual Review of Physiology* 2000, 62: 535-572.
92. Dong-yan L, Weiguo J, Pei L: Reduction of the amount of intestinal secretory IgA in fulminant hepatic failure. *Brazilian Journal of Medical and Biological Research* 2011, 44: 477-482.
93. Greger R: Role of CFTR in the colon. *Annu Rev Physiol* 2000, 62: 467-491.
94. Spitz JC, Ghandi S, Taveras M, Aoyo E, Alverdy JC: Characteristics of the intestinal epithelial barrier during dietary manipulation and glucocorticoid stress. *Critical Care Medicine* 1996, 24: 635-641.
95. Powell DW: Barrier function of epithelia. *Am J Physiol* 1981, G275-88.
96. Van Itallie CM, Anderson JM: Claudins and epithelial paracellular transport. *Annu Rev Physiol* 2006, 68: 403-429.
97. Schneeberger EE, Lynch RD: The tight junction: a multifunctional complex. *Am J Physiol Cell Physiol* 2004, 286: C1213-C1228.
98. Schneeberger EE, Lynch RD: Tight junctions. Their structure, composition, and function. *Circ Res* 1984, 55: 723-733.
99. Gonzalez-Mariscal L, Betanzos A, Nava P, Jaramillo BE: Tight junction proteins. *Prog Biophys Mol Biol* 2003, 81: 1-44.

100. Farquhar MG, Palade GE: Junctional complexes in various epithelia. *JCB* 1963, 17: 375-412.
101. Matter K, Balda MS: Signalling to and from tight junctions. *Nat Rev Mol Cell Biol* 2003, 4: 225-236.
102. Shin K, FVMB: Tight junctions and cell polarity. *Annu Rev Cell Dev Biol* 2006, 207-235.
103. Clayburgh DR, Shen L, Turner JR: A porous defense: the leaky epithelial barrier in intestinal disease. *Lab Invest* 2004, 84: 282-291.
104. Shen L, Weber CR, Raleigh DR, Yu D, Turner JR: Tight Junction Pore and Leak Pathways: A Dynamic Duo. *Annual Review of Physiology* 2011, 73: 283-309.
105. Stevenson BR, Siliciano JD, Mooseker MS, Goodenough DA: Identification of ZO-1: a high molecular weight polypeptide associated with the tight junction (zonula occludens) in a variety of epithelia. *J Cell Biol* 1986, 103: 755-766.
106. Gonzalez-Mariscal L, Betanzos A, Avila-Flores A: MAGUK proteins: structure and role in the tight junction. *Semin Cell Dev Biol* 2000, 11: 315-324.
107. Itoh M, Furuse M, Morita K, Kubota K, Saitou M, Tsukita S: Direct binding of three tight junction-associated MAGUKs, ZO-1, ZO-2, and ZO-3, with the COOH termini of claudins. *J Cell Biol* 1999, 147: 1351-1363.
108. Fanning AS, Jameson BJ, Jesaitis LA, Anderson JM: The tight junction protein ZO-1 establishes a link between the transmembrane protein occludin and the actin cytoskeleton. *J Biol Chem* 1998, 273: 29745-29753.
109. Schulzke JD, Fromm M: Tight junctions: molecular structure meets function. *Ann N Y Acad Sci* 2009, 1165: 1-6.
110. Walsh SV, Hopkins AM, Nusrat A: Modulation of tight junction structure and function by cytokines. *Adv Drug Deliv Rev* 2000, 41: 303-313.
111. Youakim A, Ahdieh M: Interferon-gamma decreases barrier function in T84 cells by reducing ZO-1 levels and disrupting apical actin. *Am J Physiol* 1999, 276: G1279-G1288.
112. Ma TY, Nguyen D, Bui V, Nguyen H, Hoa N: Ethanol modulation of intestinal epithelial tight junction barrier. *Am J Physiol* 1999, 276: G965-G974.
113. Musch MW, Walsh-Reitz MM, Chang EB: Roles of ZO-1, occludin, and actin in oxidant-induced barrier disruption. *Am J Physiol Gastrointest Liver Physiol* 2006, 290: G222-G231.
114. Furuse M, Itoh M, Hirase T, Nagafuchi A, Yonemura S, Tsukita S et al.: Direct association of occludin with ZO-1 and its possible involvement in the localization of occludin at tight junctions. *J Cell Biol* 1994, 127: 1617-1626.
115. Furuse M, Hirase T, Itoh M, Nagafuchi A, Yonemura S, Tsukita S et al.: Occludin: a novel integral membrane protein localizing at tight junctions. *J Cell Biol* 1993, 123: 1777-1788.



116. Sanchez-Pulido L, Martin-Belmonte F, Valencia A, Alonso MA: MARVEL: a conserved domain involved in membrane apposition events. *Trends Biochem Sci* 2002, 27: 599-601.
117. Tavelin S, Hashimoto K, Malkinson J, Lazorova L, Toth I, Artursson P: A new principle for tight junction modulation based on occludin peptides. *Mol Pharmacol* 2003, 64: 1530-1540.
118. Furuse M, Itoh M, Hirase T, Nagafuchi A, Yonemura S, Tsukita S et al.: Direct association of occludin with ZO-1 and its possible involvement in the localization of occludin at tight junctions. *J Cell Biol* 1994, 127: 1617-1626.
119. Al-Sadi R, Khatib K, Guo S, Ye D, Youssef M, Ma T: Occludin regulates macromolecule flux across the intestinal epithelial tight junction barrier. *Am J Physiol Gastrointest Liver Physiol* 2011, 300: G1054-G1064.
120. Ciccocioppo R, Finamore A, Ara C, Di SA, Mengheri E, Corazza GR: Altered expression, localization, and phosphorylation of epithelial junctional proteins in celiac disease. *Am J Clin Pathol* 2006, 125: 502-511.
121. Gassler N, Rohr C, Schneider A, Kartenbeck J, Bach A, Obermuller N et al.: Inflammatory bowel disease is associated with changes of enterocytic junctions. *Am J Physiol Gastrointest Liver Physiol* 2001, 281: G216-G228.
122. Coeffier M, Gloro R, Boukhattala N, Aziz M, Leclaire S, Vandaele N et al.: Increased proteasome-mediated degradation of occludin in irritable bowel syndrome. *Am J Gastroenterol* 2010, 105: 1181-1188.
123. Fries W, Mazzon E, Squarzoni S, Martin A, Martines D, Micali A et al.: Experimental colitis increases small intestine permeability in the rat. *Lab Invest* 1999, 79: 49-57.
124. Gassler N, Rohr C, Schneider A, Kartenbeck J, Bach A, Obermuller N et al.: Inflammatory bowel disease is associated with changes of enterocytic junctions. *Am J Physiol Gastrointest Liver Physiol* 2001, 281: G216-G228.
125. Sakakibara A, Furuse M, Saitou M, Ando-Akatsuka Y, Tsukita S: Possible involvement of phosphorylation of occludin in tight junction formation. *J Cell Biol* 1997, 137: 1393-1401.
126. Rao R: Occludin phosphorylation in regulation of epithelial tight junctions. *Ann N Y Acad Sci* 2009, 1165: 62-8.
127. Wong V: Phosphorylation of occludin correlates with occludin localization and function at the tight junction. *Am J Physiol* 1997, 273: 1859-1867.
128. Rao RK, Basuroy S, Rao VU, Karnaky Jr KJ, Gupta A: Tyrosine phosphorylation and dissociation of occludin-ZO-1 and E-cadherin-beta-catenin complexes from the cytoskeleton by oxidative stress. *Biochem J* 2002, 368: 471-481.
129. Atkinson KJ, Rao RK: Role of protein tyrosine phosphorylation in acetaldehyde-induced disruption of epithelial tight junctions. *Am J Physiol Gastrointest Liver Physiol* 2001, 280: G1280-G1288.

130. Tsukita S, Furuse M, Itoh M: Multifunctional strands in tight junctions. *Nat Rev Mol Cell Biol* 2001, 2: 285-293.
131. Anderson JM, Van Itallie CM: Physiology and function of the tight junction. *Cold Spring Harb Perspect Biol* 2009, 1: a002584.
132. Yamazaki Y, Tokumasu R, Kimura H, Tsukita S: Role of claudin species-specific dynamics in reconstitution and remodeling of the zonula occludens. *Mol Biol Cell* 2011, 22: 1495-1504.
133. McCarthy KM, Francis SA, McCormack JM, Lai J, Rogers RA, Skare IB et al.: Inducible expression of claudin-1-myc but not occludin-VSV-G results in aberrant tight junction strand formation in MDCK cells. *J Cell Sci* 2000, 113 Pt 19: 3387-3398.
134. Fujita H, Chiba H, Yokozaki H, Sakai N, Sugimoto K, Wada T et al.: Differential expression and subcellular localization of claudin-7, -8, -12, -13, and -15 along the mouse intestine. *J Histochem Cytochem* 2006, 54: 933-944.
135. Tamagawa H, Takahashi I, Furuse M, Yoshitake-Kitano Y, Tsukita S, Ito T et al.: Characteristics of claudin expression in follicle-associated epithelium of Peyer's patches: preferential localization of claudin-4 at the apex of the dome region. *Lab Invest* 2003, 83: 1045-1053.
136. Kucharzik T, Walsh SV, Chen J, Parkos CA, Nusrat A: Neutrophil transmigration in inflammatory bowel disease is associated with differential expression of epithelial intercellular junction proteins. *Am J Pathol* 2001, 159: 2001-2009.
137. Burgel N, Bojarski C, Mankertz J, Zeitz M, Fromm M, Schulzke JD: Mechanisms of diarrhea in collagenous colitis. *Gastroenterology* 2002, 123: 433-443.
138. Aktories K, Barbieri JT: Bacterial cytotoxins: targeting eukaryotic switches. *Nat Rev Microbiol* 2005, 3: 397-410.
139. Wang X, Li B, Zhao WD, Liu YJ, Shang DS, Fang WG et al.: Perfluorooctane sulfonate triggers tight junction "opening" in brain endothelial cells via phosphatidylinositol 3-kinase. *Biochem Biophys Res Commun* 2011, 410: 258-263.
140. Wolburg H, Wolburg-Buchholz K, Kraus J, Rascher-Eggstein G, Liebner S, Hamm S et al.: Localization of claudin-3 in tight junctions of the blood-brain barrier is selectively lost during experimental autoimmune encephalomyelitis and human glioblastoma multiforme. *Acta Neuropathol* 2003, 105: 586-592.
141. Takano K, Kojima T, Go M, Murata M, Ichimiya S, Himi T et al.: HLA-DR- and CD11c-positive dendritic cells penetrate beyond well-developed epithelial tight junctions in human nasal mucosa of allergic rhinitis. *J Histochem Cytochem* 2005, 53: 611-619.
142. Assimakopoulos SF, Tsamandas AC, Louvros E, Vagianos CE, Nikolopoulou VN, Thomopoulos KC et al.: Intestinal epithelial cell proliferation, apoptosis and expression of tight junction proteins in patients with obstructive jaundice. *Eur J Clin Invest* 2011, 41: 117-125.

143. Kwon O, Nelson WJ, Sibley R, Huie P, Scandling JD, Dafoe D et al.: Backleak, tight junctions, and cell- cell adhesion in postischemic injury to the renal allograft. *J Clin Invest* 1998, 101: 2054-2064.
144. Sabath E, Denker BM: Cell-cell interactions in the kidney: inducible expression of mutant G protein alpha-subunits in Madin-Darby canine kidney cells for studies of epithelial cell junction structure and function. *Methods Mol Biol* 2006, 341: 61-72.
145. Felinski EA, Antonetti DA: Glucocorticoid regulation of endothelial cell tight junction gene expression: novel treatments for diabetic retinopathy. *Curr Eye Res* 2005, 30: 949-957.
146. Turksen K, Troy TC: Junctions gone bad: claudins and loss of the barrier in cancer. *Biochim Biophys Acta* 2011, 1816: 73-79.
147. Sawada N, Murata M, Kikuchi K, Osanai M, Tobioka H, Kojima T et al.: Tight junctions and human diseases. *Med Electron Microsc* 2003, 36: 147-156.
148. Salim SY, Soderholm JD: Importance of disrupted intestinal barrier in inflammatory bowel diseases. *Inflamm Bowel Dis* 2011, 17: 362-381.
149. Henderson P, van Limbergen JE, Schwarze J, Wilson DC: Function of the intestinal epithelium and its dysregulation in inflammatory bowel disease. *Inflamm Bowel Dis* 2011, 17: 382-395.
150. Clayburgh DR, Barrett TA, Tang Y, Meddings JB, Van Eldik LJ, Watterson DM et al.: Epithelial myosin light chain kinase-dependent barrier dysfunction mediates T cell activation-induced diarrhea in vivo. *J Clin Invest* 2005, 115: 2702-2715.
151. Hering NA, Schulzke JD: Therapeutic options to modulate barrier defects in inflammatory bowel disease. *Dig Dis* 2009, 27: 450-454.
152. Brown GR, Lindberg G, Meddings J, Silva M, Beutler B, Thiele D: Tumor necrosis factor inhibitor ameliorates murine intestinal graft-versus-host disease. *Gastroenterology* 1999, 116: 593-601.
153. Turner JR, Rill BK, Carlson SL, Carnes D, Kerner R, Mrsny RJ et al.: Physiological regulation of epithelial tight junctions is associated with myosin light-chain phosphorylation. *Am J Physiol* 1997, 273: C1378-C1385.
154. Lowe PJ, Miyai K, Steinbach JH, Hardison WG: Hormonal regulation of hepatocyte tight junctional permeability. *Am J Physiol* 1988, 255: G454-G461.
155. Kinoshita N, Takahashi T, Tada S, Shinozuka K, Mizuno N, Takahashi K: Activation of P2Y receptor enhances high-molecular compound absorption from rat ileum. *J Pharm Pharmacol* 2006, 58: 195-200.
156. Nusrat A, Parkos CA, Bacarra AE, Godowski PJ, Delp-Archer C, Rosen EM et al.: Hepatocyte growth factor/scatter factor effects on epithelia. Regulation of intercellular junctions in transformed and nontransformed cell lines, basolateral polarization of c-met receptor in transformed and natural intestinal epithelia, and induction of rapid wound repair in a transformed model epithelium. *J Clin Invest* 1994, 93: 2056-2065.

157. Harhaj NS, Barber AJ, Antonetti DA: Platelet-derived growth factor mediates tight junction redistribution and increases permeability in MDCK cells. *J Cell Physiol* 2002, 193: 349-364.
158. Soler AP, Laughlin KV, Mullin JM: Effects of epidermal growth factor versus phorbol ester on kidney epithelial (LLC-PK1) tight junction permeability and cell division. *Exp Cell Res* 1993, 207: 398-406.
159. Söderholm JD, Perdue MH: II. Stress and intestinal barrier function. *American Journal of Physiology - Gastrointestinal and Liver Physiology* 2001, 280: G7-G13.
160. Ulluwishewa D, Anderson RC, McNabb WC, Moughan PJ, Wells JM, Roy NC: Regulation of Tight Junction Permeability by Intestinal Bacteria and Dietary Components. *J Nutr* 2011, 141: 769-776.
161. Drago S, El Asmar R, Di Pierro M, Grazia Clemente M, Sapone ATA, Thakar M et al.: Gliadin, zonulin and gut permeability: Effects on celiac and non-celiac intestinal mucosa and intestinal cell lines. *Scandinavian Journal of Gastroenterology* 2006, 41: 408-419.
162. Amasheh S, Barmeyer C, Koch CS, Tavalali S, Mankertz J, Epple HJ et al.: Cytokine-dependent transcriptional down-regulation of epithelial sodium channel in ulcerative colitis. *Gastroenterology* 2004, 126: 1711-1720.
163. Barmeyer C, Amasheh S, Tavalali S, Mankertz J, Zeitz M, Fromm M et al.: IL-1beta and TNF alpha regulate sodium absorption in rat distal colon. *Biochem Biophys Res Commun* 2004, 317: 500-507.
164. Schmitz H, Barmeyer C, Gitter AH, Wullstein F, Bentzel CJ, Fromm M et al.: Epithelial barrier and transport function of the colon in ulcerative colitis. *Ann N Y Acad Sci* 2000, 915: 312-326.
165. Grotjohann I, Schmitz H, Fromm M, Schulzke JD: Effect of TNF alpha and IFN gamma on epithelial barrier function in rat rectum in vitro. *Ann N Y Acad Sci* 2000, 915: 282-286.
166. Stefanelli T, Malesci A, Repici A, Vetrano S, Danese S: New insights into inflammatory bowel disease pathophysiology: paving the way for novel therapeutic targets. *Curr Drug Targets* 2008, 9: 413-418.
167. Suenaeert P, Bulteel V, Lemmens L, Noman M, Geypens B, Van AG et al.: Anti-tumor necrosis factor treatment restores the gut barrier in Crohn's disease. *Am J Gastroenterol* 2002, 97: 2000-2004.
168. Zolotarevsky Y, Hecht G, Koutsouris A, Gonzalez DE, Quan C, Tom J et al.: A membrane-permeant peptide that inhibits MLC kinase restores barrier function in vitro models of intestinal disease. *Gastroenterology* 2002, 123: 163-172.
169. Clayburgh DR, Musch MW, Leitges M, Fu YX, Turner JR: Coordinated epithelial NHE3 inhibition and barrier dysfunction are required for TNF-mediated diarrhea in vivo. *J Clin Invest* 2006, 116: 2682-2694.

170. Marchiando AM, Graham WV, Turner JR: Epithelial barriers in homeostasis and disease. *Annu Rev Pathol* 2010, 5: 119-144.
171. Santos J, Yang PC, Söderholm JD, Benjamin M, Perdue MH: Role of mast cells in chronic stress induced colonic epithelial barrier dysfunction in the rat. *Gut* 2001, 48: 630-636.
172. O'Sullivan M, Clayton, Breslin, Harman, Bountra, McLaren et al.: Increased mast cells in the irritable bowel syndrome. *Neurogastroenterology & Motility* 2000, 12: 449-457.
173. Alican I, Kubes P: A critical role for nitric oxide in intestinal barrier function and dysfunction. *American Journal of Physiology - Gastrointestinal and Liver Physiology* 1996, 270: G225-G237.
174. Berkes J, Viswanathan VK, Savkovic SD, Hecht G: Intestinal epithelial responses to enteric pathogens: effects on the tight junction barrier, ion transport, and inflammation. *Gut* 2003, 52: 439-451.
175. García-Lafuente A, Antolín M, Guarner F, Crespo E, Malagelada JR: Modulation of colonic barrier function by the composition of the commensal flora in the rat. *Gut* 2001, 48: 503-507.
176. Davidson G, Kritas S, Butler R: Stressed mucosa. *Nestle Nutr Workshop Ser Pediatr Program* 2007, 59: 133-142.
177. Rao R: Oxidative stress-induced disruption of epithelial and endothelial tight junctions. *Front Biosci* 2008, 1: 7210-26.
178. Anderson JM, Balda MS, Fanning AS: The structure and regulation of tight junctions. *Curr Opin Cell Biol* 1993, 5: 772-778.
179. Balda MS, Gonzalez-Mariscal L, Contreras RG, Macias-Silva M, Torres-Marquez ME, Garcia-Sainz JA et al.: Assembly and sealing of tight junctions: possible participation of G-proteins, phospholipase C, protein kinase C and calmodulin. *J Membr Biol* 1991, 122: 193-202.
180. Madara JL, Parkos C, Colgan S, Nusrat A, Atisook K, Kaoutzani P: The movement of solutes and cells across tight junctions. *Ann N Y Acad Sci* 1992, 664: 47-60.
181. Gonzalez-Mariscal L, Tapia R, Chamorro D: Crosstalk of tight junction components with signaling pathways. *Biochim Biophys Acta* 2008, 1778: 729-756.
182. Anderson JM, Van Itallie CM: Tight junctions and the molecular basis for regulation of paracellular permeability. *Am J Physiol* 1995, 269: G467-G475.
183. Hartsock A, Nelson WJ: Adherens and tight junctions: structure, function and connections to the actin cytoskeleton. *Biochim Biophys Acta* 2008, 1778: 660-669.
184. Shen L, Black ED, Witkowski ED, Lencer WI, Guerriero V, Schneeberger EE et al.: Myosin light chain phosphorylation regulates barrier function by remodeling tight junction structure. *J Cell Sci* 2006, 119: 2095-2106.

185. Madara JL: Intestinal absorptive cell tight junctions are linked to cytoskeleton. *Am J Physiol* 1987, 253: C171-5.
186. Shen L, Su L, Turner JR: Mechanisms and functional implications of intestinal barrier defects. *Dig Dis* 2009, 27: 443-449.
187. Staddon JM, Herrenknecht K, Smales C, Rubin LL: Evidence that tyrosine phosphorylation may increase tight junction permeability. *J Cell Sci* 1995, 108: 609-619.
188. Tsukamoto T, Nigam SK: Role of tyrosine phosphorylation in the reassembly of occludin and other tight junction proteins. *Am J Physiol* 1999, 276: F737-F750.
189. Gopalakrishnan S, Raman N, Atkinson SJ, Marrs JA: Rho GTPase signaling regulates tight junction assembly and protects tight junctions during ATP depletion. *Am J Physiol* 1998, 275: C798-C809.
190. Bruewer M, Hopkins AM, Hobert ME, Nusrat A, Madara JL: RhoA, Rac1, and Cdc42 exert distinct effects on epithelial barrier via selective structural and biochemical modulation of junctional proteins and F-actin. *Am J Physiol Cell Physiol* 2004, 287: C327-C335.
191. Terry S, Nie M, Matter K, Balda MS: Rho signaling and tight junction functions. *Physiology (Bethesda)* 2010, 25: 16-26.
192. Raleigh DR, Boe DM, Yu D, Weber CR, Marchiando AM, Bradford EM et al.: Occludin S408 phosphorylation regulates tight junction protein interactions and barrier function. *J Cell Biol* 2011, 193: 565-582.
193. Fujibe M, Chiba H, Kojima T, Soma T, Wada T, Yamashita T et al.: Thr203 of claudin-1, a putative phosphorylation site for MAP kinase, is required to promote the barrier function of tight junctions. *Exp Cell Res* 2004, 295: 36-47.
194. Nusrat A, Giry M, Turner JR, Colgan SP, Parkos CA, Carnes D et al.: Rho protein regulates tight junctions and perijunctional actin organization in polarized epithelia. *Proceedings of the National Academy of Sciences* 1995, 92: 10629-10633.
195. Al-Sadi R, Ye D, Said HM, Ma TY: Cellular and molecular mechanism of interleukin-1beta modulation of Caco-2 intestinal epithelial tight junction barrier. *J Cell Mol Med* 2011, 15: 970-982.
196. Al-Sadi RM, Ma TY: IL-1beta causes an increase in intestinal epithelial tight junction permeability. *J Immunol* 2007, 178: 4641-4649.
197. Moriez R, Salvador-Cartier C, Theodorou V, Fioramonti J, Eutamene H, Bueno L: Myosin light chain kinase is involved in lipopolysaccharide-induced disruption of colonic epithelial barrier and bacterial translocation in rats. *Am J Pathol* 2005, 167: 1071-1079.
198. Rao RK.: Acetaldehyde-induced barrier disruption and paracellular permeability in Caco-2 cell monolayer. *Methods Mol Biol* 2008, 447: 171-183.

199. Yuhan R, Koutsouris A, Savkovic SD, Hecht G: Enteropathogenic *Escherichia coli*-induced myosin light chain phosphorylation alters intestinal epithelial permeability. *Gastroenterology* 1997, 113: 1873-1882.
200. Manjarrez-Hernandez HA, Baldwin TJ, Williams PH, Haigh R, Knutton S, Aitken A: Phosphorylation of myosin light chain at distinct sites and its association with the cytoskeleton during enteropathogenic *Escherichia coli* infection. *Infect Immun* 1996, 64: 2368-2370.
201. Fedwick JP, Lapointe TK, Meddings JB, Sherman PM, Buret AG: *Helicobacter pylori* activates myosin light-chain kinase to disrupt claudin-4 and claudin-5 and increase epithelial permeability. *Infect Immun* 2005, 73: 7844-7852.
202. Wroblewski LE, Shen L, Ogden S, Romero-Gallo J, Lapierre LA, Israel DA et al.: *Helicobacter pylori* dysregulation of gastric epithelial tight junctions by urease-mediated myosin II activation. *Gastroenterology* 2009, 136: 236-246.
203. Scott KG, Meddings JB, Kirk DR, Lees-Miller SP, Buret AG: Intestinal infection with *Giardia* spp. reduces epithelial barrier function in a myosin light chain kinase-dependent fashion. *Gastroenterology* 2002, 123: 1179-1190.
204. Walsh SV, Hopkins AM, Chen J, Narumiya S, Parkos CA, Nusrat A: Rho kinase regulates tight junction function and is necessary for tight junction assembly in polarized intestinal epithelia. *Gastroenterology* 2001, 121: 566-579.
205. Koizumi Ji, Kojima T, Ogasawara N, Kamekura R, Kurose M, Go M et al.: Protein Kinase C enhances tight junction barrier function of human nasal epithelial cells in primary culture by transcriptional regulation. *Molecular Pharmacology* 2008, 74: 432-442.
206. Banan A, Zhang LJ, Shaikh M, Fields JZ, Choudhary S, Forsyth CB et al.: Theta isoform of protein kinase C Alters barrier function in intestinal epithelium through modulation of distinct claudin isoforms: A novel mechanism for regulation of permeability. *Journal of Pharmacology and Experimental Therapeutics* 2005, 313: 962-982.
207. Turner JR, Angle JM, Black ED, Joyal JL, Sacks DB, Madara JL: PKC-dependent regulation of transepithelial resistance: roles of MLC and MLC kinase. *American Journal of Physiology - Cell Physiology* 1999, 277: C554-C562.
208. Basuroy S, Seth A, Elias B, Naren AP, Rao R: MAPK interacts with occludin and mediates EGF-induced prevention of tight junction disruption by hydrogen peroxide. *Biochem J* 2006, 393: 69-77.
209. Samak G, Aggarwal S, Rao RK: ERK is involved in EGF-mediated protection of tight junctions, but not adherens junctions, in acetaldehyde-treated Caco-2 cell monolayers. *American Journal of Physiology - Gastrointestinal and Liver Physiology* 2011, 301: G50-G59.
210. Cereijido M, Robbins ES, Dolan WJ, Rotunno CA, Sabatini DD: Polarized monolayers formed by epithelial cells on a permeable and translucent support. *J Cell Biol* 1978, 77: 853-880.

211. Balimane PV, Chong S: Cell culture-based models for intestinal permeability: a critique. *Drug Discov Today* 2005, 10: 335-343.
212. Balimane PV, Chong S, Morrison RA: Current methodologies used for evaluation of intestinal permeability and absorption. *J Pharmacol Toxicol Methods* 2000, 44: 301-312.
213. Madara JL: Regulation of the movement of solutes across tight junctions. *Annu Rev Physiol* 1998, 60: 143-159.
214. Weber CR, Raleigh DR, Su L, Shen L, Sullivan EA, Wang Y et al.: Epithelial myosin light chain kinase activation induces mucosal interleukin-13 expression to alter tight junction ion selectivity. *J Biol Chem* 2010, 285: 12037-12046.
215. Yu D, Marchiando AM, Weber CR, Raleigh DR, Wang Y, Shen L et al.: MLCK-dependent exchange and actin binding region-dependent anchoring of ZO-1 regulate tight junction barrier function. *Proc Natl Acad Sci U S A* 2010, 107: 8237-8241.
216. Hidalgo IJ, Raub TJ, Borchardt RT: Characterization of the human colon carcinoma cell line (Caco-2) as a model system for intestinal epithelial permeability. *Gastroenterology* 1989, 96: 736-749.
217. Wilson G, Hassan IF, Dix CJ, Williamson I, Shah R, Mackay M et al.: Transport and permeability properties of human Caco-2 cells: An in vitro model of the intestinal epithelial cell barrier. *Journal of Controlled Release* 1990, 11: 25-40.
218. Sambruy Y, Ferruzza S, Ranaldi G, de A, I: Intestinal cell culture models: applications in toxicology and pharmacology. *Cell Biol Toxicol* 2001, 17: 301-317.
219. Fogh J, Fogh JM, Orfeo T: One hundred and twenty-seven cultured human tumor cell lines producing tumors in nude mice. *J Natl Cancer Inst* 1977, 59: 221-226.
220. Braun A, Hammerle S, Suda K, Rothen-Rutishauser B, Gunthert M, Kramer SD et al.: Cell cultures as tools in biopharmacy. *Eur J Pharm Sci* 2000, 11 Suppl 2: S51-S60.
221. Pinto M., Robine LS., Appay D., Kedinger M., Triadou N., Dussaulx E. et al.: Enterocyte-like differentiation and polarization of the human colon carcinoma cell line Caco-2 in culture. *Biol Cell* 1983, 47: 323-330.
222. Delie F, Rubas W: A human colonic cell line sharing similarities with enterocytes as a model to examine oral absorption: advantages and limitations of the Caco-2 model. *Crit Rev Ther Drug Carrier Syst* 1997, 14: 221-286.
223. Ward PD, Tippin TK, Thakker DR: Enhancing paracellular permeability by modulating epithelial tight junctions. *Pharm Sci Technol Today* 2000, 3: 346-358.
224. Borlak J, Zwadlo C: Expression of drug-metabolizing enzymes, nuclear transcription factors and ABC transporters in Caco-2 cells. *Xenobiotica* 2003, 33: 927-943.
225. Artursson P, Karlsson J: Correlation between oral drug absorption in humans and apparent drug permeability coefficients in human intestinal epithelial (Caco-2) cells. *Biochemical and Biophysical Research Communications* 1991, 175: 880-885.



226. Artursson P: Cell cultures as models for drug absorption across the intestinal mucosa. *Rev Ther Drug Carrier Syst* 1991, 8: 305-330.
227. Quaroni A, Hochman J: Development of intestinal cell culture models for drug transport and metabolism studies. *Advanced Drug Delivery Reviews* 1996, 22: 3-52.
228. Hartmann F, Owen R, Bissell DM: Characterization of isolated epithelial cells from rat small intestine. *Am J Physiol* 1982, 242: G147-G155.
229. Gumbiner B, Simons K: A functional assay for proteins involved in establishing an epithelial occluding barrier: identification of a uvomorulin-like polypeptide. *J Cell Biol* 1986, 102: 457-468.
230. Staddon JM, Herrenknecht K, Smales C, Rubin LL: Evidence that tyrosine phosphorylation may increase tight junction permeability. *J Cell Sci* 1995, 108: 609-619.
231. Lo CM, Keese CR, Giaever I: Cell-substrate contact: another factor may influence transepithelial electrical resistance of cell layers cultured on permeable filters. *Exp Cell Res* 1999, 250: 576-580.
232. Balimane PV, Chong S, Morrison RA: Current methodologies used for evaluation of intestinal permeability and absorption. *Journal of Pharmacological and Toxicological Methods* 2007, 44: 301-312.
233. Harhaj NS, Antonetti DA: Regulation of tight junctions and loss of barrier function in pathophysiology. *The International Journal of Biochemistry & Cell Biology* 2004, 36: 1206-1237.
234. Claude P: Morphological factors influencing transepithelial permeability: A model for the resistance of the Zonula Occludens. *Journal of Membrane Biology* 1978, 39: 219-232.
235. Obert G, Peiffer I, Servin AL: Rotavirus-induced structural and functional alterations in tight junctions of polarized intestinal Caco-2 cell monolayers. *J Virol* 2000, 74: 4645-4651.
236. Al-Sadi R, Ye D, Said HM, Ma TY: Cellular and molecular mechanism of interleukin-1beta modulation of Caco-2 intestinal epithelial tight junction barrier. *J Cell Mol Med* 2011, 15: 970-982.
237. Ma TY, Iwamoto GK, Hoa NT, Akotia V, Pedram A, Boivin MA et al.: TNF-alpha-induced increase in intestinal epithelial tight junction permeability requires NF-kappa B activation. *Am J Physiol Gastrointest Liver Physiol* 2004, 286: G367-G376.
238. Kawedia JD, Jiang M, Kulkarni A, Waechter HE, Matlin KS, Pauletti GM et al.: The protein kinase A pathway contributes to Hg<sup>2+</sup>-induced alterations in phosphorylation and subcellular distribution of occludin associated with increased tight junction permeability of salivary epithelial cell monolayers. *J Pharmacol Exp Ther* 2008, 326: 829-837.
239. Schipper NGM, Vsrum KM, Stenberg P, Ocklind Gr, LennernSs H, Artursson P: Chitosans as absorption enhancers of poorly absorbable drugs: 3: Influence of mucus

- on absorption enhancement. *European Journal of Pharmaceutical Sciences* 1999, 8: 335-343.
240. Cui W, Li LX, Sun CM, Wen Y, Zhou Y, Dong YL et al.: Tumor necrosis factor alpha increases epithelial barrier permeability by disrupting tight junctions in Caco-2 cells. *Braz J Med Biol Res* 2010, 43: 330-337.
  241. Dvorak HF, Nagy JA, Feng D, Brown LF, Dvorak AM: Vascular permeability factor/vascular endothelial growth factor and the significance of microvascular hyperpermeability in angiogenesis. *Curr Top Microbiol Immunol* 1999, 237: 97-132.
  242. Messina E, Gazzaniga P, Micheli V, Guaglianone MR, Barbato S, Morrone S et al.: Guanine nucleotide depletion triggers cell cycle arrest and apoptosis in human neuroblastoma cell lines. *Int J Cancer* 2004, 108: 812-817.
  243. Nagai M, Natsumeda Y, Konno Y, Hoffman R, Irino S, Weber G: Selective up-regulation of type II inosine 5'-monophosphate dehydrogenase messenger RNA expression in human leukemias. *Cancer Res* 1991, 51: 3886-3890.
  244. Park YJ, Ahn HJ, Chang HK, Kim JY, Huh KH, Kim MS et al.: The RhoGDI-alpha/JNK signaling pathway plays a significant role in mycophenolic acid-induced apoptosis in an insulin-secreting cell line. *Cell Signal* 2009, 21: 356-364.
  245. von VS, Ouyang H, Ley K: Mycophenolic acid suppresses granulopoiesis by inhibition of interleukin-17 production. *Kidney Int* 2010, 79-88.
  246. Ha H, Kim MS, Park J, Huh JY, Huh KH, Ahn HJ et al.: Mycophenolic acid inhibits mesangial cell activation through p38 MAPK inhibition. *Life Sci* 2006, 79: 1561-1567.
  247. Heller T, Asif AR, Petrova DT, Doncheva Y, Wieland E, Oellerich M et al.: Differential proteomic analysis of lymphocytes treated with mycophenolic acid reveals caspase 3-induced cleavage of rho GDP dissociation inhibitor 2. *Ther Drug Monit* 2009, 31: 211-217.
  248. Villarroel MC, Hidalgo M, Jimeno A: Mycophenolate mofetil: An update. *Drugs Today (Barc)* 2009, 45: 521-532.
  249. Van den Branden C, Ceysens B, Pauwels M, Van WG, Heirman I, Jie N et al.: Effect of mycophenolate mofetil on glomerulosclerosis and renal oxidative stress in rats. *Nephron Exp Nephrol* 2003, 95: e93-e99.
  250. Stassen PM, Kallenberg CG, Stegeman CA: Use of mycophenolic acid in non-transplant renal diseases. *Nephrol Dial Transplant* 2007, 22: 1013-1019.
  251. Shipkova M, Armstrong VW, Oellerich M, Wieland E: Mycophenolate mofetil in organ transplantation: focus on metabolism, safety and tolerability. *Expert Opin Drug Metab Toxicol* 2005, 1: 505-526.
  252. Bradford MM: A rapid and sensitive method for the quantitation of microgram quantities of protein utilizing the principle of protein-dye binding. *Anal Biochem* 1976, 72: 248-254.

253. Asif AR, Armstrong VW, Voland A, Wieland E, Oellerich M, Shipkova M: Proteins identified as targets of the acyl glucuronide metabolite of mycophenolic acid in kidney tissue from mycophenolate mofetil treated rats. *Biochimie* 2007, 89: 393-402.
254. Gorg A, Obermaier C, Boguth G, Harder A, Scheibe B, Wildgruber R et al.: The current state of two-dimensional electrophoresis with immobilized pH gradients. *Electrophoresis* 2000, 21: 1037-1053.
255. blum H, Beier H, Gross HJ: Improved silver staining of plant proteins, RNA and DNA in polyacrylamide gels. *Electrophoresis* 1987, 8: 93-99.
256. Luhn S, Berth M, Hecker M, Bernhardt J: Using standard positions and image fusion to create proteome maps from collections of two-dimensional gel electrophoresis images. *Proteomics* 2003, 3: 1117-1127.
257. Shevchenko A, Wilm M, Vorm O, Mann M: Mass spectrometric sequencing of proteins silver-stained polyacrylamide gels. *Anal Chem* 1996, 68: 850-858.
258. Tatusov RL, Fedorova ND, Jackson JD, Jacobs AR, Kiryutin B, Koonin EV et al.: The COG database: an updated version includes eukaryotes. *BMC Bioinformatics* 2003, 4: 41.
259. Rozen S, Skaletsky H: Primer3 on the WWW for general users and for biologist programmers. *Methods Mol Biol* 2000, 132: 365-386.
260. Schmittgen TD, Livak KJ: Analyzing real-time PCR data by the comparative C(T) method. *Nat Protoc* 2008, 3: 1101-1108.
261. Hubner GI, Eismann R, Sziegoleit W: Relationship between mycophenolate mofetil side effects and mycophenolic acid plasma trough levels in renal transplant patients. *Arzneimittelforschung* 2000, 50: 936-940.
262. Prat O, Berenguer F, Malard V, Tavan E, Sage N, Steinmetz G et al.: Transcriptomic and proteomic responses of human renal HEK293 cells to uranium toxicity. *Proteomics* 2005, 5: 297-306.
263. MacDonald ML, Lamerdin J, Owens S, Keon BH, Bilter GK, Shang Z et al.: Identifying off-target effects and hidden phenotypes of drugs in human cells. *Nat Chem Biol* 2006, 2: 329-337.
264. Sohn SH, Ko E, Jo Y, Kim SH, Kim Y, Shin M et al.: The genome-wide expression profile of *Paeonia suffruticosa*-treated cisplatin-stimulated HEK 293 cells. *Environ Toxicol Pharmacol* 2009, 28: 453-458.
265. Suizu F, Ueda K, Iwasaki T, Murata-Hori M, Hosoya H: Activation of Action-Activated MgATPase Activity of Myosin II by Phosphorylation with MAPK-Activated Protein Kinase-1b (RSK-2). *Journal of Biochemistry* 2000, 128: 435-440.
266. Mondin M, Moreau V, Genot E, Combe C, Ripoche J, Dubus I: Alterations in cytoskeletal protein expression by mycophenolic acid in human mesangial cells requires Rac inactivation. *Biochem Pharmacol* 2007, 73: 1491-1498.

267. Dubus I, L'Azou B, Gordien M, Delmas Y, Labouyrie JP, Bonnet J et al.: Cytoskeletal reorganization by mycophenolic acid alters mesangial cell migration and contractility. *Hypertension* 2003, 42: 956-961.
268. Yuan SY, Wu MH, Ustinova EE, Guo M, Tinsley JH, De LP et al.: Myosin light chain phosphorylation in neutrophil-stimulated coronary microvascular leakage. *Circ Res* 2002, 90: 1214-1221.
269. Zhao Y, Rhoades RA, Packer CS: Hypoxia-induced pulmonary arterial contraction appears to be dependent on myosin light chain phosphorylation. *Am J Physiol* 1996, 271: L768-L774.
270. Ishii T, Yanagawa T: Stress-induced peroxiredoxins. *Subcell Biochem* 2007, 44: 375-384.
271. Neumann CA, Krause DS, Carman CV, Das S, Dubey DP, Abraham JL et al.: Essential role for the peroxiredoxin Prdx1 in erythrocyte antioxidant defence and tumour suppression. *Nature* 2003, 424: 561-565.
272. Mowbray AL, Kang DH, Rhee SG, Kang SW, Jo H: Laminar shear stress up-regulates peroxiredoxins (PRX) in endothelial cells: PRX 1 as a mechanosensitive antioxidant. *J Biol Chem* 2008, 283: 1622-1627.
273. Schreibelt G, van HJ, Haseloff RF, Reijerkerk A, van der Pol SM, Nieuwenhuizen O et al.: Protective effects of peroxiredoxin-1 at the injured blood-brain barrier. *Free Radic Biol Med* 2008, 45: 256-264.
274. Jung JY, Kang GC, Jeong YJ, Kim SH, Kwak YG, Kim WJ: Proteomic analysis in cyclosporin A-induced overgrowth of human gingival fibroblasts. *Biol Pharm Bull* 2009, 32: 1480-1485.
275. de CM, Silva S, Cruz D, Basso F, Corradi V, Lentini P et al.: Oxidative stress and 'monocyte reprogramming' after kidney transplant: a longitudinal study. *Blood Purif* 2008, 26: 105-110.
276. Land W, Vincenti F: Toxicity-sparing protocols using mycophenolate mofetil in renal transplantation. *Transplantation* 2005, 80: S221-S234.
277. Cao J, Schulte J, Knight A, Leslie NR, Zagozdzon A, Bronson R et al.: Prdx1 inhibits tumorigenesis via regulating PTEN/AKT activity. *EMBO J* 2009, 28: 1505-1517.
278. Yanagawa T, Iwasa S, Ishii T, Tabuchi K, Yusa H, Onizawa K et al.: Peroxiredoxin I expression in oral cancer: a potential new tumor marker. *Cancer Lett* 2000, 156: 27-35.
279. Hoshino I, Matsubara H, Hanari N, Mori M, Nishimori T, Yoneyama Y et al.: Histone deacetylase Inhibitor FK228 activates tumor suppressor Prdx1 with apoptosis induction in esophageal cancer cells. *Clin Cancer Res* 2011, 11: 7945-7952.
280. Rawe VY, Payne C, Schatten G: Profilin and actin-related proteins regulate microfilament dynamics during early mammalian embryogenesis. *Hum Reprod* 2006, 21: 1143-1153.

281. Das T, Bae YH, Wells A, Roy P: Profilin-1 overexpression upregulates PTEN and suppresses AKT activation in breast cancer cells. *J Cell Physiol* 2009, 218: 436-443.
282. Zou L, Ding Z, Roy P: Profilin-1 overexpression inhibits proliferation of MDA-MB-231 breast cancer cells partly through p27kip1 upregulation. *J Cell Physiol* 2010, 223: 623-629.
283. Rubin CI, Atweh GF: The role of stathmin in the regulation of the cell cycle. *J Cell Biochem* 2004, 93: 242-250.
284. Feichtiger H, Wieland E, Armstrong VW, Shipkova M: The acyl glucuronide metabolite of mycophenolic acid induces tubulin polymerization in vitro. *Clin Biochem* 2010, 43: 208-213.
285. Miyashita H, Kanemura M, Yamazaki T, Abe M, Sato Y: Vascular endothelial zinc finger 1 is involved in the regulation of angiogenesis: possible contribution of stathmin/OP18 as a downstream target gene. *Arterioscler Thromb Vasc Biol* 2004, 24: 878-884.
286. Alli E, Yang JM, Hait WN: Silencing of stathmin induces tumor-suppressor function in breast cancer cell lines harboring mutant p53. *Oncogene* 2007, 26: 1003-1012.
287. Liu F, Rong YP, Zeng LC, Zhang X, Han ZG: Isolation and characterization of a novel human thioredoxin-like gene hTLP19 encoding a secretory protein. *Gene* 2003, 315: 71-78.
288. Trotta R, Ciarlariello D, Dal CJ, Allard J, Neviani P, Santhanam R et al.: The PP2A inhibitor SET regulates natural killer cell IFN-gamma production. *J Exp Med* 2007, 204: 2397-2405.
289. Seo SB, McNamara P, Heo S, Turner A, Lane WS, Chakravarti D: Regulation of histone acetylation and transcription by INHAT, a human cellular complex containing the set oncoprotein. *Cell* 2001, 104: 119-130.
290. Sontag E: Protein phosphatase 2A: the Trojan Horse of cellular signaling. *Cell Signal* 2001, 13: 7-16.
291. Neviani P, Santhanam R, Trotta R, Notari M, Blaser BW, Liu S et al.: The tumor suppressor PP2A is functionally inactivated in blast crisis CML through the inhibitory activity of the BCR/ABL-regulated SET protein. *Cancer Cell* 2005, 8: 355-368.
292. Sun XX, Dai MS, Lu H: Mycophenolic acid activation of p53 requires ribosomal proteins L5 and L11. *J Biol Chem* 2008, 283: 12387-12392.
293. Wu D, Ingram A, Lahti JH, Mazza B, Grenet J, Kapoor A et al.: Apoptotic release of histones from nucleosomes. *J Biol Chem* 2002, 277: 12001-12008.
294. Spencer VA, Davie JR: Role of covalent modifications of histones in regulating gene expression. *Gene* 1999, 240: 1-12.
295. Petrova DT, Heller T, Hitt R, Wieland E, Oellerich M, Armstrong VW et al.: Regulation of IL2 and NUCB1 in mononuclear cells treated with acyl glucuronide of mycophenolic

- acid reveals effects independent of inosine monophosphate dehydrogenase inhibition. *Ther Drug Monit* 2009, 31: 31-41.
296. Huang M, Ji Y, Itahana K, Zhang Y, Mitchell B: Guanine nucleotide depletion inhibits pre-ribosomal RNA synthesis and causes nucleolar disruption. *Leuk Res* 2008, 32: 131-141.
  297. Yoshioka N, Wang L, Kishimoto K, Tsuji T, Hu GF: A therapeutic target for prostate cancer based on angiogenin-stimulated angiogenesis and cancer cell proliferation. *Proc Natl Acad Sci U S A* 2006, 103: 14519-14524.
  298. Sanchez-Alcazar JA, Khodjakov A, Schneider E: Anticancer drugs induce increased mitochondrial cytochrome c expression that precedes cell death. *Cancer Res* 2001, 61: 1038-1044.
  299. Taylor PR, Carugati A, Fadok VA, Cook HT, Andrews M, Carroll MC et al.: A hierarchical role for classical pathway complement proteins in the clearance of apoptotic cells in vivo. *J Exp Med* 2000, 192: 359-366.
  300. Botto M, Dell'Agnola C, Bygrave AE, Thompson EM, Cook HT, Petry F et al.: Homozygous C1q deficiency causes glomerulonephritis associated with multiple apoptotic bodies. *Nat Genet* 1998, 19: 56-59.
  301. Matter K, Balda MS: Signalling to and from tight junctions. *Nat Rev Mol Cell Biol* 2003, 4: 225-236.
  302. Steed E, Balda MS, Matter K: Dynamics and functions of tight junctions. *Trends Cell Biol* 2010, 20: 142-149.
  303. Catalioto RM, Maggi CA, Giuliani S: Intestinal epithelial barrier dysfunction in disease and possible therapeutical interventions. *Curr Med Chem* 2011, 18: 398-426.
  304. Shin K, Fogg VC, Margolis B: Tight junctions and cell polarity. *Annu Rev Cell Dev Biol* 2006, 22: 207-235.
  305. Helderman JH: Prophylaxis and treatment of gastrointestinal complications following transplantation. *Clin Transplant* 2001, 15 Suppl 4: 29-35.
  306. Arslan H, Inci EK, Azap OK, Karakayali H, Torgay A, Haberal M: Etiologic agents of diarrhea in solid organ recipients. *Transpl Infect Dis* 2007, 9: 270-275.
  307. Helderman JH, Goral S: Gastrointestinal complications of transplant immunosuppression. *J Am Soc Nephrol* 2002, 13: 277-287.
  308. Ponticelli C, Passerini P: Gastrointestinal complications in renal transplant recipients. *Transpl Int* 2005, 18: 643-650.
  309. Dalle IJ, Maes BD, Geboes KP, Lemahieu W, Geboes K: Crohn's-like changes in the colon due to mycophenolate? *Colorectal Dis* 2005, 7: 27-34.
  310. Maes BD, Dalle I, Geboes K, Oellerich M, Armstrong VW, Evenepoel P et al.: Erosive enterocolitis in mycophenolate mofetil-treated renal-transplant recipients with persistent afebrile diarrhea. *Transplantation* 2003, 75: 665-672.

311. Papadimitriou JC, Cangro CB, Lustberg A, Khaled A, Nogueira J, Wiland A et al.: Histologic features of mycophenolate mofetil-related colitis: a graft-versus-host disease-like pattern. *Int J Surg Pathol* 2003, 11: 295-302.
312. Kim HC, Park SB: Mycophenolate mofetil-induced ischemic colitis. *Transplant Proc* 2000, 32: 1896-1897.
313. Clayburgh DR, Shen L, Turner JR: A porous defense: the leaky epithelial barrier in intestinal disease. *Lab Invest* 2004, 84: 282-291.
314. Alvarez-Hernandez X, Nichols GM, Glass J: Caco-2 cell line: a system for studying intestinal iron transport across epithelial cell monolayers. *Biochimica et Biophysica Acta (BBA) - Biomembranes* 1991, 1070: 205-208.
315. Peterson MD, Mooseker MS: Characterization of the enterocyte-like brush border cytoskeleton of the C2BBE clones of the human intestinal cell line, Caco-2. *Journal of Cell Science* 1992, 102: 581-600.
316. Levy P, Robin H, Bertrand F, Kornprobst M, Capeau J: Butyrate-treated colonic Caco-2 cells exhibit defective integrin-mediated signaling together with increased apoptosis and differentiation. *J Cell Physiol* 2003, 197: 336-347.
317. Koeneman BA, Zhang Y, Westerhoff P, Chen Y, Crittenden JC, Capco DG: Toxicity and cellular responses of intestinal cells exposed to titanium dioxide. *Cell Biol Toxicol* 2010, 26: 225-238.
318. Schlegel N, Burger S, Golenhofen N, Walter U, Drenckhahn D, Waschke J: The role of VASP in regulation of cAMP- and Rac 1-mediated endothelial barrier stabilization. *Am J Physiol Cell Physiol* 2008, 294: C178-C188.
319. Schlegel N, Meir M, Spindler V, Germer CT, Waschke J: Differential role of Rho GTPases in intestinal epithelial barrier regulation in vitro. *J Cell Physiol* 2011, 226: 1196-1203.
320. Rozen S SH: Primer3 on the WWW for general users and for biologist programmers. *Methods Mol Bio* 2000, 132: 365-386.
321. Dodane V, Amin KM, Merwin JR: Effect of chitosan on epithelial permeability and structure. *Int J Pharm* 1999, 182: 21-32.
322. Ranaldi G, Marigliano I, Vespignani I, Perozzi G, Sambuy Y: The effect of chitosan and other polycations on tight junction permeability in the human intestinal Caco-2 cell line(1). *J Nutr Biochem* 2002, 13: 157-167.
323. Qasim M, Rahman H, Oellerich M, Asif A: Differential proteome analysis of human embryonic kidney cell line (HEK-293) following mycophenolic acid treatment. *Proteome Science* 2011, 9: 57.
324. Turner JR, Black ED, Ward J, Tse CM, Uchwat FA, Alli HA et al.: Transepithelial resistance can be regulated by the intestinal brush-border Na<sup>+</sup>/H<sup>+</sup> exchanger NHE3. *American Journal of Physiology - Cell Physiology* 2000, 279: C1918-C1924.

325. Jain S, Suzuki T, Seth A, Samak G, Rao R: Protein kinase C phosphorylates occludin and promotes assembly of epithelial tight junctions. *Biochemical Journal* 2011, 437: 289-299.
326. Madara JL, Pappenheimer JR: Structural basis for physiological regulation of paracellular pathways in intestinal epithelia. *J Membr Biol* 1987, 100: 149-164.
327. Xu Lf, Xu C, Mao ZQ, Teng X, Ma L, Sun M: Disruption of the F-actin cytoskeleton and monolayer barrier integrity induced by PAF and the protective effect of ITF on intestinal epithelium. *Archives of Pharmacol Research* 2011, 34: 245-251.
328. Ma TY, Hoa NT, Tran DD, Bui V, Pedram A, Mills S et al.: Cytochalasin B modulation of Caco-2 tight junction barrier: role of myosin light chain kinase. *Am J Physiol Gastrointest Liver Physiol* 2000, 279: G875-G885.
329. Feighery LM, Cochrane SW, Quinn T, Baird AW, O'Toole D, Owens SE et al.: Myosin light chain kinase inhibition: correction of increased intestinal epithelial permeability in vitro. *Pharm Res* 2008, 25: 1377-1386.
330. Schliwa M: Action of cytochalasin D on cytoskeletal networks. *J Cell Biol* 1982, 92: 79-91.
331. Scott KGE, Meddings JB, Kirk DR, Lees-Miller SP, Buret AG: Intestinal infection with *Giardia* spp. reduces epithelial barrier function in a myosin light chain kinase-dependent fashion. *Gastroenterology* 2002, 123: 1179-1190.
332. Subramanian VS, Marchant JS, Ye D, Ma TY, Said HM: Tight junction targeting and intracellular trafficking of occludin in polarized epithelial cells. *American Journal of Physiology - Cell Physiology* 2007, 293: C1717-C1726.
333. Shimizu M.: Interaction between food substances and the intestinal epithelium. *Biosci Biotechnol Biochem* 2010, 74: 232-241.
334. Duggan C, Gannon J, Walker WA: Protective nutrients and functional foods for the gastrointestinal tract. *Am J Clin Nutr* 2002, 75: 789-808.
335. Clayburgh DR, Barrett TA, Tang Y, Meddings JB, Van Eldik LJ, Watterson DM et al.: Epithelial myosin light chain kinase-dependent barrier dysfunction mediates T cell activation-induced diarrhea in vivo. *J Clin Invest* 2005, 115: 2702-2715.
336. Dunlop SP, Hebden J, Campbell E, Naesdal J, Olbe L, Perkins AC et al.: Abnormal intestinal permeability in subgroups of diarrhea-predominant irritable bowel syndromes. *Am J Gastroenterol* 2006, 101: 1288-1294.
337. Clayburgh DR, Barrett TA, Tang Y, Meddings JB, Van Eldik LJ, Watterson DM et al.: Epithelial myosin light chain kinase-dependent barrier dysfunction mediates T cell activation-induced diarrhea in vivo. *J Clin Invest* 2005, 115: 2702-2715.
338. Davies NM, Grinyo J, Heading R, Maes B, Meier-Kriesche HU, Oellerich M: Gastrointestinal side effects of mycophenolic acid in renal transplant patients: a reappraisal. *Nephrol Dial Transplant* 2007, 22: 2440-2448.

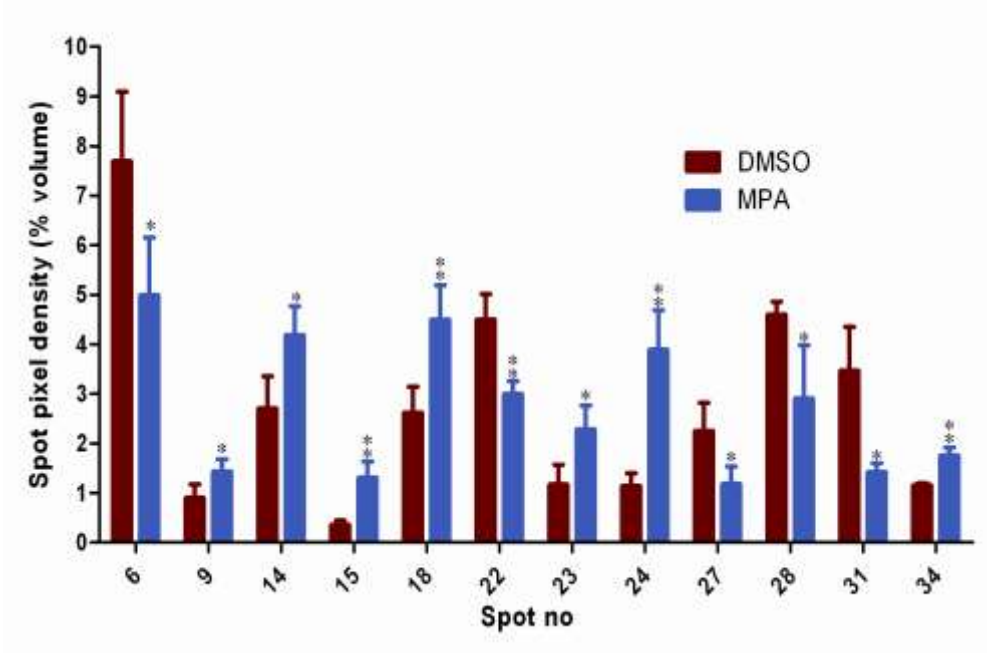


339. Parfitt JR, Jayakumar S, Driman DK: Mycophenolate mofetil-related gastrointestinal mucosal injury: variable injury patterns, including graft-versus-host disease-like changes. *Am J Surg Pathol* 2008, 32: 1367-1372.
340. Dalle IJ, Maes BD, Geboes KP, Lemahieu W, Geboes K: Crohn's-like changes in the colon due to mycophenolate? *Colorectal Dis* 2005, 7: 27-34.
341. Sambuy Y, de A, I, Ranaldi G, Scarino ML, Stammati A, Zucco F: The Caco-2 cell line as a model of the intestinal barrier: influence of cell and culture-related factors on Caco-2 cell functional characteristics. *Cell Biol Toxicol* 2005, 21: 1-26.
342. van Breemen RB, Li Y: Caco-2 cell permeability assays to measure drug absorption. *Expert Opin Drug Metab Toxicol* 2005, 1: 175-185.
343. von Bonsdorff CH, Fuller SD, Simons K: Apical and basolateral endocytosis in Madin-Darby canine kidney (MDCK) cells grown on nitrocellulose filters. *EMBO J* 1985, 4: 2781-2792.
344. Malinowski M, Martus P, Lock JF, Neuhaus P, Stockmann M: Systemic influence of immunosuppressive drugs on small and large bowel transport and barrier function. *Transpl Int* 2011, 24: 184-193.
345. Furuse M, Itoh M, Hirase T, Nagafuchi A, Yonemura S, Tsukita S et al.: Direct association of occludin with ZO-1 and its possible involvement in the localization of occludin at tight junctions. *J Cell Biol* 1994, 127: 1617-1626.
346. Wang F, Graham WV, Wang Y, Witkowski ED, Schwarz BT, Turner JR: Interferon-gamma and tumor necrosis factor-alpha synergize to induce intestinal epithelial barrier dysfunction by up-regulating myosin light chain kinase expression. *Am J Pathol* 2005, 166: 409-419.
347. Saitoh M, Ishikawa T, Matsushima S, Naka M, Hidaka H: Selective inhibition of catalytic activity of smooth muscle myosin light chain kinase. *J Biol Chem* 1987, 262: 7796-7801.
348. Guntaka SR, Samak G, Seth A, Larusso NF, Rao R: Epidermal growth factor protects the apical junctional complexes from hydrogen peroxide in bile duct epithelium. *Lab Invest* 2011.
349. Stevenson BR, Begg DA: Concentration-dependent effects of cytochalasin D on tight junctions and actin filaments in MDCK epithelial cells. *Journal of Cell Science* 1994, 107: 367-375.
350. Subramanian VS, Marchant JS, Ye D, Ma TY, Said HM: Tight junction targeting and intracellular trafficking of occludin in polarized epithelial cells. *Am J Physiol Cell Physiol* 2007, 293: C1717-C1726.

# 6. Appendix

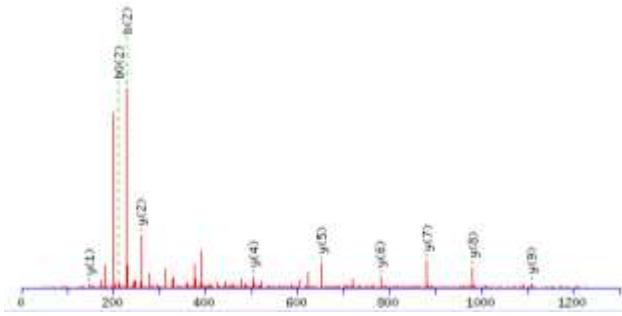
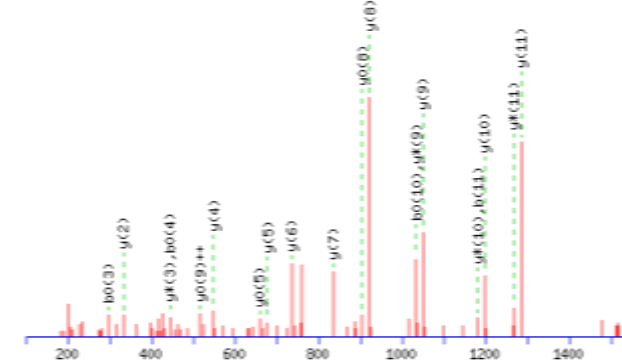

**Figure 5.1: A graphical representation of relative abundance (% volume) of all differentially regulated proteins.**

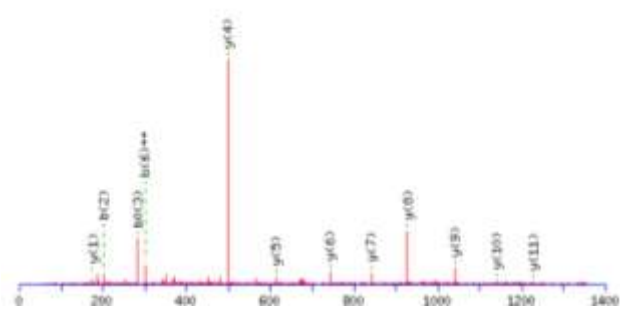
Relative abundance of the proteins differentially expressed in DMSO and MPA treated HEK-293 cells. Results shown as mean of four independent experiments (\*p < 0.05 or \*\*p < 0.005).



**Table 5.1: MS/MS analysis table of all differentially regulated proteins.**

Spot no: the spot identification number on 2-DE; Accession no: Swiss-prot protein identification number; Sequence coverage: the percentage of the protein's sequence represented by the peptides identified by MS/MS; MS/MS analysis: peptides sequences (bold & red) identified for a particular protein, including MS/MS queries, and the MS/MS spectra of an exemplary peptide.

Spot no.	Accession no.	Sequence Coverage	Protein name	MS/MS Analysis																																																	
6	Q01105	11	Protein SET	<p>1 MAPKRQSPPLP PQKKKPRPPP ALGPEETSAS AGLPKKGEKE QQEAIHIDE                      51 VQNEIDRLNE <b>QASEILK</b>VE QKYNKLRQPF FQKRSELIK IPNFVWTFV                      101 NHPQVSALLG EEDEEALHYL TR<b>VEVTEFED</b>IKSGYRIDFY FDENPYFENK                      151 VLSK<b>EFHLNE</b> <b>SGDPSK</b>STE IKWKSGKDLT KRSSQTQNK SRKRQHEEPE                      201 SFTWFTDHS DAGADELGEV IKDDIWPNPL QYYLVPDMD EEEGEEEDDD                      251 DDEEEEGLED IDEEGDEDEG EEDEDDDEGE EGEDEGEDD</p> <table border="1"> <thead> <tr> <th>Start-End</th> <th>Observed</th> <th>Mr(expt)</th> <th>Mr(calc)</th> <th>Delta</th> <th>Miss</th> <th>Sequence</th> </tr> </thead> <tbody> <tr> <td>58 - 68</td> <td>637.3448</td> <td>1272.6750</td> <td>1272.6561</td> <td>0.0190</td> <td>0</td> <td>R.LNEQASEEILK.V</td> </tr> <tr> <td>123 - 132</td> <td>604.8156</td> <td>1207.6166</td> <td>1207.5972</td> <td>0.0194</td> <td>0</td> <td>R.VEVTEFEDIK.S</td> </tr> <tr> <td>155 - 167</td> <td>482.8923</td> <td>1445.6551</td> <td>1445.6423</td> <td>0.0128</td> <td>0</td> <td>K.EFHLNESGDPSK.S</td> </tr> </tbody> </table> <p>MS/MS Fragmentation of <b>VEVTEFEDIK</b></p> 	Start-End	Observed	Mr(expt)	Mr(calc)	Delta	Miss	Sequence	58 - 68	637.3448	1272.6750	1272.6561	0.0190	0	R.LNEQASEEILK.V	123 - 132	604.8156	1207.6166	1207.5972	0.0194	0	R.VEVTEFEDIK.S	155 - 167	482.8923	1445.6551	1445.6423	0.0128	0	K.EFHLNESGDPSK.S																					
Start-End	Observed	Mr(expt)	Mr(calc)	Delta	Miss	Sequence																																															
58 - 68	637.3448	1272.6750	1272.6561	0.0190	0	R.LNEQASEEILK.V																																															
123 - 132	604.8156	1207.6166	1207.5972	0.0194	0	R.VEVTEFEDIK.S																																															
155 - 167	482.8923	1445.6551	1445.6423	0.0128	0	K.EFHLNESGDPSK.S																																															
9	Q07021	9	Complement component 1 Q subcomponent-binding protein, mitochondrial	<p>1 MLPLLRVCPV VLGSSVAGLR AAAPASPFRR LLQPAPRLCT RPFGLLSVRA                      51 GSERRPGLLR PRGPCACGCG CGSLHTDGDK AFVDFLSDEI KEERKIQKHK                      101 TLPK<b>MSGGWE</b> <b>LELNGTEAK</b>L VRKVAGEKIT VTFNINNSIP PTFDGEIEPS                      151 QGQKVEEQEP ELTSTPNFVV EVIKNDDGKK ALVLDCHYPE DEVGQDEAE                      201 SDIFSIRE<b>EV</b> <b>FQSTGESEWK</b> DTNYTLNTDS LDWALYDHLM DFLADRGVND                      251 TFADELVELS TALEHQEYIT FLEDLKSFKV SQ</p> <table border="1"> <thead> <tr> <th>Start-End</th> <th>Observed</th> <th>Mr(expt)</th> <th>Mr(calc)</th> <th>Delta</th> <th>Miss</th> <th>Sequence</th> </tr> </thead> <tbody> <tr> <td>105-119</td> <td>819.3414</td> <td>1636.6682</td> <td>1636.7403</td> <td>-0.0720</td> <td>0</td> <td>K.MSGGWELELNGTEAK.L</td> </tr> <tr> <td>208 - 220</td> <td>757.3123</td> <td>1512.6100</td> <td>1512.6732</td> <td>-0.0632</td> <td>0</td> <td>R.EVSFQSTGESEWK.D</td> </tr> </tbody> </table> <p>MS/MS Fragmentation of <b>EVSFQSTGESEWK</b></p> 	Start-End	Observed	Mr(expt)	Mr(calc)	Delta	Miss	Sequence	105-119	819.3414	1636.6682	1636.7403	-0.0720	0	K.MSGGWELELNGTEAK.L	208 - 220	757.3123	1512.6100	1512.6732	-0.0632	0	R.EVSFQSTGESEWK.D																												
Start-End	Observed	Mr(expt)	Mr(calc)	Delta	Miss	Sequence																																															
105-119	819.3414	1636.6682	1636.7403	-0.0720	0	K.MSGGWELELNGTEAK.L																																															
208 - 220	757.3123	1512.6100	1512.6732	-0.0632	0	R.EVSFQSTGESEWK.D																																															
14	P38117	22	Electron transfer flavoprotein subunit beta	<p>1 MAELRVLVAV KRVIDYAVKI RVKPDRT<b>GVV</b> <b>TDGVK</b>HSMNP FCEIAVEEAV                      51 RLKEKLVKE VIAVSCGPAQ CQETIR<b>TALA</b> <b>MGADR</b>GIHVE VPPAEAE<b>RLG</b>                      101 <b>PLQVAR</b>VLAK LAEKEKVDLV LLGQAIDDD CNQTGQMTAG FLDWPGGTFA                      151 SQVTLEGDKL KVER<b>EIDGGL</b> <b>ETLRL</b>KLPAV VTADLRLNEP RYATLPNIMK                      201 AKKKKIEVIK PGDLGVDLTS <b>KLSVISVEDP</b> <b>PQRTAGVK</b><b>VE</b> <b>TEDLVA</b>KLK                      251 EIGRI</p> <table border="1"> <thead> <tr> <th>Start-End</th> <th>Observed</th> <th>Mr(expt)</th> <th>Mr(calc)</th> <th>Delta</th> <th>Miss</th> <th>Sequence</th> </tr> </thead> <tbody> <tr> <td>27 - 35</td> <td>438.2605</td> <td>874.5064</td> <td>874.4760</td> <td>0.0304</td> <td>0</td> <td>R.TGVVTDGVK.H</td> </tr> <tr> <td>77 - 85</td> <td>461.2477</td> <td>920.4808</td> <td>920.4386</td> <td>0.0423</td> <td>0</td> <td>R.TALAMGADR.G</td> </tr> <tr> <td>99 - 106</td> <td>427.2842</td> <td>852.5538</td> <td>852.5181</td> <td>0.0357</td> <td>0</td> <td>R.LGPLQVAR.V</td> </tr> <tr> <td>165 - 174</td> <td>551.8152</td> <td>1101.6158</td> <td>1101.5666</td> <td>0.0493</td> <td>0</td> <td>R.EIDGGLLETLR.L</td> </tr> <tr> <td>222 - 233</td> <td>670.3985</td> <td>1338.7824</td> <td>1338.7143</td> <td>0.0681</td> <td>0</td> <td>K.LSVISVEDPPQR.T</td> </tr> <tr> <td>239 - 248</td> <td>552.8170</td> <td>1103.6194</td> <td>1103.5710</td> <td>0.0484</td> <td>0</td> <td>K.VETTEDLVAK.L</td> </tr> </tbody> </table> <p>MS/MS Fragmentation of <b>LSVISVEDPPQR</b></p> 	Start-End	Observed	Mr(expt)	Mr(calc)	Delta	Miss	Sequence	27 - 35	438.2605	874.5064	874.4760	0.0304	0	R.TGVVTDGVK.H	77 - 85	461.2477	920.4808	920.4386	0.0423	0	R.TALAMGADR.G	99 - 106	427.2842	852.5538	852.5181	0.0357	0	R.LGPLQVAR.V	165 - 174	551.8152	1101.6158	1101.5666	0.0493	0	R.EIDGGLLETLR.L	222 - 233	670.3985	1338.7824	1338.7143	0.0681	0	K.LSVISVEDPPQR.T	239 - 248	552.8170	1103.6194	1103.5710	0.0484	0	K.VETTEDLVAK.L
Start-End	Observed	Mr(expt)	Mr(calc)	Delta	Miss	Sequence																																															
27 - 35	438.2605	874.5064	874.4760	0.0304	0	R.TGVVTDGVK.H																																															
77 - 85	461.2477	920.4808	920.4386	0.0423	0	R.TALAMGADR.G																																															
99 - 106	427.2842	852.5538	852.5181	0.0357	0	R.LGPLQVAR.V																																															
165 - 174	551.8152	1101.6158	1101.5666	0.0493	0	R.EIDGGLLETLR.L																																															
222 - 233	670.3985	1338.7824	1338.7143	0.0681	0	K.LSVISVEDPPQR.T																																															
239 - 248	552.8170	1103.6194	1103.5710	0.0484	0	K.VETTEDLVAK.L																																															



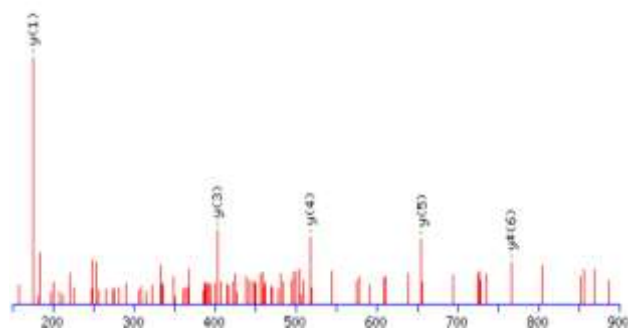
15 P47985 16

Cytochrome b-c1 complex subunit Rieske, mitochondrial

1 MLSVASRSGP FAPVLSATSR GVAGALRPLV QATVPATPEQ PVLDLKRPF  
 51 SRESLSGQAV RRPLVASVGL NVPASVCYSH TDIKVPDFSE YRRLEVLDS  
 101 KSSRESSEAR KGFSYLVTGV TTVGVAYAANK NAVTQFVSSM SASADVLALA  
 151 KIEIKLSDIP EGKNMAFKWR GKPLFVVRHRT QKEIEQEAAV ELSQLRDPQH  
 201 DLDRVKKPEW VILIGVCTHL GCVPIANAGD FGGYYCPCGH SHYDASGRIR  
 251 LGPAPLNLEV PTYEFTSDDM VIVG

Start-End	Observed	Mr(expt)	Mr(calc)	Delta	Miss	Sequence
85 - 92	506.7550	1011.4954	1011.4662	0.0293	0	K.VPDFSEYR.R
93 - 101	530.8184	1059.6222	1059.5924	0.0298	1	R.RLEVLDSK.S
94 - 101	452.7524	903.4902	903.4913	-0.0011	0	R.LEVLDSK.S
171 - 177	408.7669	815.5192	815.5018	0.0175	0	R.GKPLFVR.H
183 - 196	807.9452	1613.8758	1613.8260	0.0498	0	K.EIEQEAAVELSQLR.D
197 - 204	498.2446	994.4746	994.4468	0.0278	0	R.DPQHDLDR.V

MS/MS Fragmentation of DPQHDLDR



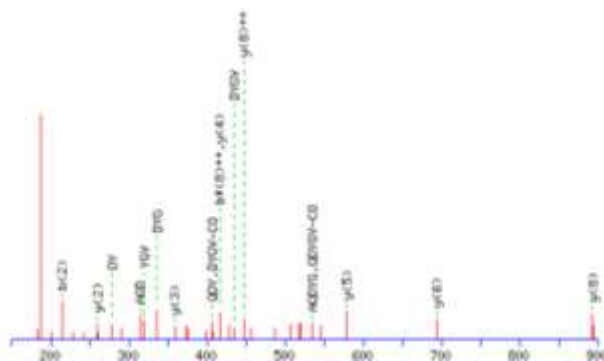
18 Q06830 10

Peroxiredoxin-1

1 MSSGNAKIGH PPNFKATAV MPDGGFKDIS LSDYKGYVVF FFFYPLDFTF  
 51 VCPTEIIAFS DRAEEFKKLN CQVIGASVDS HFCHLAWVNT PPKQGGGLGPM  
 101 NIPLVSDPKR TIAQDYGVLK ADEGISFRGL FIIDDKGILR QITVNDLPVG  
 151 RSVDELRLV QAFQFTDKHG EVCPAGWKPG SDTIKPDVQK SKEYFSKQK

Start-End	Observed	Mr(expt)	Mr(calc)	Delta	Miss	Sequence
111 - 120	554.2855	1106.5564	1106.5972	-0.0407	0	R.TIAQDYGVLK.A
141 - 151	606.3233	1210.6320	1210.6670	-0.0349	0	R.QITVNDLPVGR.S

MS/MS Fragmentation of TIAQDYGVLK.



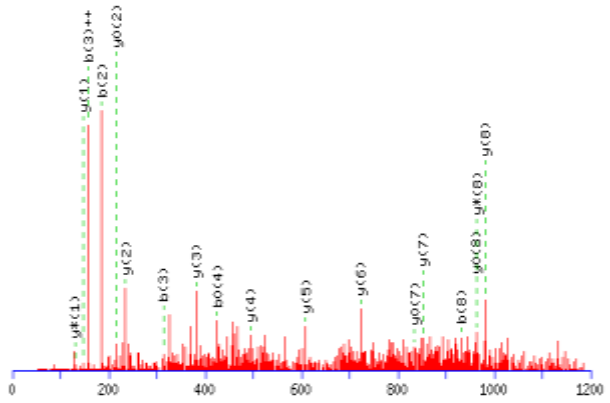
22 P16949 18

Stathmin

1 MASSDIQVKE LEKRASGQAF ELILSPRSKE SVPEFPLSPP KKKDLSLEEI  
 51 QKLEAAEER RKSHEAEVLK QLAEKREHEK EVLQKAIEN NNFSKMAEEK  
 101 LTHKMEANKE NREAQMAAKL ERLREKDKHI EEVRKNKESK DPADETEAD

Start-End	Observed	Mr(expt)	Mr(calc)	Delta	Miss	Sequence
44 - 52	537.7797	1073.5448	1073.5604	-0.0156	0	K.DLSLEEEIK.
53 - 60	473.2399	944.4652	944.4927	-0.0274	1	K.KLEAAEER.R
86 - 95	583.2628	1164.5110	1164.5411	-0.0300	0	K.AIEENNNFSK.M

MS/MS Fragmentation of AIEENNNFSK



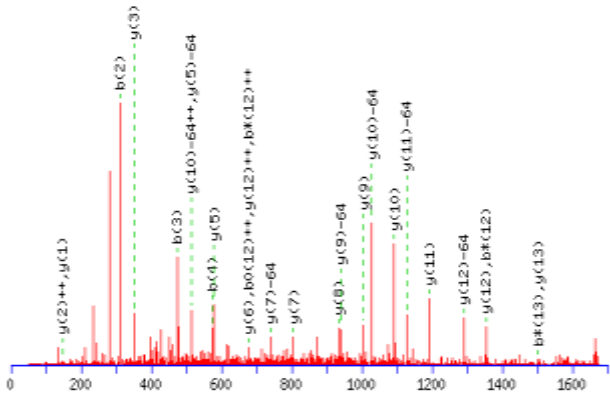
23 O95881 13

Thioredoxin domain-containing protein 12

1 METRPRLGAT CLLGFSFLLL VISSDGHNGL KGFQGDHIHW RTLEDGKKEA  
 51 AASGLPLMVI IHKSWCGACK ALKPKFAEST EISELSHNFV MVNLEDEEPP  
 101 KDEDSPDGG YIPRILFLDP **SGK**VHPEIIN ENGNPSYK**YF YVSAEQVVQGMK**  
 151 **M**KEAQERLTG DAFRKKHLED EL

Start-End	Observed	Mr(expt)	Mr(calc)	Delta	Miss	Sequence
115 - 123	495.3159	988.6172	988.5593	0.0579	0	R.IFLFLDPSGK.V
115 - 123	495.3221	988.6296	988.5593	0.0703	0	R.IFLFLDPSGK.V
139 - 152	832.9714	1663.9282	1663.7916	0.1367	0	K.YFVSAEQVVQGMK.E
139 - 152	832.9721	1663.9296	1663.7916	0.1381	0	K.YFVSAEQVVQGMK.E

MS/MS Fragmentation of **YFVSAEQVVQGMK**



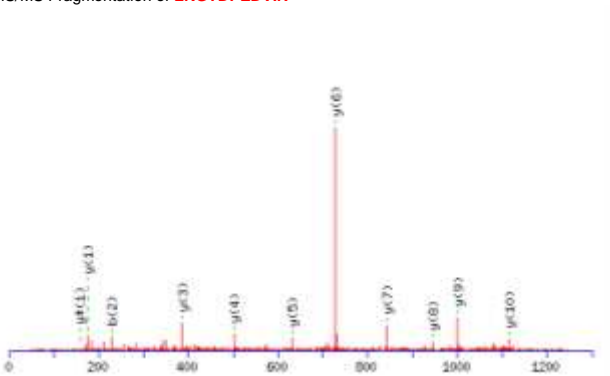
24 O14950 23

Myosin regulatory light chain MRLC2

1 MSSKKAKTKT TKKRPQRATS NVFAMFDQSQ IQEFKEAFNM IDQNRDGFID  
 51 KEDLDMLAS LGKNPTDAYL DAMMNEAPGP INFTMFLTMF GEKL**NGTDP**EDR  
 101 **D**VIRNAFACF DEEATGTIQE DYLR**ELLTTM GDRFTDEEVD ELY**REAPIDK  
 151 **KGNFN**YIEFT RILKHGAKDK DD

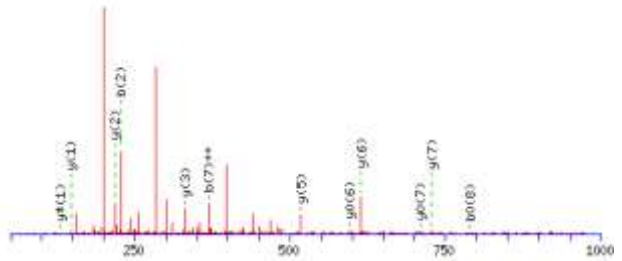
Start - End	Observed	Mr(expt)	Mr(calc)	Delta	Miss	Sequence
94 - 104	614.8414	1227.6682	1227.6095	0.0587	0	K.LNGTDPEDVIR.N
125 - 133	526.2847	1050.5548	1050.5016	0.0533	0	R.ELLTTMGDR.F
134 - 144	708.3533	1414.6920	1414.6252	0.0668	0	R.FTDEEVD ELYR.E
152 - 161	630.8325	1259.6504	1259.5935	0.0570	0	K.GNFN YIEFTR.I

MS/MS Fragmentation of **LNGTDPEDVIR**



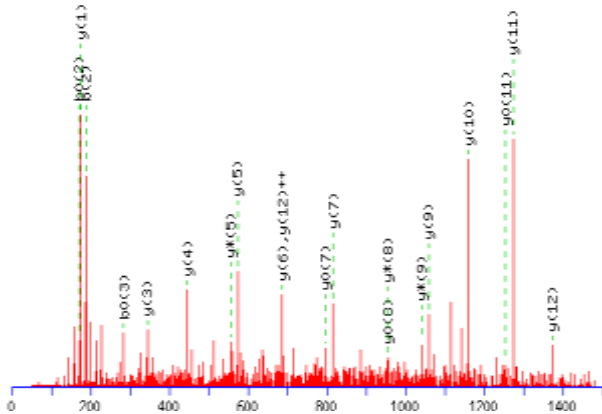
27 Q96A08 12 Histone H2B type 1-A

1 MPEVSSKAT ISKKGFKAV VKTQKKEGKK RKRTRKESYS IYIYKVLKQV  
 51 HPDTGISSKA MSIMNSFVTD IFERIASEAS RLAHYSKRST ISSR**EIQTAV**  
 101 **LLLLPGELAK** HAVSEGTKAV TKYTSSK  
**Start - End Observed Mr(expt) Mr(calc) Delta Miss Sequence**  
 95 - 101 408.7352 815.4558 815.4501 0.0057 0 R.EIQTAVR.L  
 102 - 110 477.3018 952.5890 952.5957 -0.0066 0 R.LLLPGELAK.  
 MS/MS Fragmentation of **LLLLPGELAK**



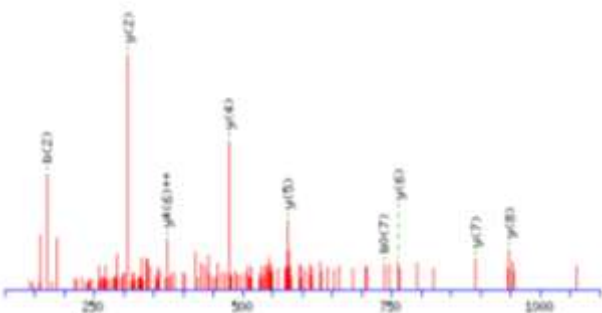
28 P62807 57 Histone H2B type 1-C/E/F/G/I

1 MPEPAKAPA PKKGSKKAVT KAQKKDGKKR KRSR**ESYSV YVYKVLKQVH**  
 51 **PDTGISSKAM GIMNSFVNDI FERIAGEASR LAHYNKRSTI TSREIQTAVR**  
 101 **LLLLPGELAKH AVSEGTKAVT KYTSK**  
**Start - End Observed Mr(expt) Mr(calc) Delta Miss Sequence**  
 36 - 44 569.2944 1136.5742 1136.5390 0.0353 0 K.ESYSVYVYK.V  
 45 - 58 503.6217 1507.8433 1507.8358 0.0074 1  
**K.VLKQVHPDTGISSK.A**  
 48 - 58 584.8140 1167.6134 1167.5884 0.0250 0 K.QVHPDTGISSK.A  
 59 - 73 888.4241 1774.8336 1774.8018 0.0318 0  
**K.AMGIMNSFVNDIFER.I**  
 88 - 100 487.9460 1460.8162 1460.7947 0.0215 1 R.STITSREIQTAVR.L  
 94 - 100 408.7277 815.4408 815.4501 -0.0093 0 R.EIQTAVR.L  
 101 - 109 477.2920 952.5694 952.5957 -0.0262 0 R.LLLPGELAK.H  
 101 - 109 477.3095 952.6044 952.5957 0.0088 0 R.LLLPGELAK.H  
 110 - 121 409.8952 1226.6638 1226.6619 0.0019 1 K.HAVSEGTKAVTK.Y  
 MS/MS Fragmentation of **STITSREIQTAVR**



31 P25398 14 40S ribosomal protein S12

1 MAEEGIAAGG VMDVNTALQE VLK**TALIH DG LARG**IREAAK ALDKRQAHLK  
 51 VLASNCDEPM YVKLVEALCA EHQINLIKVD DNKK**LGEWVG LCK**IDREGKP  
 101 RKVVGCSVV VKDYGKESQA KDVIEEYFKC KK  
**Start - End Observed Mr(expt) Mr(calc) Delta Miss Sequence**  
 24 - 33 533.7745 1065.5344 1065.5931 -0.0586 0 K.TALIH**DGLAR.G** )  
 24 - 33 533.7747 1065.5348 1065.5931 -0.0582 0 K.TALIH**DGLAR.G**  
 85 - 93 531.2432 1060.4718 1060.5376 0.0657 0 K.L**GEWVGLCK.I**  
 MS/MS Fragmentation of **LGEWVGLCK**



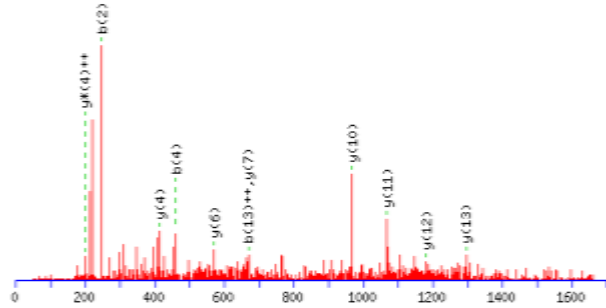
1 MAGWNYIDN LMADGTCQDA AIVGYKDSPS VWAAVPGK**TF VNITPAEVGV**  
**51 LVGKDRSSFY** VNGLTGGGQK CSVIR**DSLLQ DGEFSMDLR**T **KSTGGAPTFN**  
**101 VTVTKDKTL VLLMGKEGVH GGLINKKCYE MASHLR**RSQY

Start - End	Observed	Mr(expt)	Mr(calc)	Delta	Miss	Sequence
39 - 54	822.4751	1642.9356	1642.9294	0.0062	0	K.TFVNITPAEVGVLVGK.D

K.TFVNITPAEVGVLVGK.D

76 - 89	813.3810	1624.7474	1624.7403	0.0072	0	R.DSLLQDGEFSMDLR.T
92 - 105	690.3588	1378.7030	1378.7093	-0.0062	0	K.STGGAPTFNVTVK.
106 - 116	609.8624	1217.7102	1217.7053	0.0049	1	K.TDKTLVLLMGK.E
117 - 127	576.3310	1150.6474	1150.6458	0.0016	1	K.EGVHGGGLINKK.C
128 - 136	583.7573	1165.5000	1165.5008	-0.0008	0	K.CYEMASHLR.R

MS/MS Fragmentation of **TFVNITPAEVGVLVGK**



## 7. Acknowledgements

My sincere gratitude to Prof. Dr. Michael Oellerich and PD. Dr. Abdul Rahman Asif for their constant encouraging guidance, support, and invaluable suggestions. They provide me inspiring energy and have always been ready for both scientific and social discussions during this period. Their creativity and expertise in research, patience, and motivational skills are exceptional.

I would like to express my gratitude to Prof. Dr. Uwe Groß and Prof. Dr. Stefan Pöggeler for serving on my thesis committee, and for their constructive criticisms and endless help throughout this study. I also have the deepest gratitude for my subject examination committee members, Dr. Michael Hoppert, Dr. Rolf Daniel, Prof. Dr. Petr Karlovsky, and Dr. Marko Rohlf for their thoughtful comments and suggestions.

Special thanks to Hazir Rahman and Misbah Tauseef for giving me critical advice during our discussions and helped me to turn results into science. They were with me through the thick and thin of this long and arduous PhD journey.

I was fortunate to work with great colleagues Dr. Darinka Petrova, Dr. Christoph Eberle, Dr. Gunner Brandhorst, Prof. Dr. Nico Von Ahsen, Dr. Lutz Binder, Dr. Raees Ahmed for their invaluable support and perceptive comments. I am deeply indebted to my former colleagues Saima Zafar, Saadia Zahid, Bharat Singh and Dr. Saagarika Biswas for their always being there and helping me in more ways than one probably know. I would like to express my appreciation to our proteomics laboratory technicians, especially Christina Wiese, Christa Schultz, Susanne Goldmann for their technical support and expertise. I also wish to thank Ulrike Bonitz, Rainer Andaq and Sandra Hartung, for creating a supportive and pleasant work atmosphere.

I wish to express my gratitude to Prof. Dr. Philips Walson for their constructive criticism and for giving me valuable suggestions for improvement of my dissertation. I also offer special thanks to Vicky Maixner for editing support for my thesis and manuscripts. I am grateful to Prof. Dr. Gabor Kottra for providing me TER instrument and special thanks to Prof. Dr. Giuliano Ramadori for the providing access to the immunofluorescence microscope facility.

I would like to pay special thanks to Kohat University of Science and Technology and Higher Education Commission of Pakistan for giving me the opportunity, and financial support to complete PhD work in such a world class University.



I express gratitude to my friends Abdul Malik, Waheed Murad, Hayat Khan Sherani, Muhammad Naveed, Muhammad Adnan, Sajjad Ahmed, Tayyab Tahir, Ihtzaz Ahmed, Naeem Misdaq, Naila Naz, Sadaf Sultan, Aneela Javed, Saadia Qammar, Nazim Khan, Abdullah Jalal, Noor Muhammad, Kalimullah Khan, Jamil-ur-Rehman, Adeel, Altaf Husain, Muhammad Haroon, Nouman, and many others, for supporting me in difficult moments and understanding my needs. Wholehearted thanks to the peoples of Göttingen especially Pakistani community for all the good care and great help throughout the way. In addition, I share my success to all of the wonderful people who have supported, assisted, and loved me in Germany and also those back in Pakistan.

I would especially like to acknowledge my past teachers Prof. Dr. Mansoor-ul-Hassan Alvi, Prof. Dr. Shahida Hasnain, and Prof. Dr. Abdul Rauf Shakoori, for guiding me during the earlier days in my scientific career. They have been a continuous source of inspiration and motivation to me in this tough journey.

Last but not the least; words are insufficient to express my thanks to my parents, sisters and brother for all their undying love, constant support, encouragement and blessings through out my PhD course. My warmest thanks belong to my wife and children for their understanding, never-ending support, love and sharing my affection.

## 8. Curriculum Vitae

Name: Muhammad Qasim

Date and Place of birth: 25<sup>th</sup> December 1978, Mardan, Pakistan

Nationality: Pakistani

### Educational background

2008 – continue PhD (Biology) from Georg-August University, Goettingen, Germany.

2004 – 2006 M.Sc (Microbiology and Molecular Genetics) from University of the Punjab, Lahore, Pakistan.

2000 – 2003 B.Sc (Medical Laboratory Technology) from University of the Punjab, Lahore Pakistan

### Professional experience

2003 - 2005 Lecturer Microbiology, Institute of Health Management, Lahore, Pakistan.

2004 - 2005 Research Scholar, Department of Microbiology, Children Hospital, Lahore, Pakistan.

2006 - 2008 Medical Technologist (Clinical scientist), Department of Microbiology, Federal Post Graduate Medical Institute, Shaikh Zayed Hospital Lahore, Pakistan.

2008 – to date Lecturer Microbiology, Department of Microbiology, Kohat University of Science and Technology, Kohat, Pakistan (study leave).

### Publications

1. **Qasim M**, Rahman H, Oellerich M, Asif AR. Differential proteome analysis of human embryonic kidney cell line following mycophenolic acid treatment. *Proteome Sci.* 2011 Sep 20;9:57.
2. Rahman H, **Qasim M**, Schultze FC, Oellerich M, Asif AR. Influence of fetal calf serum heat inactivation and lipopolysaccharides contamination on human T lymphoblasts proteome and phosphoproteome. *Proteome Sci.* 2011 Nov 15;9(1):71.
3. **Qasim M**, Rahman H, Ahmed R, Oellerich M, Asif AR. Mycophenolic acid mediated disruption of the intestinal epithelial tight junctions. *Submitted.*
4. Rahman H, **Qasim M**, Ahmed R, Oellerich M, Asif AR. mTORC1 interactomics; mtorc1 interplay in the mRNA decapping through Edc4. *Submitted.*

## Abstracts published

1. **Qasim M**, Rahman H, Oellerich M, Asif AR. Protein alterations in human cell line in response to mycophenolic acid. *Clin Chem*. 2010; 57(S10): A78.
2. **Qasim M**, Rahman H, Ahmed R, Oellerich M, Asif AR. Mycophenolic acid modulation of epithelial tight junctions-a mechanism of gastrointestinal toxicity? *Clin Chem Lab Med*. 2011; 49(9): A112.

## Research presentations

1. **Qasim M**, Hasnain S, Zafar A. Bacteria isolated from indwelling medical devices and their antibiotic susceptibility pattern in children. International Symposium on Genomics, Proteomics and Metabolomics at University of the Punjab, Lahore, Pakistan (22<sup>nd</sup> to 23<sup>rd</sup> Oct 2007) (*Poster*).
2. **Qasim M**, Rahman H, Oellerich M, Asif AR. Protein alterations in human cell line in response to mycophenolic acid. DGKL Congress Mannheim, Germany (29<sup>th</sup> Sept to 2<sup>nd</sup> Oct 2010) (*Poster*).
3. Rahman H, **Qasim M**, Schultze FC, Oellerich M, Asif AR. Dynamin 2: is a new interacting partner of mechanistic target of rapamycin complex 1 in human T lymphocytes. Berlin Proteomic Forum, Germany (3<sup>rd</sup> to 7<sup>th</sup> April 2011) (*Poster*).
4. Rahman H, **Qasim M**, Schultze FC, Oellerich M, Asif AR. Fetal calf serum heat inactivation and lipopolysaccharide contamination influence the human T lymphoblasts proteome and phosphoproteome. Berlin Proteomic Forum, Germany (3<sup>rd</sup> to 7<sup>th</sup> April 2011) (*Poster*).
5. Tauseef M, **Qasim M**, Asif AR, Oellerich M, Ahsen NC. Differential protein profiling of thiopurines in T lymphocytes. Berlin Proteomic Forum, Germany (3<sup>rd</sup> to 7<sup>th</sup> April 2011) (*Poster*).
6. Sing B, **Qasim M**, Rahman H, Sharma GL, Oellerich M, Kumar R, Asif AR. Proteomics based identification of diagnostically relevant and vaccine candidate molecules of *Aspergillus fumigatus* at the meeting of Goettingen International Health Network, Goettingen, Germany (23<sup>rd</sup> to 24<sup>th</sup> May 2011) (*Poster*).
7. **Qasim M**, Rahman H, Ahmed R, Oellerich M, Asif AR. Mycophenolic acid modulation of epithelial tight junctions-a mechanism of gastrointestinal toxicity?. AACC annual meeting 2011, Atlanta, Georgia, USA (24<sup>th</sup> to 28<sup>th</sup> July 2011) (*Poster*).
8. **Qasim M**. Epithelial tight junction regulation by Mycophenolic acid. Symposium of Transportage 2011 at the Department of Physiology and Patho physiology, University Medical Center, Goettingen, Germany (22<sup>nd</sup> to 23<sup>rd</sup> Oct 2011) (*Oral*).

## Distinction and award

1. Second position in the institute in BSc Medical Lab Technology (2003), University of the Punjab, Lahore, Pakistan.
2. PhD scholarship for Germany under the faculty development scholarship program from the Kohat University Science and Technology, Pakistan (2008-2011).